INFORMATION TO USERS

This material was produced from a microfilm copy of the original document. While the most advanced technological means to photograph and reproduce this document have been used, the quality is heavily dependent upon the quality of the original submitted.

The following explanation of techniques is provided to help you understand markings or patterns which may appear on this reproduction.

1. The sign or "target" for pages apparently lacking from the document photographed is "Missing Page(s)". If it was possible to obtain the missing page(s) or section, they are spliced into the film along with adjacent pages. This may have necessitated cutting thru an image and duplicating adjacent pages to insure you complete continuity.

2. When an image on the film is obliterated with a large round black mark, it is an indication that the photographer suspected that the copy may have moved during exposure and thus cause a blurred image. You will find a good image of the page in the adjacent frame.

3. When a map, drawing or chart, etc., was part of the material being photographed the photographer followed a definite method in "sectioning" the material. It is customary to begin photoing at the upper left hand corner of a large sheet and to continue photoing from left to right in equal sections with a small overlap. If necessary, sectioning is continued again — beginning below the first row and continuing on until complete.

4. The majority of users indicate that the textual content is of greatest value, however, a somewhat higher quality reproduction could be made from "photographs" if essential to the understanding of the dissertation. Silver prints of "photographs" may be ordered at additional charge by writing the Order Department, giving the catalog number, title, author and specific pages you wish reproduced.

5. PLEASE NOTE: Some pages may have indistinct print. Filmed as received.

University Microfilms International
300 North Zeeb Road
Ann Arbor, Michigan 48106 USA
St. John's Road, Tyler's Green
High Wycombe, Bucks, England HP10 8HR

77-18,091

PARK, Jung-Yong, 1943-
BIOPHYSICAL MODEL APPROACH TO THE MECHANISTIC STUDIES OF INTESTINAL ABSORPTION OF DRUGS.

The University of Michigan, Ph.D., 1977
Health Sciences, pharmacy

Xerox University Microfilms, Ann Arbor, Michigan 48106

BIOPHYSICAL MODEL APPROACH TO THE MECHANISTIC STUDIES OF INTESTINAL ABSORPTION OF DRUGS

by

Jung-Yong Park

A dissertation submitted in partial fulfillment
of the requirement for the degree of
Doctor of Philosophy
(Pharmaceutical Chemistry)
in The University of Michigan
1977

Doctoral Committee:

Associate Professor Norman F. H. Ho, Chairman
Associate Professor Gordon L. Flynn
Professor Arthur B. French
Professor William I. Higuchi
Associate Professor Norman D. Weiner
Dr. Walter Morozowich, Research Scientist IV,
Pharmacy Research, The Upjohn Company

To my mother
and
my wife, Myoung-Hee
and
my daughter, Sissela SayEun

ACKNOWLEDGEMENTS

This project was completed with the help of individuals who deserve special mention. I wish to pay tribute to them.

It is my privilege to have been associated with Dr. Norman F. H. Ho and Dr. William I. Higuchi. Their dedication and scientific knowledge have been a constant source of inspiration. It has been their guidance and encouragement that has enabled me to complete this study. Their efforts in my education are deeply appreciated.

To Dr. Walter Morozowich for his support and invaluable suggestions for the conceptualization and successful completion of the prostaglandin studies.

To Mr. Scott Douglas of the Upjohn Company for the radiosynthesis of the prostaglandin $F_{2\alpha}$ C_1-amide analogs.

To the members of the Doctoral Committee: Dr. Gordon L. Flynn, Dr. Arthur B. French and Dr. Norman D. Weiner for their time and effort in providing helpful suggestions.

To Dr. Kishor Desai for his friendship and valuable discussions throughout the experiments.

To Mark Langworthy for his help in the thin layer chromatography studies.

To my wife, Myoung-Hee, for her typing of this manuscript and her constant support throughout my graduate career.

In addition, to The Upjohn Company for financial support through a predoctoral fellowship.

TABLE OF CONTENTS

DEDICATION ii

ACKNOWLEDGEMENTS iii

LIST OF TABLES vi

LIST OF FIGURES ix

NOMENCLATURE xii

INTRODUCTION 1

LITERATURE REVIEW 3

A. Aspects of Intestinal Physiology Relevant to Absorption 3
   1. Gross Intestinal Structure 3
   2. The Absorption Cell Barrier 3
   3. The Aqueous Boundary (Diffusion) Layer . . 7
   4. Lumenal and Membrane Drug Metabolism . . . 8
   5. Intestinal Blood Flow 8
B. Transport Across Aqueous Boundary Layer . . . 9
C. Prostaglandins 11
   1. Gastrointestinal Tract 13
   2. Intestinal Absorption 14
   3. Metabolism 15
   4. Physical Properties and Stability 18

STATEMENT OF THE PROBLEM 19

EXPERIMENTAL 21

A. Materials and Apparatus 21
B. In Situ Rat Intestinal Absorption Procedures . 23
C. Non-Steady State Disappearance of Drugs . . . 27
D. Thin Layer Chromatography of Prostaglandins. . 28

CHAPTER I. PASSIVE TRANSPORT OF DRUGS 31

A. Theoretical Considerations 31
   1. General Description of the Physical Model. 31
   2. Special Case of the General Model 34
   3. Determination of the Permeability Coefficients 34
   4. Incremental Partition Constant . . . . . .
B. Influence of the Aqueous Diffusion Layer on the Rat Intestinal Transport of Various Solutes 38
   1. Introduction 38
   2. Absorption of Hydrocortisone and Prednisolone 39

3. Absorption of n-Octanol, n-Butanol and Salicylic Acid 46
4. Permeability Coefficients 54
5. General Discussion 58
C. Intestinal Absorption of n-Alkanoic Acids . . 64
1. General Absorption Studies 64
2. Permeability Coefficients and Incremental Partition Constant per CH_2 Group 71
3. General Discussion 74

CHAPTER II. SIMULTANEOUS PASSIVE TRANSPORT AND BIOCONVERSION OF DRUGS 76

A. Theoretical Consideration 76
1. General Description of the Physical Model. 76
2. Steady-State Fluxes 78
3. Special Case of Simple Passive Transport . 82
4. Factorization of the Effective Transport-Bioconversion Permeability Coefficients. . 83
5. The π^* Concept 84
B. Intestinal Absorption of Prostaglandin $F_{2\alpha}$ . . 86
1. Introduction 86
2. General Absorption Studies 88
3. Assessment of the Physiological Effects of $PGF_{2\alpha}$ on the Membrane 92
4. Mechanism of Membrane Transport 98
5. Metabolism Studies 102
6. Permeability Coefficients 107
7. General Observation of Buffer Capacity on In Situ $PGF_{2\alpha}$ Absorption 112
C. Quantitative Assessment of the Influence of Molecular Substituents Groups on the Intestinal Absorption Process of Prostaglandins . . 114
1. Introduction 114
2. General Results 115
3. π^* Analysis Between PGE_2 and $PGF_{2\alpha}$ 120
4. π^* Analysis Between $PGF_{2\alpha}$ and $PGF_{2\alpha}$ C_1-Amide 121
5. π^* Analysis Between $PGF_{2\alpha}$ C_1-n-Amide and $PGF_{2\alpha}$ C_1-Carbamoylmethylamide 122
6. π^* Analysis of $PGF_{2\alpha}$ C_1-n-Alkylamide Homologs 124

SUMMARY 126

REFERENCES 128

APPENDIX 133

LIST OF TABLES

Table		Page
I	Standard Isotonic Buffer Solutions	22
II	Nonsteady-State Disappearance of Various Solutes at pH 6.0 in the Initial 30 Seconds in the Rat Jejunum before the Experimental Zero Time Sampling	29
III	Successive Absorption Experiments at pH 6.0 in Same Jejunum Segment at Different Hydrocortisone Concentrations and Static 150 Sec Sampling Intervals	45
IV	Independence of the Sampling Intervals on the Absorption Rate When Oscillating Procedures Producing Continuous Hydrodynamics in the Intestinal Solution are Employed	45
V	Estimation of r* between the Permeability Coefficients of the Unstirred Aqueous Layer under Various Hydrodynamic Conditions	57
VI	Rate Constants and Permeability Coefficients of Steroids in the Jejunum at 37°C and pH 6.0	59
VII	Rate Constants and Permeability Coefficients of n-Alkanols and Salicylic Acid in Jejunum at 37°C	60
VIII	Influence of the Unstirred Aqueous Layer on the Experimental Rate Constants	62
IX	The First Order Rate Constants of the n-Alkanoic Acids at Various pH and Two Hydrodynamic Conditions	67
X	Estimation of the Permeability Coefficients and Effective Thickness of the Aqueous Boundary Layer	71
XI	In Situ Permeability Coefficients of n-Alkanoic Acids for the Rat Jejunum	73
XII	In Situ Absorption of ^{3}H-$PGF_{2\alpha}$ (5×10^{-3} µg/ml) in Rat Jejunum at 37°C: Apparent Rate Constants	91

XIII	Successive Absorption Experiments of ^{3}H-$PGF_{2\alpha}$ in Same Jejunum Segment at Various Buffer pH Combinations	94
XIV	Successive Absorption Experiments at pH 6.0 in Same Jejunum Segment at Various $PGF_{2\alpha}$ Concentration Combinations	95
XV	Absorption of ^{14}C-n-Butanol in Jejunum at pH 6.0 in the Absence and Presence of $PGF_{2\alpha}$	96
XVI	In Situ Absorption of ^{14}C-Benzoate at pH 8.5 in the Absence and Presence of $PGF_{2\alpha}$ in the Jejunum	96
XVII	In Situ Absorption of ^{3}H-$PGF_{2\alpha}$ at Various Concentrations and Buffer pH	100
XVIII	Absorption of ^{3}H-$PGF_{2\alpha}$ in the Absence and Presence of Indomethacin at Buffer pH 7.5	100
XIX	In Situ Absorption of ^{3}H-$PGF_{2\alpha}$ in the Absence and Presence of Iodoacetic Acid at Buffer pH 6.0	102
XX	Absorption of ^{3}H-$PGF_{2\alpha}$ in the Absence and Presence of Furosemide at Buffer pH 4.5, 6.0 and 7.5	105
XXI	Permeability Coefficients of the Aqueous Diffusion Layer	109
XXII	Factorization of the Effective Permeability Coefficients of the Jejunal Membrane at Various Buffer pH into the Permeability Coefficients of the Aqueous Pores and Principal Membrane Pathway	110
XXIII	Influence of the Aqueous Diffusion Layer on the Transport Rate of $PGF_{2\alpha}$ in the Jejunum	111
XXIV	Permeability Coefficients of Various Prostaglandins Obtained from In Situ Rat Jejunal Studies at 37°C	118
XXV	Michaelis Constant and v_{max} of Various Prostaglandins Using Monkey Lung Prostaglandin Dehydrogenase	119

XXVI	Analysis of π Values Between PGE_2 and $PGF_{2\alpha}$	120
XXVII	Analysis of π Values Between $PGF_{2\alpha}$ and $PGF_{2\alpha}$ C_1-Amide	122
XXVIII	In Vitro Partition Coefficients of $PGF_{2\alpha}$ and $PGF_{2\alpha}$ C_1-Amide	123
XXIX	Analysis of π Values Between $PGF_{2\alpha}$ C_1-Amide and $PGF_{2\alpha}$ C_1-Carbamoylmethylamide. .	123
XXX	Analysis of π Values Among $PGF_{2\alpha}$ C_1-n-Alkylamides Including $PGF_{2\alpha}$ C_1-Amide	124

LIST OF FIGURES

1. Schematic diagram of two sectioned villi and a crypt to illustrate the histologic organization of the small intestinal mucosa 4

2. Schematic diagram of an intestinal absorptive cell 6

3. Modified Doluisio system for *in situ* rat intestinal absorption studies 25

4. Schematic diagram of the physical model for the passive transport of solutes across the intestinal membrane 32

5. Semilogarithmic plot of the fraction of hydrocortisone remaining in the lumen with time at 37°C and pH 6.0 under various constant hydrodynamic situations 40

6. Semilogarithmic plot of the fraction of hydrocortisone remaining in the lumen with time at 37°C and pH 6.0 41

7. Semilogarithmic plot of the fraction of prednisolone remaining in the lumen with time at 37°C and pH 6.0 under various constant hydrodynamic situations 43

8. Semilogarithmic plot of the fraction of prednisolone remaining in the lumen with time at 37°C and pH 6.0 44

9. First order absorption of n-octanol at 37°C and pH 6.0 under constant hydrodynamic conditions 48

10. First order absorption of n-octanol at 37°C and pH 6.0 49

11. First order absorption of n-butanol at 37°C and pH 6.0 under constant hydrodynamic conditions 50

12. First order absorption of n-butanol at 37°C and pH 6.0 51

13. Absorption of salicylic acid at 37°C and pH 6.0 under constant hydrodynamic conditions . . . 52

14. Absorption of salicylic acid at 37°C and pH 6.0 . 53

15. First order absorption rate constants versus number of carbons in the n-alkanol series under various hydrodynamic situations 56

16. Semilogarithmic plots in the fraction of n-alkanoic acids remaining in the lumen with time at pH 6.0 and oscillation hydrodynamic condition. 65

17. Absorption of n-butyric and n-octanoic acids in the rat jejunum at two different hydrodynamic situations 66

18. First order absorption rate constant-buffer pH profiles of n-alkanoic acid homologs 68

19. Profiles of absorption rate constant versus carbon number in n-alkanoic acid series as a function of buffer pH and hydrodynamic conditions 70

20. Physical model for the simultaneous intestinal membrane transport and bioconversion of a substrate drug 77

21. Semilogarithmic change in the fraction of ^{3}H-$PGF_{2\alpha}$ remaining in the lumen with time 89

22. Comparison of the in situ absorption of $PGF_{2\alpha}$ at buffer pH 3.5 and 4.5 under two hydrodynamic conditions 90

23. Apparent first order rate constants versus high buffer pH under two hydrodynamic conditions in the rat jejunum 93

24. Semilogarithmic plots of the concentration of ^{14}C-n-octanol remaining in the lumen of the jejunum with time in the presence and absence of $PGF_{2\alpha}$ under static, 150 seconds sampling interval, hydrodynamics 97

25. Comparison of the absorption-pH profiles of $PGF_{2\alpha}$ and n-butyric acid under oscillation 0.075 ml/sec hydrodynamics in the rat jejunum . . 99

26. Effect of $PGF_{2\alpha}$ concentration on the intestinal absorption rate constant at pH 6.0 and oscillation hydrodynamics 101

27. Percent of radiolabeled $PGF_{2\alpha}$ and metabolites found in the lumen of the rat jejunum in situ with time 103

28. Percent of radiolabeled $PGF_{2\alpha}$ and metabolites found in the lumenal solution jejunal gut segment and blood after 20 minutes from *in situ* absorption experiments and in the lumenal solution and after 20 minutes exposure from *in vitro* experiments 104

29. Percent of radiolabeled $PGF_{2\alpha}$ and metabolites found in the lumen of the rat jejunum after 20 minutes *in situ* experiments in the presence and absence of furosemide at pH 6.0 106

30. Semilogarithmic plots of the concentration of ^{14}C-n-butanol remaining in the lumen of the jejunum within the absence and presence of furosemide to assess membrane damage at pH 6.0. . 108

31. Semilogarithmic change in the lumenal concentration of $PGF_{2\alpha}$ and bulk pH change with time for the pH 3.5 and 4.5 cases under oscillation hydrodynamics and two buffer strengths 113

32. Apparent first order rate constants *versus* high buffer capacity pH under two hydrodynamic conditions in the rat jejunum 116

33. *In situ* absorption rate constants of the $PGF_{2\alpha}$ C_1-*n*-alkylamide, including $PGF_{2\alpha}$ amide 117

NOMENCLATURE

A	= apparent geometric surface area
C	= total drug concentration in the membrane
C_b	= total drug concentration in the lumen
cpm	= counts per minute
C_p^o	= concentration of nondissociated species in the aqueous pores
C_s	= total drug concentration at the membrane interface
C_s^o	= concentration of nondissociated species at the membrane interface
$C_{s,m}^o$	= concentration of nondissociated species at the surface on the membrane side
D	= diffusion coefficient of drug in the passive diffusional-bioconversion pathway of the membrane
D_{aq}	= aqueous diffusion coefficient
D_p	= diffusion coefficient of drug in the aqueous pores
J_{aq}	= total flux in the aqueous boundary layer per unit area
J_m	= flux in the membrane per unit apparent surface area
J_p	= flux per unit apparent surface area across the aqueous pores
K	= membrane lipoidal biophase-water partition coefficient for the nondissociated species
K_a	= dissociation constant of a weak acid or weak base
K_u	= apparent first order absorption rate constant
$K_{u,max}$	= apparent maximum absorption rate constant
K_M	= Michaelis enzyme constant

K_i, K_{i+1} = lipoidal biophase-aqueous partition coefficient of a n-alkanol and the next higher homolog

L = effective thickness of the membrane

L_{aq} = effective thickness of the aqueous boundary layer

MW = molecular weight

pK_a = negative logarithm of the dissociation constant K_a

P_{app} = apparent permeability coefficient

P_{aq} = permeability coefficient of aqueous boundary layer for a drug molecule

$P_{e,m}$ = effective permeability coefficient of the membrane

P_o = permeability coefficient of the lipoidal pathway of the membrane for the nondissociated species

$P_{o,i}; P_{o,i+1}$ = permeability coefficient of a n-alkanol and the next higher homolog across the lipoidal pathway

P_p, P_p^- = permeability coefficient of the aqueous pore pathway of the membrane for the nondissociated and charged species, respectively

$P_{e,lipid}$ = effective permeability coefficient of the lipoidal biophase and is equal to $P_o X_s$

PGE_2 = prostaglandin E_2

$PGF_{2\alpha}$ = prostaglandin $F_{2\alpha}$

R_g = universal gas constant

T = absolute temperature

V = volume solution in the intestinal lumen

X_s = fraction of nondissociated species at the membrane surface on the aqueous boundary layer side

k = first order bioconversion rate constant

n_{CH_2} = incremental partition constant per methylene group

r = effective radius of the lumen

s = subscript denoting the surface boundary

t = time .

tanh = hyperbolic tangent function

* = superscript denoting the structurally modified drug

α = volume fraction of lipoidal biophase of the membrane

$(1-\alpha)$ = volume fraction of aqueous pores of the membrane

$\delta\Delta F^*_{CH_2}$ = incremental free energy change per CH_2 group

υ = steady-state rate of enzyme catalysis

υ_{max} = maximum steady-state rate of enzyme catalysis

π_{CH_2} = dimensionless incremental free energy change per CH_2 group

π_k = dimensionless incremental free energy change in the enzymatic rate constant of the reference drug molecule by the addition of a substituent group

π_{PC} = same definition as π_{CH_2}, but used in context with a drug undergoing simultaneous passive membrane transport and metabolism

π^* = total dimensionless incremental free energy changes in the transfer of a substituent group from water to the lipoidal phase and in the substituent group effect on the change in the enzyme rate constant of the reference drug molecule

INTRODUCTION

In the process of developing a new drug, the traditional approach is to select that drug with the highest activity out of a series of closely related structural variants. Quite often the "lead drug" has the desired potency and specificity of action but it may not have the optimal pharmaceutical properties (solubility, stability and related physico-chemical properties) and biological properties (absorption, duration of action, side effects and related pharmacodynamic properties). The approach to optimizing these pharmaceutical and biological properties employs additional molecular modification of the lead compound via derivative or analog synthesis.

One of the most common problems with drugs is their failure to show complete oral absorption or bioavailability. The scientific and patent literature abounds with a number of empirically obtained derivatives and analogs of drugs with improved oral absorption but there is little rationale given for their design or the specifics of structural modification. In an attempt to place structure-intestinal absorptivity relationships on a sound basis, this thesis concerned with theoretical and experimental studies of the process of intestinal drug absorption of drugs to quantitatively formulate rigorous mathematical relationships between absorption and the relevant physico-chemical processes involved. These studies are referred to as the physical model approach to the intestinal absorption of

drugs.

The fundamental physical properties that influence the intestinal absorption of drugs are diffusion, partitioning, ionic equilibria in the case of ionizable solutes, solubility and metabolism. The understanding of the relationships of these factors together with the aqueous boundary layer and the biophysicochemical property of the intestinal membrane barrier should provide the essential body of knowledge to quantitatively predict the rate of absorption of the lead drug and the molecular modified drug as well as to provide the basis for the rational development and manipulation of formulation concepts.

LITERATURE REVIEW

A. Aspects of Intestinal Physiology Relevant to Absorption.

1. Gross Intestinal Structure: A rational approach to the understanding of the intestinal absorption of drugs, among other important considerations relating to the physicochemical properties of the drug molecule and pharmaceutical formulation, requires some degree of knowledge of the intestinal tract: morphology, organization and function of the different components of the cells, geometry, ultrastructure, biochemical processes, hydrodynamics in the intestinal lumen, and transport mechanisms. Excellent reviews on intestinal structure in relation to absorption are available.[1,2,3]

The small intestine is divided into the duodenum, jejunum and ileum. The mucosa consists of three layers (Figure 1): (a) the absorptive layer, a single sheet of columnar epithelium, (b) the lamina propia, a layer heterogeneous in composition and cell types, and (c) the muscularis mucosa, a muscular layer separating the mucosa and the submucosa. In man the villi (fingerlike projections) are 0.5-1.0 mm in height.

2. The Absorption Cell Barrier: The epithelium layer consists of a distribution of cell types and functionality that vary with location. Absorption cells are found about the tips of the villi while the Goblet cells (mucous-

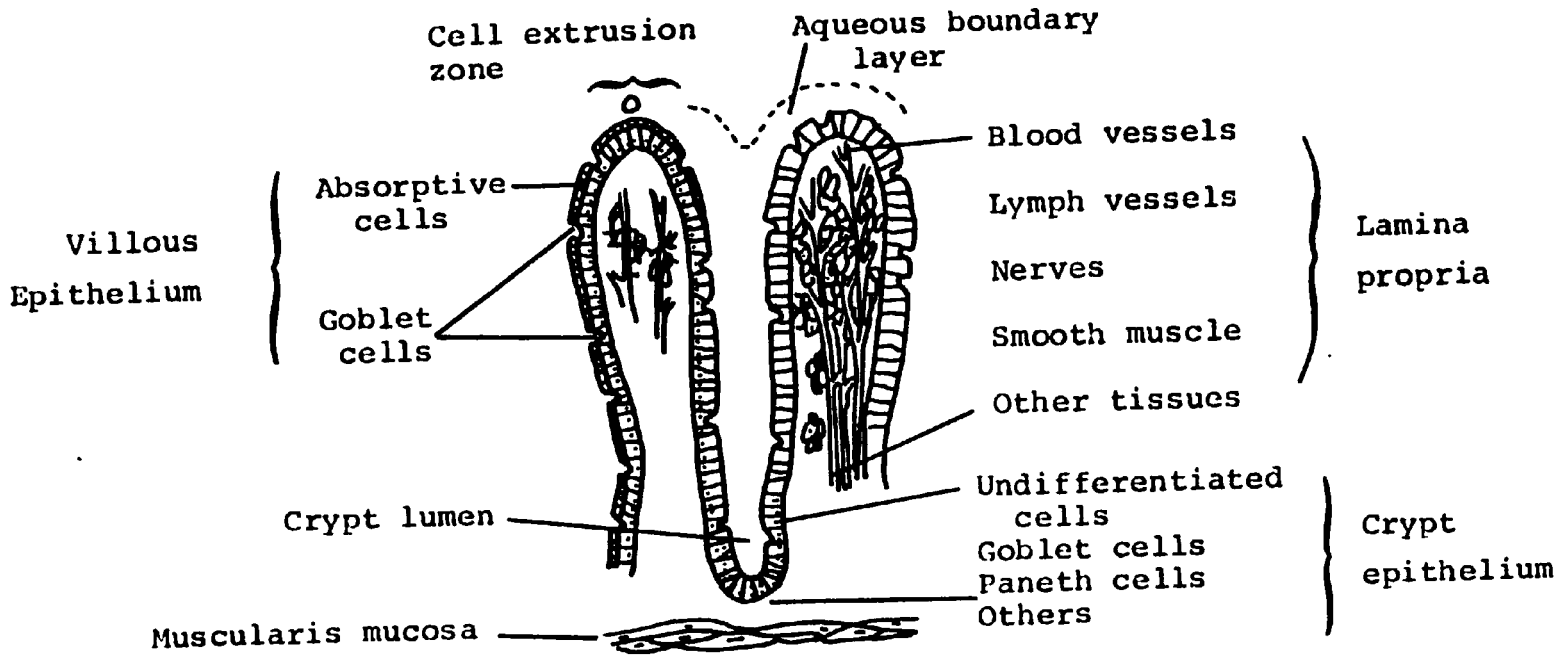


Figure 1. Schematic diagram of two sectioned villi and a crypt to illustrate the histologic organization of the small intestinal mucosa.

secreting) are dispersed throughout the surface. Undifferentiated, Paneth and endocrine cells are located in the crypts of the villi. The epithelium undergoes continuous surface renewal. Cell multiplication occurs in the crypts and as the undifferentiated cells migrate toward the villous tip they differentiate into specific cell types.

Absorption cells (commonly called columnar enterocytes or brush border cells) are the predominant type of cells and most important from the point of view of absorption (Figure 2). It is noteworthy that the composite barrier separating the drug in the lumen from the blood supply is this single layer of cells. In man the cells are 20-30 microns in height and 8-10 microns in width. The mucosal surface of this cell is characterized by the presence of microvilli (the brush border, about 1.0 micron in height and 0.1-0.2 in width). The microvillous membrane is a trilaminar structure (70-90°A thick) composed of proteins, neutral lipids, phospholipids and glycolipids. An important structure, which is regarded to be an integral part of the plasma membrane, is the glycocalyx (or fuzzy coat). It is composed of very fine filaments, glycoprotein in nature, radiating about 0.1-0.5 microns into the lumen. The plasma membrane plays important roles in maintaining the internal environment of the cell different from the external environment and in possessing specialized permeability and transport properties. The epithelial cells rest on the basement membrane, a protein-polysaccaride

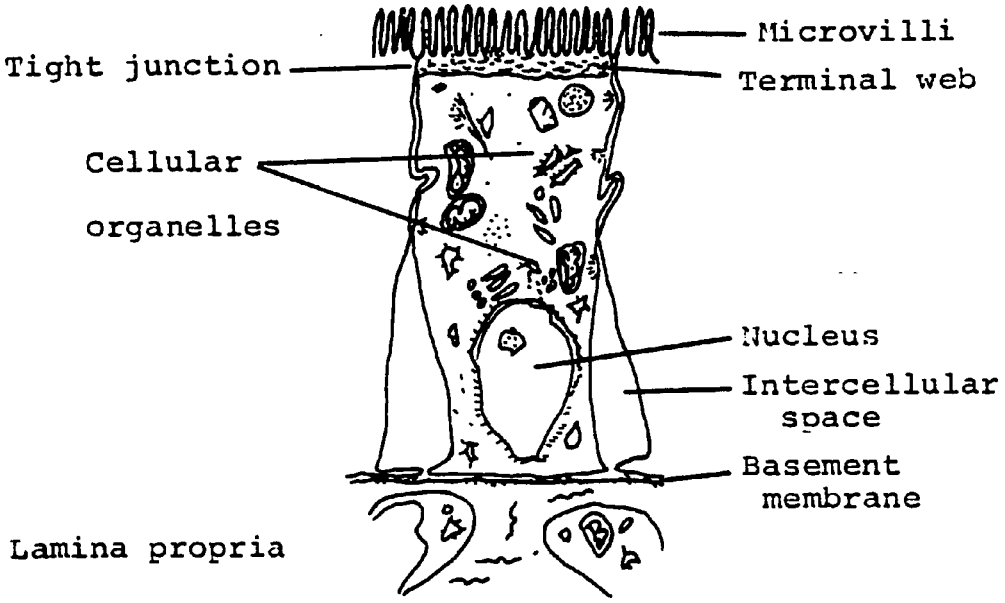


Figure 2. Schematic diagram of an intestinal absorptive cell.[4]

structure about 300°A thick, below which is a rich blood capillary network. Adjacent cells are connected by a junctional complex. The apical junction is called the tight junction which has an intercellular space of 200°A over a distance of 0.3-0.5 microns.

3. The Aqueous Boundary (Diffusion) Layer: Figure 1 depicts an aqueous boundary layer (often referred to as the stagnant, unstirred, or aqueous diffusion layer) which is an important hydrodynamic barrier that the drug must traverse before arriving at the surface of the mucosal membrane. In reality, the liquid in the layer is not static as the term "unstirred" implies but represents a film at the surface where diffusive and natural convective mixing are more important than forced convective mixing. Due to the agitated flow of fluid along the intestinal tract and intrinsic villous motility, drug transport in this hydrodynamic boundary layer thus occurs by natural convection and diffusion. Although the villi increase the surface area eight-fold and the microvilli by another factor of 30-40, the effective surface area for absorption has proven to be less than the theoretical anatomical area of the membrane.[5] This is due to a combination of reasons, i.e., the prevalent distribution of specialized absorption cells about the tips of the villi and the tendency of the aqueous boundary layer to contour about the apical region of the densely populated villi. The effective thickness of the aqueous layer is thinner about the tips and thicker and less stirred in the valleys of the villi. The exist-

ence of the aqueous boundary layer is physically sound and experimentally demonstrable.[6,7]

The contractile activity of the small intestines is thought to serve three functions: (a) mixing of ingested substance with secretions, (b) mixing of intestinal contents with the intestinal mucosa, and (c) peristaltic propulsion of the contents along the tract.

4. Luminal and Membrane Drug Metabolism: In meaningful studies on drug absorption, it is prerequisite to recognize and distinguish between cavital, membrane contact and intracellular drug metabolism.[8,9] Cavital metabolism takes place in the intestinal lumen with a variety of enzyme systems secreted by the pancreas and intestinal cells. In a broad sense drug metabolism by the intestinal bacterial flora may be included here. Membrane contact metabolism is carried out by enzymes localized on the surface of the membrane and is generally characterized spacially as intermediate between extra- and intracellular metabolism. Enzyme systems usually associated with the membrane surface include the carbohydrases, peptidases, lipases, hydrolyases and isoenzymes of alkaline phosphatase. Various enzymes such as the non-specific esterase, phosphatase, dehydrogenase, oxidase, and glucuronidase are found with different organelles in the cell.

5. Intestinal Blood Flow: The mechanistic relationship between intestinal blood flow and absorption, secre-

tion and metabolic activity of the intestinal mucosa is unclear.[10] However, there is evidence that impaired flow rates slow down absorption.[11,13] It has been postulated that reduced blood flow reduces the absorption rate by (a) decreasing the effective concentration gradient across the epithelial layer for passively absorbed solutes by not rapidly carrying the solute away, (b) lowering oxygen supply to the absorption cells needed to maintain the active transport mechanism, and (c) affecting metabolic changes attending the integrity of the membrane.[12]

B. Transport Across the Aqueous Boundary Layer.

The concept of the unstirred aqueous layer was originally developed by Noyes and Whitney[14] and Nernst[15] in their studies of heterogeneous reactions. According to the theory of Nernst, there is thin layer of static liquid immediately adjacent to the surface of a solid body immersed in fluid. Within this layer there is a concentration gradient. Later, Levich[16] placed the aqueous boundary layer on a physically sound basis in terms of convective and pure diffusive components.

Many investigators,[17-20] working with isolated tissues and biological membranes bathed in an electrolyte solution, have found the stagnant water layer to be important. Often it becomes the rate-limiting transport factor. Wilson et al.[21,22] recognized the relevance of the stagnant water layer in their initial absorption

rate studies with everted rat jejunum. They pointed out that the passive transport of fatty acids (n-heptanoic to n-nonanoic acids) from dilute solutions did not exhibit the aqueous diffusion layer-dependence at high stirring conditions in contrast to micellar solutions of fatty acids (myristic to stearic acids). Later, they demonstrated that the uptake of short chain fatty acid monomers was rate-limited by the lipid cell membrane but became increasingly rate-limited by the diffusion layer with increasing chain length.[23,24]

Wilson and Dietschy[5] and Winne[25] studied the effect of the aqueous diffusion layer on carrier-mediated transport processes and found that the Michaelis constant K_M of a carrier-mediated transport system in a membrane was overestimated when an aqueous diffusion layer is ignored. They also concluded that the apparent differences between Michaelis constants obtained from *in vitro* and *in vivo* absorption experiments can be explained partly by differences in the thickness of the diffusion layer between the two kinds of experiments.

Lewis and Fordtran[26] investigated the effect of perfusion rate on absorption, surface area, unstirred water layer thickness, permeability, and intralumenal pressure in the rat ileum *in vivo*. They pointed out that high flow rates increase the intralumenal pressure and, thereby, cause an increase in surface area and passive permeability

of the aqueous channels. This concern of the effect of intralumenal pressure tended to add confusion to the interpretation of increased absorption rates due only to the thinning of the aqueous diffusion layer with increasing flow rates.

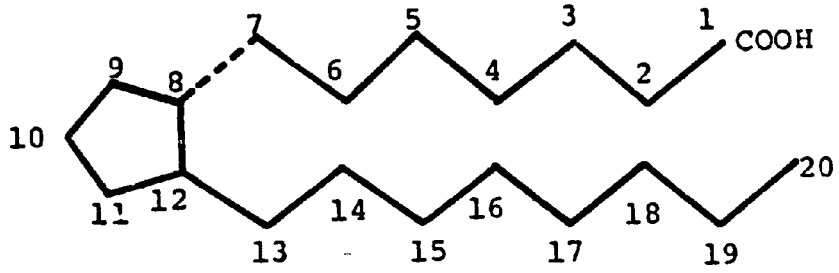
Recently, Desai[7] carried out unique baseline experiments with the n-alkanol homologs to study the influence of the aqueous diffusion layer upon intestinal absorption. He used a modified Doluisio technique to provide good control of the degree of stirring of the solution in the lumen of the rat intestinal tract. At high agitation, the absorption rates for n-butanol and higher homologs were faster than observed with mild agitation. Depending upon the hydrodynamic conditions employed, the effective aqueous diffusion layer thickness ranged from 270 to 850 microns.

C. Prostaglandins.

Prostaglandins are hormone-like substances found in the body tissues and fluids. They affect a wide range of physiological processes from the contraction of the uterus to secretion from the stomach wall. For some 30 years after the original discovery of the prostaglandins in the early 1930's, little was known about their chemistry and specific physical properties. One of the reasons is that the body produces these substances in minute quantities. However, the literature has recently grown exponentionally.

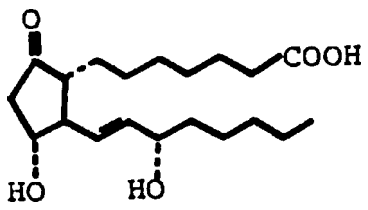
The prostaglandins are of considerable biological

interest and have been the subject of several excellent general reviews.[27-35] They are analogs of prostanoic acid, a 20 carbon fatty acid.



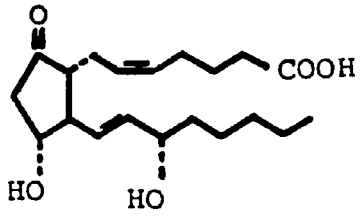
Prostanoic Acid

Some of the naturally occurring prostaglandins are prostaglandin E_1, E_2, $F_{1\alpha}$ and $F_{2\alpha}$ as shown below.



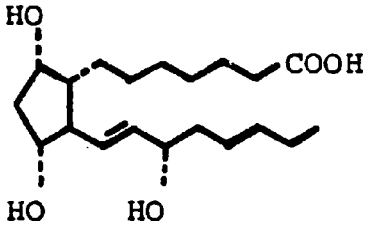
Prostaglandin E_1

(PGE_1)



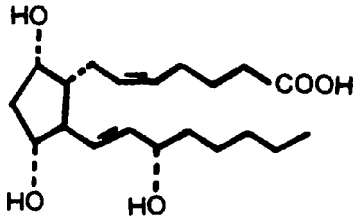
Prostaglandin E_2

(PGE_2)



Prostaglandin $F_{1\alpha}$

($PGF_{1\alpha}$)



Prostaglandin $E_{2\alpha}$

($PGF_{2\alpha}$)

The E series differ from the F series by a keto group at C_9. The subscripts 1 and 2 denote carbon-carbon double bonds. The subscript, α, refers to the orientation of the hydroxy group at C_9.

The following literature review on the prostaglandins will be restricted to prostaglandin, $F_{2\alpha}$, E_1 and E_2 and to such topics as physiological effects, membrane transport, metabolism and physicochemical properties which are deemed pertinent to this thesis.

1. Gastrointestinal Tract: Prostaglandins $F_{2\alpha}$, E_1 and E_2 are found in gut tissue and effect the smooth muscle in small concentrations. The human and animal longitudinal muscles of the small and large intestine are contracted by the three aforementioned prostaglandins,[36,37] while the circular muscle is relaxed by the PGE_1 and PGE_2 and contracted by the $PGF_{2\alpha}$.[38] The presence of prostaglandins in the gastrointestinal tract and their effect on the gastrointestinal strips *in vitro* have led to studies on the action of prostaglandins on gastric secretion. Robert *et al.*[39] showed that intravenous administration of PGE_1 and PGE_2 inhibited gastric secretion in the dog which was previously stimulated by either food or histamine. $PGF_{2\alpha}$ was ineffective against histamine-induced gastric secretion. There is some evidence that the inhibitory action of PGE_1 on gastric secretion may be due to inhibition of adenyl cyclase.[40] However, since gastric blood flow is affected by prostaglandins infused intravenously, the possibility

that diminution in secretory response is secondary to reduced blood flow must also be considered.[41] Jacobson[42] measured the ratio of blood flow to secretion rate in conscious dogs and concluded that the inhibition of gastric secretion following PGE_1 administration is not secondary to vascular changes.

Karim and Filshie[43] observed that the intravenous administration of $PGF_{2\alpha}$ in humans produces diarrhea. Prostaglandins cause increased contractility of small bowel smooth muscles and it has been suggested that they cause diarrhea by increasing small bowel mobility and decreasing intestinal transit time.[44] Pierce et al.[45] reported that infusions of $PGF_{2\alpha}$ induce net secretion of water and electrolyte from the jejunum in the dog. The stimulation of jejunum secretion of water and electrolytes by $PGF_{2\alpha}$ indicates that this process might be mediated by an effect upon the intracellular level of cAMP.

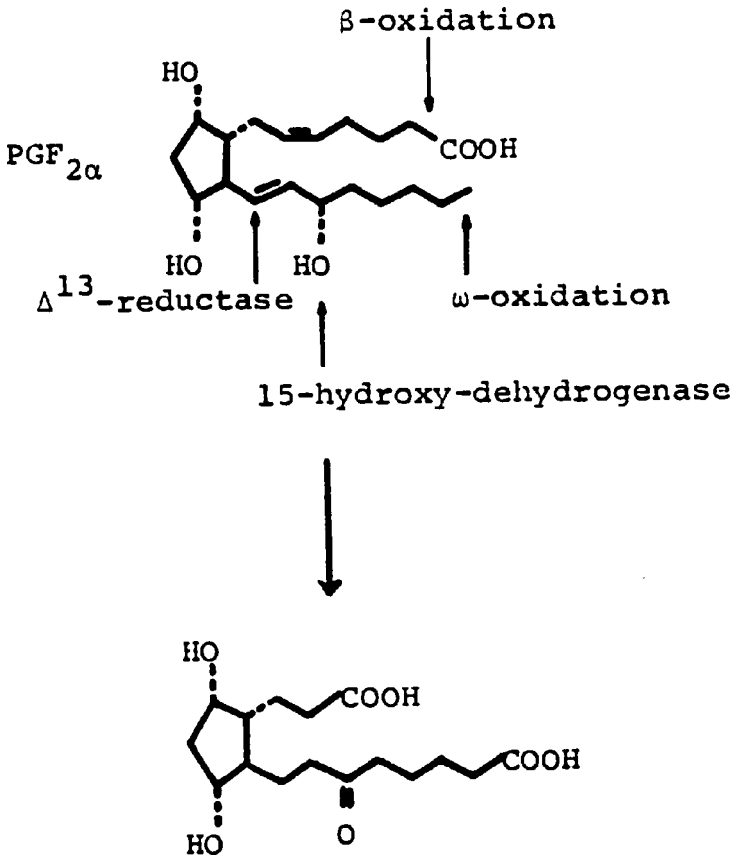
2. Intestinal Absorption: The amount of literature on the intestinal absorption of the prostaglandins is sparse. Parkinson and co-workers[46] studied the oral absorption of PGE_1 in rats by lymphatic and bile duct fistula. About 58 percent of the dose administered orally was excreted as expired CO_2 collected in metabolic cages after 24 hours and an additional 0.5-5 percent was found in the thoracic duct lymph. They indicated that the intestine may be the primary site of oxidation of orally administered PGE_1. This hypothesis was later supported

with studies[47] using jejunum segments *in vitro*. Magee and co-workers[48] followed the *in situ* absorption of prostaglandins (PGE_1, $PGF_{2\alpha}$, 15(s)-methyl $PGF_{2\alpha}$ and 15(s)-methyl $PGF_{2\alpha}$ methyl ester) in the small intestines and vagina of the rat. They observed that PGE_1 disappeared from the lumen with a half-life of 37 minutes. The half-lives were 60-70 minutes for $PGF_{2\alpha}$ and 15-methyl $PGF_{2\alpha}$, respectively. They also recovered 2-3 percent of PGE_1, 2 percent $PGF_{2\alpha}$ and 0.8 percent 15-methyl $PGF_{2\alpha}$ in the blood. The disappearance of 15-methyl $PGF_{2\alpha}$ methyl ester was very rapid initially and followed by a second much slower rate of absorption. These results correlated with the rapid rate of hydrolysis of the methyl ester in the lumen of the intestine which was slower at higher doses. Robert *et al.*[49] studied the intestinal absorption of $PGF_{2\alpha}$ in the dog and found that 8 to 19 percent of initial radioactivity accumulated in the blood in 60 min after the introduction of $PGF_{2\alpha}$ in the intestinal lumen. Extensive metabolism occurred in the mucosal membrane.

Rogers[50] provided a rather in-depth analysis of the rat intestinal absorption of $PGF_{2\alpha}$, PGE_1 and PGE_2. He quantitatively assessed the separate contribution of the chemical substituent differences among these prostaglandins to passive diffusion and enzyme kinetics in explaining the differences in the absorption rates.

3. Metabolism: In general, the major metabolic pathways of prostaglandins are (a) oxidation of 15-hydroxy

group to the keto form by 15-hydroxy prostaglandin dehydrogenase with diphosphopyridine nucleotide (DPNH) being the co-factor, (b) reduction of the C_{13} double bond by Δ^{13}-reductase, (c) stepwise β-oxidation of the carbonyl side chain and (d) ω-oxidation of the lower hydrocarbon chain.[51-56] Enzymatic activity of Δ^{13}-reductase is sequential to the enzymatic attack by dehydrogenase.



5α, 7α-dihydroxy-11-ketotetra-norprosta-1,16-dioic acid

Prostaglandin dehydrogenase and Δ^{13}-reductase are found in tissues of the lung, spleen, kidney, stomach, testicle and small intestines in the swine.[55] Samuelson et al.[55] also found that β-oxidation occurred in lung tissue and kidney in rat and ω-oxidation in human seminal plasma. The sequence of β-oxidation and ω-oxidation processes is not known.[57] Pace-Asciak and co-workers[58] showed that rat gut homogenates convert $PGF_{1\alpha}$ to 15-keto- 13,14-dihydro $PGF_{1\alpha}$. Nekano and Prancan[59] noted that a little metabolism occurred in rat plasma. Magee and co-workers showed that dehydrogenase activity was readily detected in intestinal washes and 15-methyl $PGF_{2\alpha}$ was taken up almost quantitatively by the liver and metabolized to polar acids which reentered the circulation and also were excreted into the bile. 15-Epi-$PGF_{2\alpha}$ and 15-methyl $PGF_{2\alpha}$ are not subject to enzymatic attack by dehydrogenase.[48,60]

Biological degradation of prostaglandin $F_{2\alpha}$ has been extensively investigated in rat,[48,51,61] swine,[52] monkey,[62] rabbit,[63] guinea pig[64,65] and human subjects.[53,66,67] The metabolic patterns of the animal species are similar but not identical to that of human subjects.

Paulsrud et al.[68] showed the inhibition of dehydrogenase with several diuretic drugs (furosemide, and ethacrynic acid). Bito[69] reported that PGE_1 and $PGF_{2\alpha}$ are accumulated against a concentration gradient when anterior uvea, choriod plexus, rabbit vaginal tissues or kidney cortex slices are incubated in a medium containing pros-

taglandin. This active accumulation is prevented by indomethacin, an inhibitor of prostaglandin synthesis. Fried and co-workers[70] found that rac-prostanoic acid and racemic-7,13-prostanoic acid are the most potent inhibitors of human placental prostaglandin 15-OH dehydrogenase. Salicylic acid is a weak inhibitor of dehydrogenase.[50]

4. Physical Properties and Stability: The aqueous solubility of $PGF_{2\alpha}$ (free acid) is 1.5 mg/ml and its pK_a is 4.90. The tromethamine salt of $PGF_{2\alpha}$ is readily soluble (200 mg/ml) in distilled water[71] and is stable for at least one year at room temperature in the crystalline state. Aqueous solutions of 5 mg/ml $PGF_{2\alpha}$ tromethamine are stable for at least three months at room temperature in the pH range of 7-9. Chemical kinetic data show that the degradation of $PGF_{2\alpha}$ is acid-catalyzed,[72] particularly below pH 3.0. Karim et al.[73] reported that $PGF_{2\alpha}$ in 0.9 percent saline solution at pH 5-11 showed no loss in activity after 6 months at room temperature. $PGF_{2\alpha}$ retained its original activity after one hour at 240°F and 10 psi.

STATEMENT OF THE PROBLEM

We believe that the physical model approach is essential to the meaningful study of a problem so complex as drug absorption in the gastrointestinal tract. Through a systematic theoretical and experimental investigation, it is planned to obtain a quantitative mechanistic interpretation of the factors involved in the intestinal absorption of the drugs. This will be accomplished through the use of baseline experiments involving *in situ* rat intestinal absorption technique of Doluisio and the subsequent assessment of the data by an appropriate physical model.

This thesis is divided into two principal parts. The first part is concerned with the passive transport of model nonelectrolytes and weak electrolytes such as the steroids, *n*-alkanoic acids and selected *n*-alkanols. These studies are aimed at the general understanding of the interplay of hydrodynamics, passive transport mechanism of the membrane, pH and pK_a (as the case may be) leading to the quantitative factorization of the permeability coefficients of the aqueous boundary layer, the lipoidal and aqueous pore pathways of the membrane.

The second major effort is involved with the simultaneous passive transport and membrane metabolism of drugs, as exemplified by the prostaglandins. The specific aims are the development of experimental methodology and physical model assessment of the data leading to quantitative understanding of:

1. The role of the aqueous boundary layer as a barrier to transport.
2. The transport of the prostaglandin across the passive diffusional-metabolic pathway of the membrane.
3. The transport of the prostaglandin across the aqueous pores of the membrane.
4. The relationship of pH on the transport rates.
5. The effect of molecular modification of a reference prostaglandin on the total membrane transport kinetics as well as on the passive transport and enzyme kinetic components.

Concurrently, the physical model and accompanying mathematical description will be developed.

EXPERIMENTAL

A. Material and Apparatus.

The following ^{14}C-labeled compounds[a,b] were used without further purification: (a) the n-alkanol series including n-butanol, n-hexanol, n-heptanol, n-octanol and n-decanol; (b) the n-alkanoic acid series including n-butyric acid, n-hexanoic acid, n-octanoic acid and n-decanoic acid; (c) salicylic and benzoic acids; and (d) polyethylene glycol 4000 (PEG 4000).

The following ^{3}H-labeled compounds were also used without further purification: steroid compounds[a] including hydrocortisone and prednisolone; prostaglandins $F_{2\alpha}$ ($PGF_{2\alpha}$)[a]; and other prostaglandins[c] such as 15-epi-$PGF_{2\alpha}$, $PGF_{2\alpha}$ C_1-carbamoylmethylamide, $PGF_{2\alpha}$ C_1-amide, $PGF_{2\alpha}$ C_1-ethylamide, $PGF_{2\alpha}$ C_1-n-propylamide, $PGF_{2\alpha}$ C_1-n-butylamide and $PGF_{2\alpha}$ C_1-n-hexylamide. Approximately 5 μCi of radiolabeled compound was used for each experiment.

Prostaglandin $F_{2\alpha}$ as the tromethamine salt, 15-keto-$PGF_{2\alpha}$, 15-keto-13,14-dihydro-$PGF_{2\alpha}$, indomethacin, iodoacetic acid, furosemide and reagent grade chemicals were used without further purification.[c]

---

[a] New England Nuclear Corporation, Boston, Massachusetts.

[b] International Chemical and Nuclear Corporation, Irvine, California.

[c] The Upjohn Co., Kalamazoo, Michigan.

The isotonic buffer solutions are listed in Table I.

Table I. Standard Isotonic Buffer Solutions

pH 3.5	pH 4.5	pH 6.0
Citric acid·H_2O 14.75 gm	Citric acid·H_2O 11.03 gm	KH_2PO_4 anhyd. 9.07 gm
K_2HPO_4 anhyd. 10.38 gm	K_2HPO_4 anhyd. 16.53 gm	K_2SO_4 11.93 gm
K_2SO_4 7.0 gm	K_2SO_4 2.63 gm	Dist. H_2O qs. 1 liter
Distilled H_2O qs.	Distilled H_2O qs.	Adjust with 1N NaOH

pH 7.5	pH 9.5
KH_2PO_4 9.07 gm	Boric acid 10.33 gm
K_2SO_4 11.93 gm	K_2SO_4 9.13 gm
Distilled H_2O qs. 1 liter	Distilled H_2O qs. 1 liter Adjust with 1N NaOH

Reagent grade chemicals were used without further purification. All solutions were adjusted to 300-310 mosm/Kg with K_2SO_4. For buffer solutions less than the buffer capacities of the standard preparations, the concentration of buffer reagents were reduced proportionally and adjusted to isoosmotic conditions with K_2SO_4.

All solutions were adjusted to 300-310 mosm/Kg with potassium sulfate. For buffer solutions less than the buffer capacities of the standard preparations, the concentration of buffer reagents were reduced proportionally and adjusted to isotonic condition with potassium sulfate. Stock solutions of radiolabeled solutes in the aqueous buffer used in the intestinal absorption studies were of such concen-

trations that a 20 µl sample in 10 ml of scintillation cocktail (naphthalene 100 gms, 2,5-diphenyloxazole 6.0 gms in one liter of p-dioxane) gave approximately 2 x 10^3 cpm.

The instruments employed were Beckman liquid scintillation counter (Model LS-200), Beckman research pH meter (Model 1019), osmometer (Model 68-31 LAS),[a] centrifuge (Model ss-3 automatic)[b] and FMI pump (Model RRP-G-150).[c]

B. In Situ Rat Intestinal Absorption Procedures.

The well-known in situ rate intestinal absorption method of Doluisio[74] was basically employed with male Sprague-Dawley albino rats, 220-275 Gms and fasted for 15-20 hours. Water was given during the fasting period. However, certain modifications in the method were introduced to control the hydrodynamics of the system.

The rats were anesthetized approximately one hour before surgery with ethylcarbamate 20 percent solution using an intraperitoneal injection dose of 1 mg/gm body weight. After a midline abdominal incision was made, the small intestine was taken out with careful handling to maintain an intact blood supply. Twenty-two cm jejunal segment was cannulated with L-shaped glass cannula (inside diameter of 2.5 mm and outside diameter of 3.5 mm) and

---

[a] Advanced Instruments, Inc., Newton Highlands, Mass.
[b] Ivan Sorvall, Inc., Norwalk, Connecticut.
[c] Fluid Metering, Inc., Oyster Bay, New York.

connected to a 5 ml plastic disposable hypodermic syringe barrel and a two-directional FMI pump as shown in Figure 3. The jejunal segment was washed with a sterile normal saline perfusion solution until the perfusate was visually clear. The last wash consisted of the particular isotonic buffer solution preparation intended for the ensuing experiment.

Exactly 2 ml of the radiolabeled solute in isotonic buffer solution was introduced into the lumen of the jejunum. With the aid of the FMI pump, 0.5 ml of solution was pushed up the barrel of one syringe at the rate of 0.075 ml/sec and, likewise, up the other syringe and finally up the first syringe whereupon a 20 µl sample was withdrawn with an automatic pipette[a] for assay. This first sample is regarded to be the zero time sample, which is 30-35 seconds after the initial introduction of the 2 ml drug solution into the intestinal lumen. The initial procedure of oscillating the lumenal solution is to obtain a uniform mixing of the 2 ml drug solution with the residual solution in the gut lumen from the final wash. The apparent surface area to volume ratio is 11.2. All absorption experiments were carried out at 37°C.

In those experiments involving the static hydrodynamic conditions, the drug solution remains in the lumen until at regular, predetermined sampling time intervals

---

[a] Eppendorf Microliter pipet, Brinkmann Instruments, Inc., Westbury, N.Y. 11590.

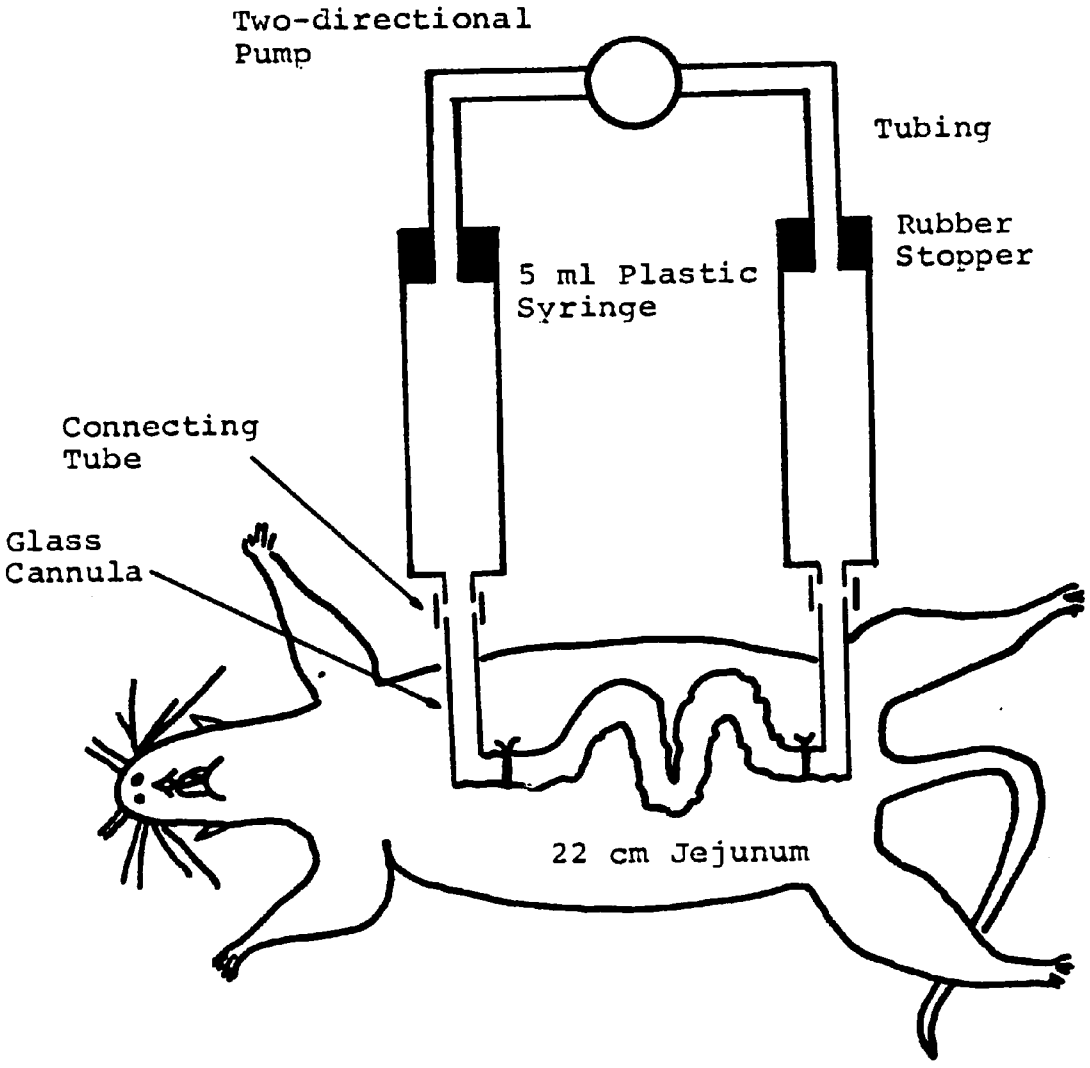


Figure 3. Modified Doluisio system for <u>in situ</u> rat intestinal absorption studies.

(150, 300, etc. second intervals), 0.5 ml of the lumenal solution is pushed up into the barrel of the syringe with the FMI pump at 0.075 ml per sec and a 20 µl sample is withdrawn. Then the solution is pumped back into the lumen and remains there until the next regular sampling interval. This sampling procedure takes no more than 10 seconds and at least 75 percent of the solution volume always remains in the lumen.

From a physicochemical point of view, the regularity of the sampling time interval under these "static" experimental conditions are important in maintaining some degree of constancy in the hydrodynamics of the solution in the gut lumen, particularly, when the transport rate is relatively determined by the permeability of the unstirred aqueous layer. It can be said that this "static" hydrodynamic situation, which is very similar to the original Doluisio method, provides a kind of discontinuous or non-uniform hydrodynamic pattern. When the solution remains in the lumen until it is time to take a sample, the permeability and thickness of the unstirred layer are smaller and thicker, respectively, as compared to the larger permeability coefficient and thinner layer when the 0.5 ml drug solution is pumped up the barrel of the syringe, a 20 µl sample taken and then the solution returned into the lumen until the next sampling interval. Consequently, the average hydrodynamics of the system will depend upon the sampling intervals taken. The shorter the sampling inter-

vals, the higher the average permeability coefficient and the thinner the average thickness of the unstirred layer.

Absorption experiments were also carried out in which there was a continuous oscillation of the solution in the lumen. This was accomplished by pushing 0.5 ml of solution up the barrel of one syringe with the FMI pump and then reversing it back into the other syringe to complete one oscillating cycle at a constant flow rate. At all times, at least 75 percent of the drug solution remained in the lumenal segment. Usually, a flow rate of 0.075 ml per sec was used; however, other flow rates can also be utilized. Each oscillating cycle takes 20 seconds. Because of the continuous hydrodynamic conditions provided by this procedure, 20 µl samples could be withdrawn at any convenient time.

C. Non-steady State Disappearance of Drugs.

Some preliminary experiments were conducted to evaluate the decrease in the concentration of prednisolone, n-butanol and salicylic acid at pH 6.0 according to the procedure used in the first 30 seconds, the period of time between the initial introduction of exactly 2 ml drug solution into the intestinal lumen and the experimental zero time sample. This 30-second period should reflect the non-steady-state disappearance of the drug and also the mixing and dilution of the 2 ml drug solution with the volume of residual solution in the lumen of the jejunum

(22 cm length) from the final wash with isotonic pH 6.0 phosphate buffer. Using C^{14}-polyethylene glycol 4000 in the phosphate buffer, a non-absorbable solute in the intestine, the average volume of residual solution is 0.42 ± 0.03 ml from five separate determinations. Table II indicates that the decrease in the drug concentration 30 seconds after the introduction of the drug solution into the empty lumen is largely due to dilution with the residual perfusion solutions (about 98 percent) and to a much less extent (a few percent) to nonsteady-state-absorption.

D. Thin Layer Chromatography of Prostaglandins.

Thin layer chromatography was carried out with silica gel F-250 precoated plates.[a] This plate was developed in solvent system AIX (ethyl acetate-acetic acid-isooctane-water, 90:20:50:100 by volume).[75] The $PGF_{2\alpha}$ and metabolites were readily observed by spraying with 15 percent ammonium sulfate solution. Zones of radioactivity were quantified by 0.5 cm scrapings in Aquasol.[b] Using this TLC system, no impurities in the original ^{3}H-$PGF_{2\alpha}$ solutions were detected.

During the course of the in situ intestinal absorption

---

[a] Analtech, Inc., 75 Blue Hen Drive, Newark, Delaware.
[b] New England Nuclear, Boston, Mass. 02118.

Table II. Nonsteady-State Disappearance of Various Solutes at pH 6.0 in the Initial 30 Seconds in the Rat Jejunum before the Experimental Zero Time Sampling.

Drug Concentration	Prednisolone		n-Butanol		Salicylic Acid	
cpm in original 2 ml solution	3564	2463	1653	874	455	454
cpm in lumenal solution accounting for mixing with residual perfusion wash solution in lumen at zero time*	2950	2040	1365	719	376	375
cpm in lumenal solution after 30 sec	2885	1975	1340	704	374	369
cpm of solute absorbed in 30 sec	65	65	25	15	2	6
Percent decrease in drug conc. in lumen after 30 sec due to absorption	2.2%	3.2%	1.8%	2.0%	0.4%	1.6%

*Using C^{14}-PEG 4000 as a nonabsorbable indicator, the volume of the residual perfusion solution is found to be 0.4 ml with 2.0 ml of initial solution, the dilution factor is 1.21.

of radiolabeled $PGF_{2\alpha}$, samples from the lumenal solution, blood and small intestines were taken and treated for TLC. One-tenth ml of lumenal solution or blood was extracted 2 to 3 times with 2 ml ethyl acetate, concentrated by evaporation with a stream of nitrogen and then spotted. One cm intestinal segment, previously washed with normal saline, was excised, homogenized in the cold and then extracted 3 times with 2 ml ethyl acetate, concentrated with the aid of a nitrogen stream and spotted.

CHAPTER I: PASSIVE TRANSPORT OF DRUGS

A. Theoretical Considerations.

1. General Description of the Physical Model: The physical model for the passive absorption of a drug in the rat small intestine is shown in Figure 4. It consists of an aqueous boundary layer (unstirred water layer) in series with a membrane compartment of parallel lipoidal and aqueous pore pathways and then a blood sink.

Let the model solute be a weak acid. Using the principles of thermodynamics and laws of interphase diffusional mass transfer, one can show that the rate of disappearance of a drug from the intestinal lumen and the appearance in the blood is given by

$$\frac{dC_b}{dt} = - \frac{A}{V} P_{app} (C_b - C_{blood}) \qquad \text{(Eq. 1)}$$

When there is no accumulation of drug on the blood side, i.e., sink conditions,

$$\frac{dC_b}{dt} = - K_u C_b \qquad \text{(Eq. 2)}$$

Here,

C_b = total drug concentration in intestinal lumen

A/V = geometrical surface area to volume ratio in the intestinal segment

P_{app} = apparent permeability coefficient

$K_u = A P_{app}/V$, the apparent first order absorption

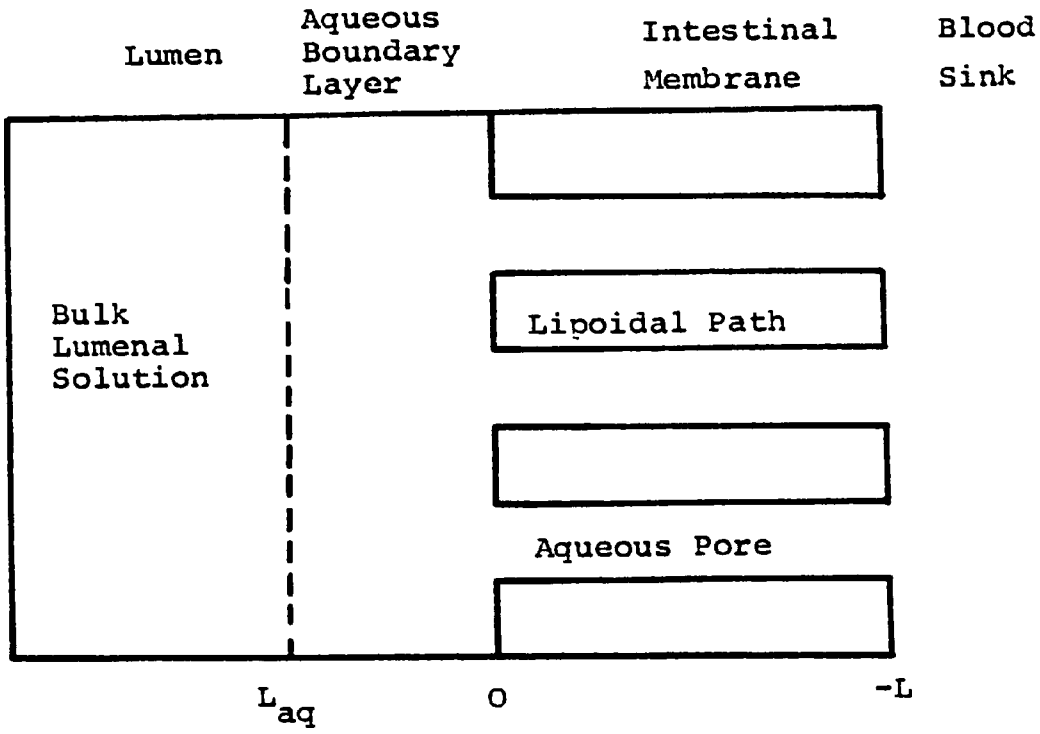


Figure 4. Schematic diagram of the physical model for the passive transport of solutes across the intestinal membrane. The bulk aqueous solution with an aqueous diffusion layer on the mucosal side is followed by a heterogeneous membrane consisting of lipoidal and aqueous channel pathways and thereafter by a sink on the serosal side.

rate constant.

The apparent first order rate constant, K_u, is

$$K_u = \frac{A}{V} \cdot \frac{1}{\frac{1}{P_{aq}} + \frac{1}{(P_o + P_p) X_s + P_p^- (1 - X_s)}} \qquad \text{(Eq. 3)}$$

or, upon rearrangement,

$$K_u = \frac{A}{V} \cdot \frac{P_{aq}}{1 + \frac{P_{aq}}{(P_o + P_p) X_s + P_p^- (1 - X_s)}} \qquad \text{(Eq. 4)}$$

where,

P_{aq} = permeability coefficient of the aqueous boundary layer for all drug species

P_o = permeability coefficient of the lipoidal pathway of the membrane for the nondissociated species

P_p, P_p^- = permeability coefficients of the aqueous pore pathway of membrane for the nondissociated and anionic species.

The fraction of nondissociated drug species, X_s, at the membrane surface on the aqueous boundary layer side is

$$X_s = \frac{1}{1 + K_a/(H^+)_s} \qquad \text{(Eq. 5)}$$

where,

K_a = dissociation constant of the weak acid drug

$(H^+)_s$ = hydrogen ion concentration at the membrane

surface.

2. Some Special Cases of the General Model: When the permeability coefficients of the nondissociated and anionic species across the aqueous pores are taken to be equal,[76] Eq. 4 reduces to

$$K_u = \frac{A}{V} \cdot \frac{P_{aq}}{1 + \frac{P_{aq}}{P_o X_s + P_p}} \qquad \text{(Eq. 6)}$$

While Eq. 4 is appropriate for weak electrolytes sufficiently small in size so that the aqueous pore pathways are accessible, in the general case of nonelectrolytes where the dissociation constant is zero, the rate constant is

$$K_u = \frac{A}{V} \cdot \frac{P_{aq}}{1 + \frac{P_{aq}}{P_o + P_p}} \qquad \text{(Eq. 7)}$$

For bulky nonelectrolytes such as the steroids, the aqueous pore route should be insignificant; thus,

$$K_u = \frac{A}{V} \cdot \frac{P_{aq}}{1 + \frac{P_{aq}}{P_o}} \qquad \text{(Eq. 8)}$$

3. Determination of the Permeability Coefficients: In Eqs. 6, 7 and 8 it is noted that as the effective per-

meability of the membrane is much greater than the permeability of the aqueous boundary layer, the ratio of the coefficients will be much less than unity. Consequently, this means that the maximum rate constant or apparent permeability coefficient will be determined by the diffusional rate of the drug across the aqueous boundary layer. In other words,

$$K_{u',max} = \frac{A}{V} \cdot P_{aq} \qquad \text{(Eq. 9)}$$

or

$$\frac{K_{u,max}}{A/V} = P_{app,max} \simeq P_{aq} \qquad \text{(Eq. 10)}$$

In practice, the factorization of the permeability coefficients of the aqueous diffusion layer, P_{aq}, can be readily accomplished by utilizing such homologous series as the n-alkanols and n-alkanoic acids. In turn, the effective thickness of the aqueous diffusion layer can be defined by

$$L_{aq} = \frac{D_{aq}}{P_{aq}} = \frac{A}{V} \cdot \frac{D_{aq}}{K_{u,max}} \qquad \text{(Eq. 11)}$$

where L_{aq} = effective thickness of the aqueous boundary layer

D_{aq} = aqueous diffusion coefficient.

The permeability of the aqueous pores of the membrane is estimated in the following manner. When the fraction of nondissociated species at the membrane surface is zero

(for example, $pH >> pK_a$ for a weak acid), Eq. 3 reduces to

$$K_u = \frac{A}{V} \cdot \frac{1}{\frac{1}{P_{aq}} + \frac{1}{P_p^-}} \qquad \text{(Eq. 12)}$$

and, upon rearrangement, the permeability coefficient of the aqueous pore for charged species is

$$P_p^- = \frac{1}{\frac{A}{V K_u} - \frac{1}{P_{aq}}} \qquad \text{(Eq. 13)}$$

But, in case of nonelectrolytes, the permeability coefficient of the aqueous pore can be gotten upon rearrangement of Eq. 7. Thus, the permeability coefficient of the aqueous pore is

$$P_p = \frac{1}{\frac{A}{V K_u} - \frac{1}{P_{aq}}} - P_o \qquad \text{(Eq. 14)}$$

The permeability coefficient of the lipoidal pathway of the membrane for a nonelectrolyte can be determined by rearrangement of Eq. 14.

$$P_o = \frac{1}{\frac{A}{V K_u} - \frac{1}{P_{aq}}} - P_p \qquad \text{(Eq. 15)}$$

For bulky molecules, such as the steroids, P_p approach zero and the permeability coefficient of lipoidal pathway is

$$P_o = \frac{1}{\frac{A}{V K_u} - \frac{1}{P_{aq}}} \qquad \text{(Eq. 16)}$$

In a homologous series such as the n-alkanols and n-alkanoic acids, the increase in the partition coefficient of one member of the series (K_i) to that of the next higher member (K_{i+1}) is given by the incremental lipid-water partition constant for a methylene group. Since P_o is proportional to the partition coefficient between water and lipoidal biophase of the membrane, the incremental partition constant can be described by

$$n_{CH_2} = \frac{K_{i+1}}{K_i} \simeq \frac{P_{o,i+1}}{P_{o,i}} \qquad \text{(Eq. 17)}$$

or

$$n^2_{CH_2} = \frac{K_{i+2}}{K_i} \simeq \frac{P_{o,i+2}}{P_{o,i}} \qquad \text{(Eq. 18)}$$

where

i = number of methylene group in n-alkyl chain

n_{CH_2} = incremental partition constant per methylene group.

The corresponding incremental free energy change in the transfer of a CH_2 group of an n-alkyl chain is defined by

$$\delta\Delta F^*_{CH_2} = -R_g T \ln \frac{K_{i+1}}{K_i} \qquad \text{(Eq. 19)}$$

where

$\delta\Delta F^{*}_{CH_2}$ = incremental free energy change per CH_2 group

R_g = universal gas constant

T = absolute temperature

In turn, the dimensionless incremental free energy change[7] is

$$\pi_{CH_2} = \frac{-\delta\Delta F^{*}_{CH_2}}{2.303\ R_g T} = \log n \qquad \text{(Eq. 20)}$$

where

π_{CH_2} = dimensionless incremental free energy change per CH_2 group.

B. Influence of the Aqueous Diffusion Layer on the Rat Intestinal Transport of Various Solutes.

1. Introduction: Using the Doluisio method with certain modifications to improve the efficiency in controlling the hydrodynamics of the drug solution in the intestinal lumen, it can be shown that certain solutes (prednisolone, hydrocortisone) which have been reported to show a biexponential decrease in the drug concentration in the lumen with time,[77] actually follow a monoexponential pattern and that certain solutes (n-butanol, n-octanol and salicylic acid), which are known in the literature[7,78] to follow a monoexponential disappearance with time can be forced into biexponential behavior by exponential design. This demonstration points out that, lack of recognition

of the significance of the aqueous boundary layer can easily mislead and produce improper interpretations of transport mechanisms.

2. Absorption of Hydrocortisone and Prednisolone: Figures 5 and 6 show the semilogarithmic plot of the fraction of hydrocortisone and prednisolone, respectively, remaining in the lumen of the jejunum with time. In the static hydrodynamic situation in which the withdrawal of samples for assay was at regular 150 and 300 second intervals, the absorption rate constant increased with shorter sampling intervals, about 27 percent. When the lumenal solution was oscillated back and forth at a rate of 0.075 ml/sec, the absorption rate constant was even larger. The differences in these rate constants reflect the differences in the hydrodynamics of the lumenal solution and, consequently, the permeability and the average thickness of the unstirred aqueous layer.

The monoexponential curves observed here contrast with previously published[77] biexponential loss of prednisolone at pH 6.0 in the rat intestinal tract with time in which the postulated mechanism was rapid distribution of the drug between the gut lumen and membrane compartment followed by a slower transfer of the drug from the membrane compartment into the blood. As will be shown next, the biexponential character in the curve is an experimental artifact that is readily explained physically by the hydrodynamics of the lumenal solution.

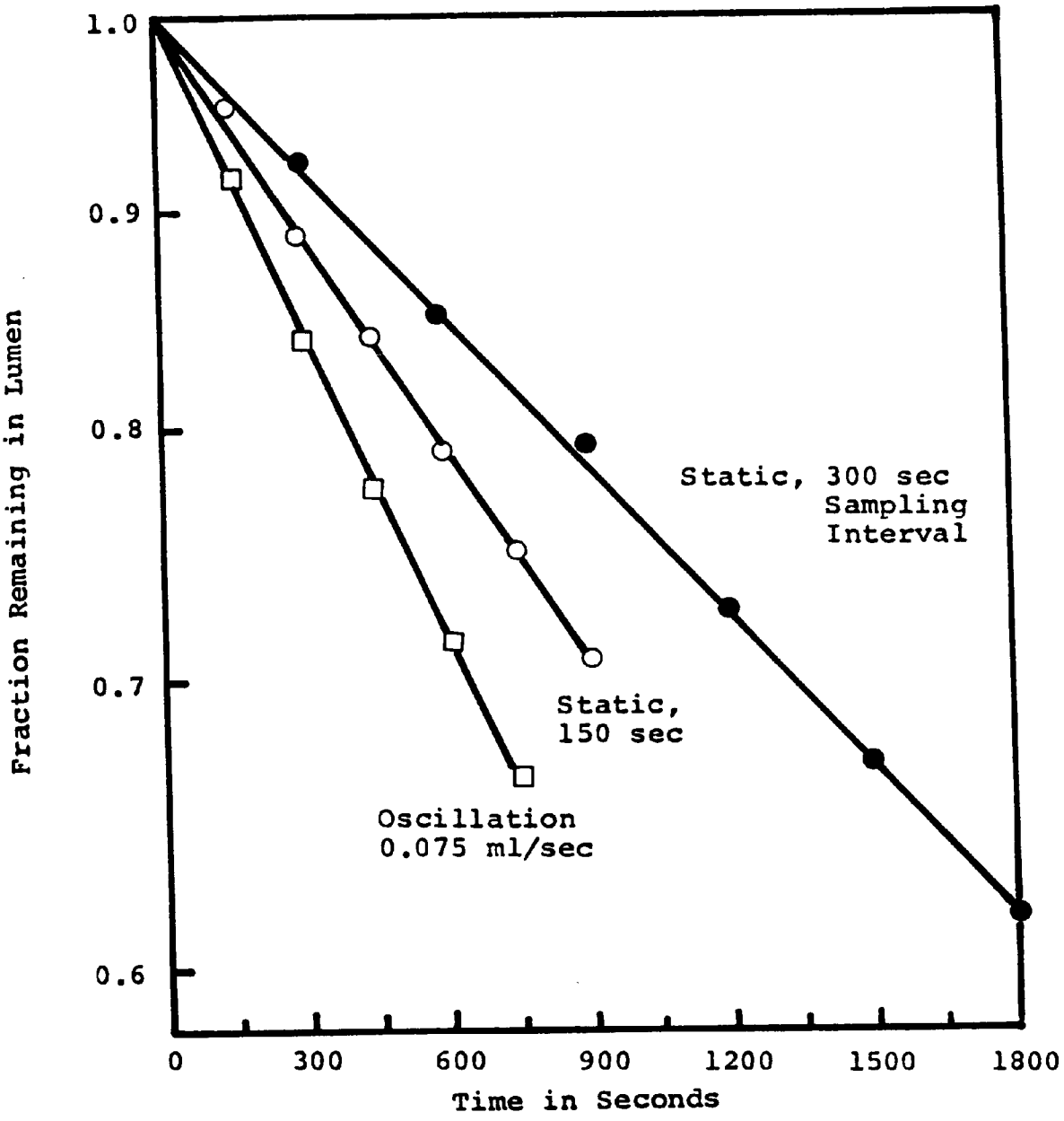


Figure 5. Semilogarithmic plot of the fraction of hydrocortisone remaining in the lumen with time at 37°C and pH 6.0 under various constant hydrodynamic situations. The solid lines are least square lines.

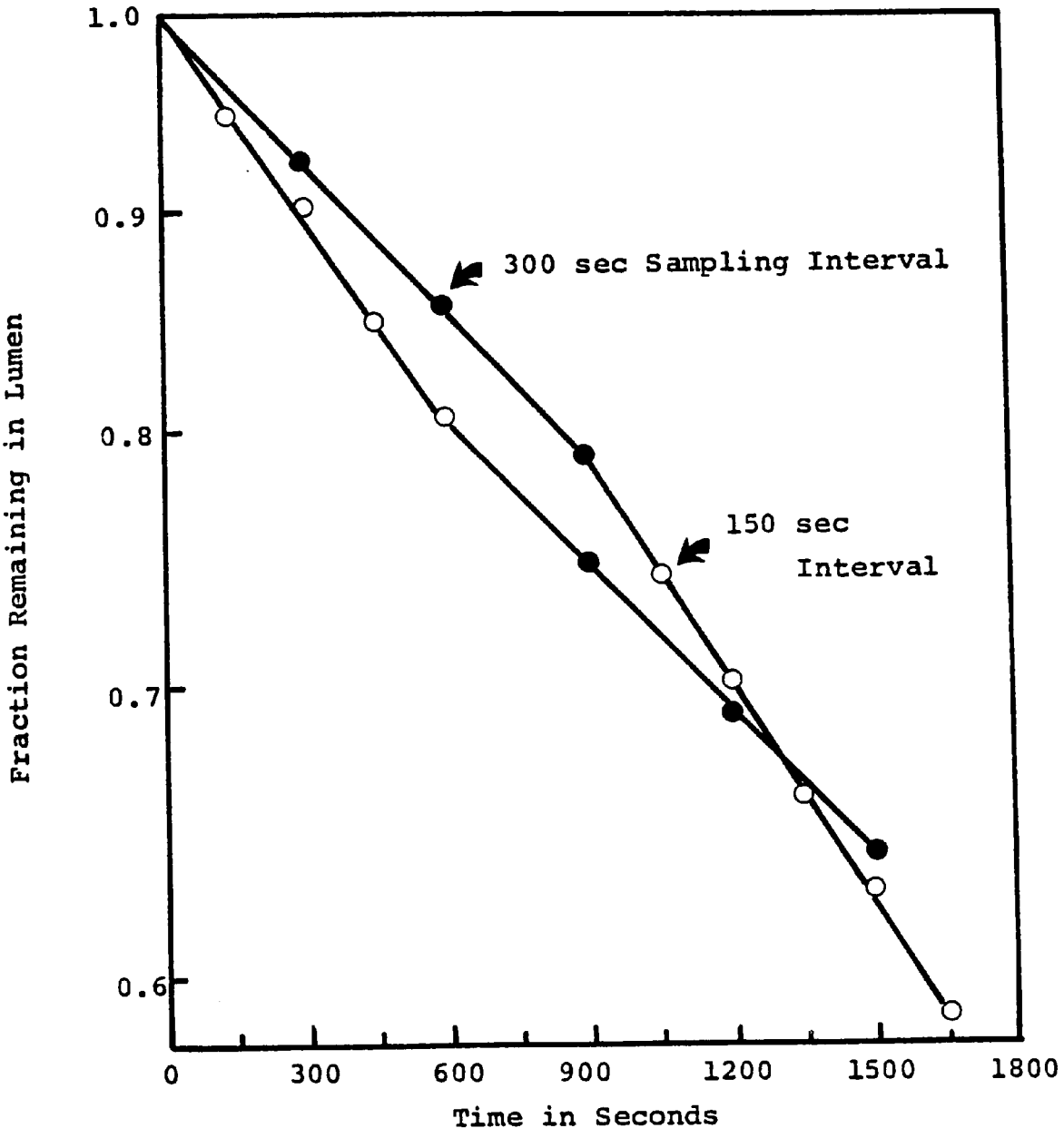


Figure 6. Semilogarithmic plot of the fraction of hydrocortisone remaining in the lumen with time at 37°C and pH 6.0. The bi-exponential character of the plots was obtained simply by changing the sampling time intervals during the absorption experiments and is attributed to changes in the average thickness of the unstirred aqueous layer in front of the mucosal membrane.

Specifically, Hayton and Levy initially employed two 5-minute sampling intervals followed by 10-minute intervals in their prednisolone studies and showed a rapid exponential disappearance of the drug during the short sampling intervals and then a slower exponential disappearance during the longer sampling intervals.

As shown in Figures 7 and 8, absorption studies were carried out with prednisolone and hydrocortisone in which the sampling intervals were changed during the time course of the experiments. Biexponential curves of the type where the initial rapid phase is followed by a slower phase were obtained by using initially the 150 second sampling intervals and then the 300 second intervals. By reversing the sampling intervals, a "mirror image" of the biexponential curve to the first one is obtained. Upon comparing Figures 7 and 8 to the corresponding Figures 5 and 6, the rate constants obtained from the biexponential curves are the same as those from the monoexponential curves of identical sampling intervals. This is a positive indication that the procedures used are not placing undue stress on the membrane. Table III shows that the results of successive absorption experiments in the same jejunal segment of a rat with different steroid concentrations (2×10^{-6} to 5×10^{-1} mM). The result indicates that there is no concentration dependence of these steroids on the transport kinetics.

To show that the sampling intervals do not affect the rate of absorption under the oscillation procedure pro-

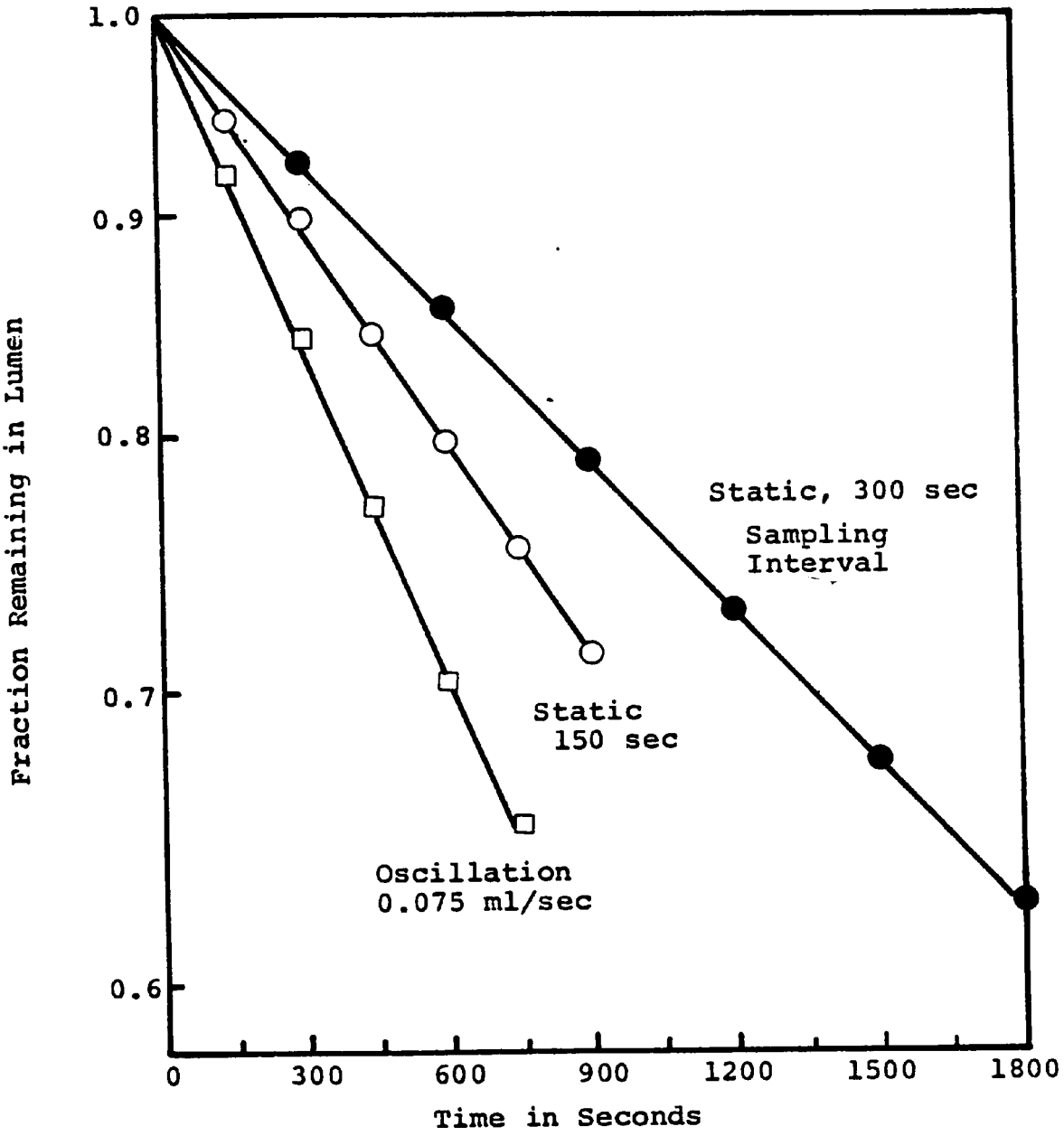


Figure 7. Semilogarithmic plot of the fraction of prednisolone remaining in the lumen with time at 37°C and pH 6.0 under various constant hydrodynamic situations.

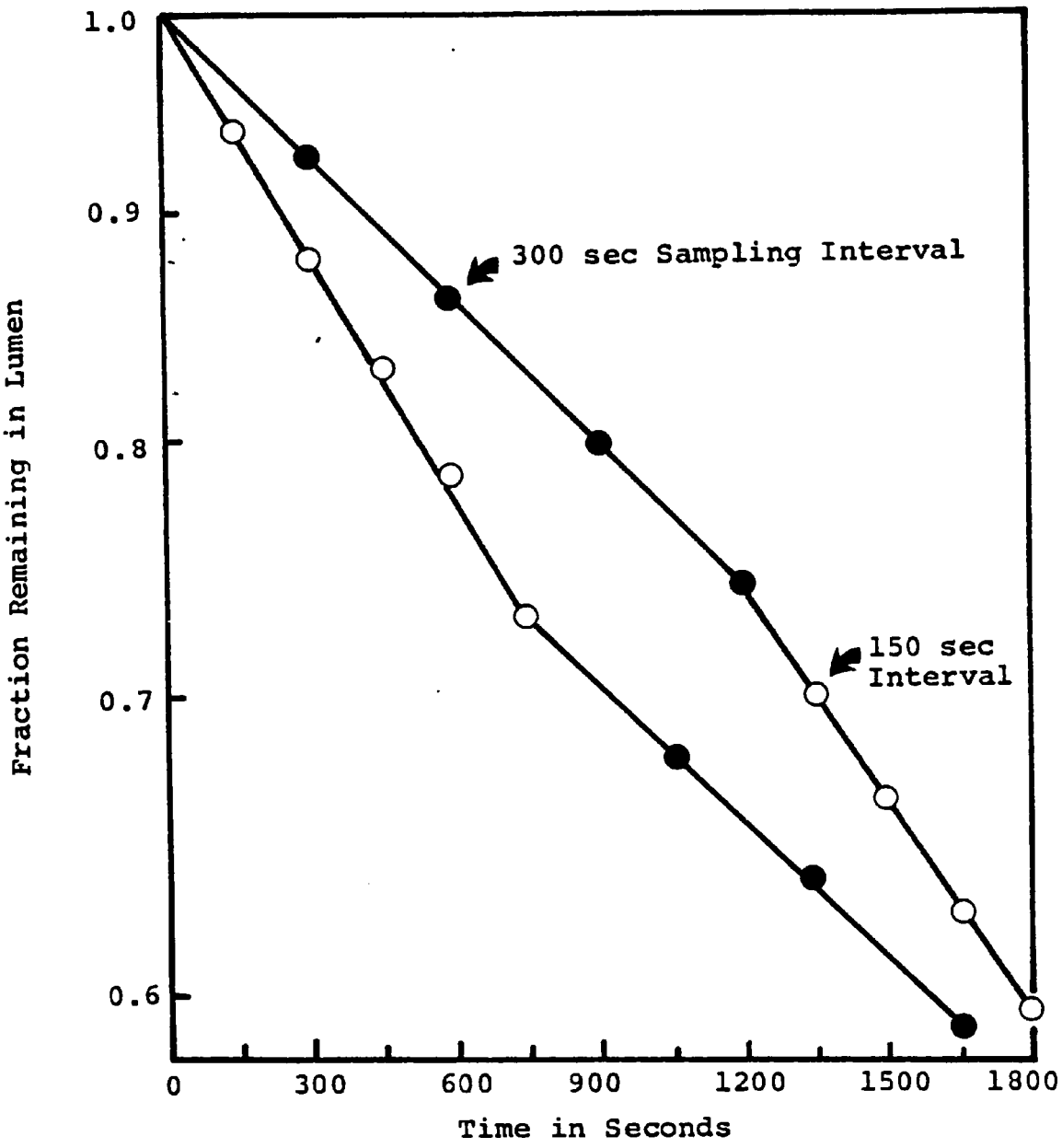


Figure 8. Semilogarithmic plot of the fraction of prednisolone remaining in the lumen with time at 37°C and pH 6.0. The biexponential character of the plots was obtained simply by changing the sampling time intervals during the absorption experiments and is attributed to changes in the average thickness of the unstirred aqueous layer in front of the mucosal membrane.

Table III. Successive Absorption Experiments at pH 6.0 in Same Jejunum Segment at Different Hydrocortisone Concentrations and Static 150 sec Sampling Intervals.

Order of Experiment in Same Jejunum Segment 22 cm	Rat A		Rat B	
	Concentration mM	$K_u \times 10^4$ sec^{-1}	Concentration mM	$K_u \times 10^4$ sec^{-1}
1	2×10^{-6}	3.54	5×10^{-1}	3.75
2	5×10^{-1}	3.48	2×10^{-6}	3.68

Table IV. Independence of the Sampling Intervals on the Absorption Rate When Oscillating Procedures Producing Continuous Hydrodynamics in the Intestinal Solution are Employed.

Sampling Intervals for the Oscillation 0.075 ml/sec Situation	Rate Constant x 10^4 sec^{-1}	
	Hydrocortisone	Prednisolone
150 sec intervals	5.60	5.85
300 sec intervals	5.26	5.70
450 sec intervals	5.71	5.50

ducing a continuous hydrodynamic condition in the intestinal solution (as would perfusion techniques at constant flow rates), sampling intervals of 150, 300 and 450 seconds were employed. Unlike the static procedures where the sampling intervals taken do change the absorption rate of prednisolone and hydrocortisone, the results in Table IV show no differences among the sampling intervals.

It should be emphasized here that, although it has been shown that the disappearance of both steroids in the intestinal lumen with time is monoexponential rather than biexponential and, accordingly, that the proposed mechanism of a rapid rate of distribution of the steroids between the lumenal solution and the intestinal membrane followed by a slow release rate into the blood is questionable, this present study does not detract from the observations of Hayton and Levy[77] that the dialkylpropionamides apparently enhances the rat intestinal absorption of the steroids.

3. Absorption of n-Octanol, n-Butanol and Salicylic Acid: The principal objective of the absorption experiments with n-octanol, n-butanol and salicylic acid is to show that the intestinal transport of these compounds can be made to follow a biexponential decrease in lumenal concentration with time although it is generally accepted to be monoexponential. The experiments will also show when the aqueous diffusion layer becomes a significant

factor in the total transport rate.

In the case of n-octanol (Figure 9) the slopes are markedly different at sampling intervals of 150, 300, and 600 seconds kept constant throughout the absorption experiment under the static hydrodynamic procedures employed. By changing the sequence of sampling intervals throughout the course of the experiment (Figure 10), multi-exponential curves are obtained. It is obvious that by employing different sequences of sampling intervals multi-exponential curves of different shapes can be tailor-made. In contrast, the biexponential curves with n-butanol are not as marked as those with n-octanol. As will be seen, this is due to the fact that the transport of n-butanol is much less aqueous diffusion-controlled and more membrane-controlled than the more lipophilic n-octanol (Figures 11 and 12).

At buffer pH 6.0 the absorption of salicylic acid is significantly influenced by the sampling intervals on the aqueous diffusion layer (Figure 13). However, there is no effect on the absorption at pH 9.0 by changing the sampling intervals (Figure 14). These two situations with salicylic acid illustrate the point more explicitly than with n-butanol that the transport rate is sensitive to changes in the hydrodynamic conditions in the lumenal solution when the transport rate is relatively aqueous diffusion-controlled and insensitive when the rate is membrane-controlled. A more detailed physical insight into the reason why the transport rate at pH 6.0 and 9.0 are different although

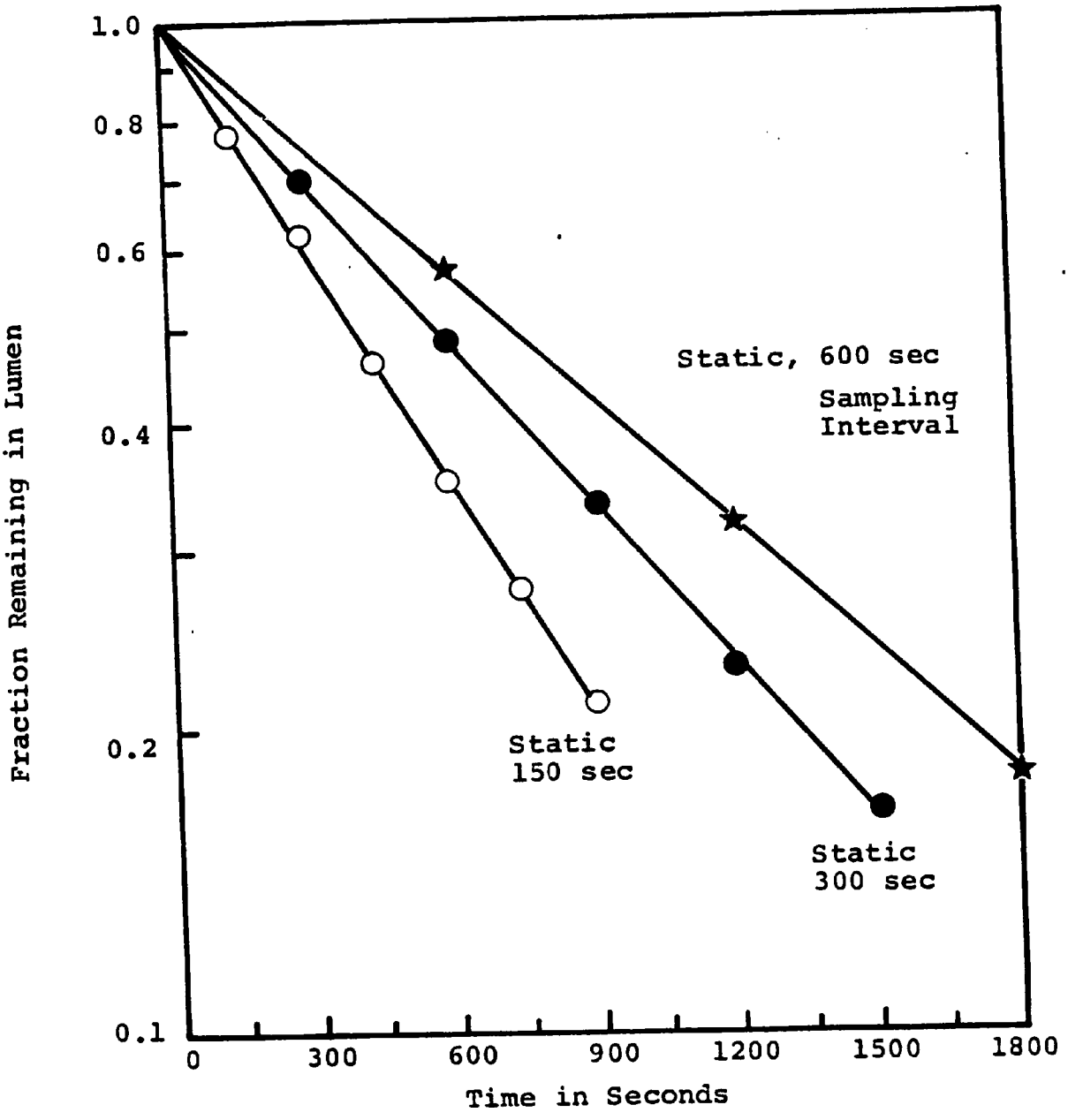


Figure 9. First order absorption of n-octanol at 37°C and pH 6.0 under constant hydrodynamic conditions.

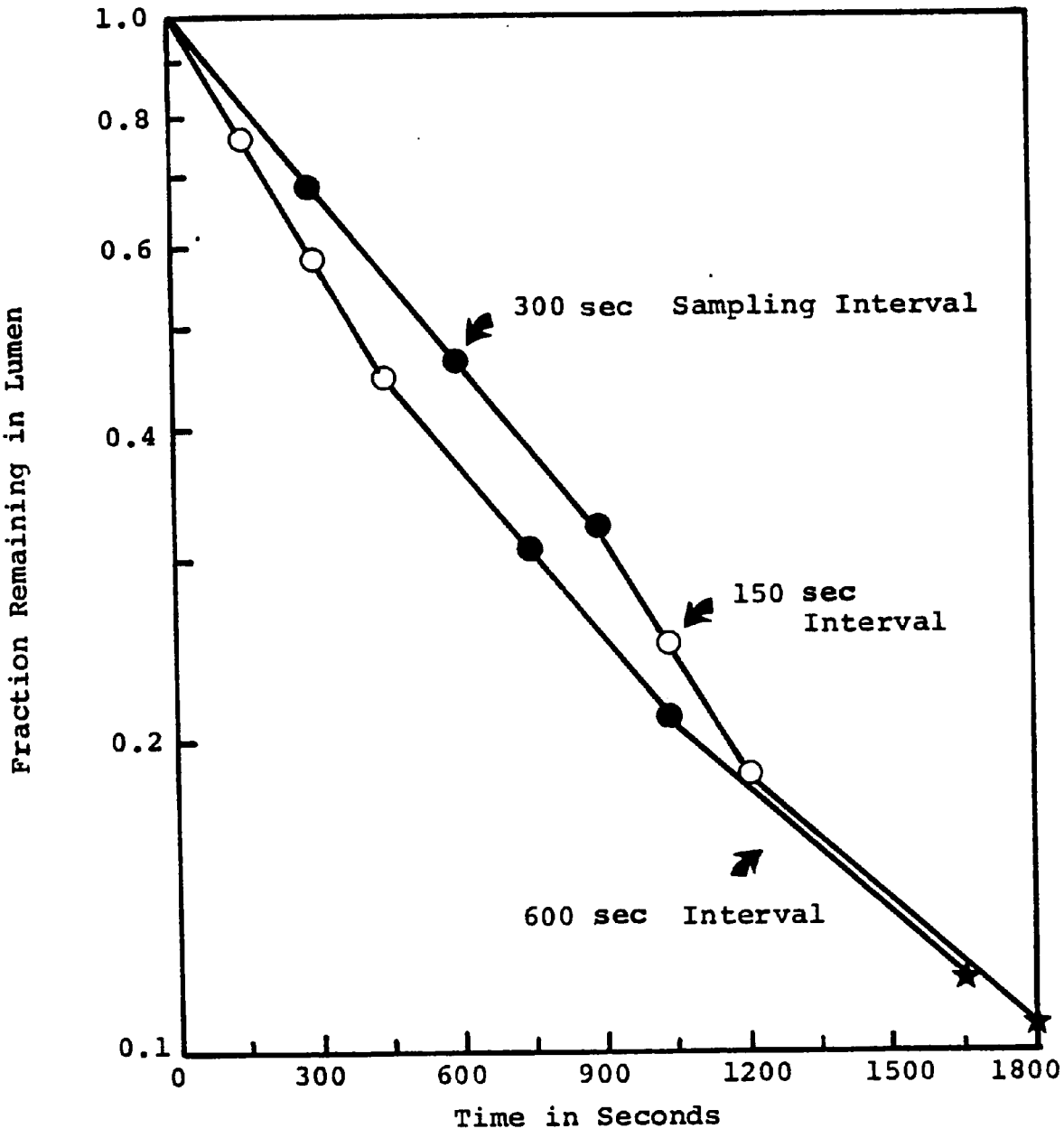


Figure 10. First order absorption of n-octanol at 37°C and pH 6.0. The various multiexponential curves obtained by changing the sampling intervals in the static hydrodynamic procedure during the course of the experiment.

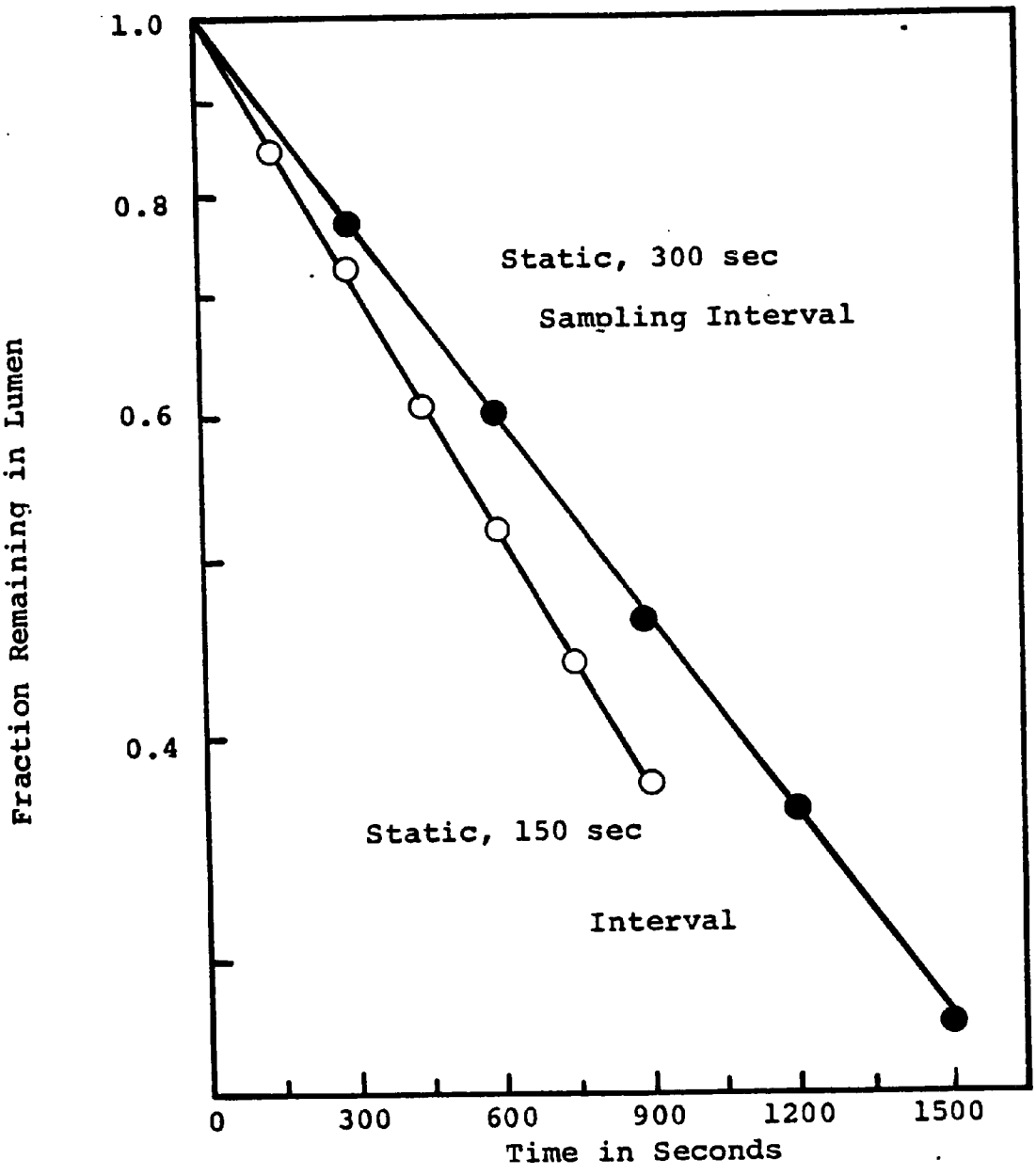


Figure 11. First order absorption of n-butanol at 37°C and pH 6.00 under constant hydrodynamic conditions.

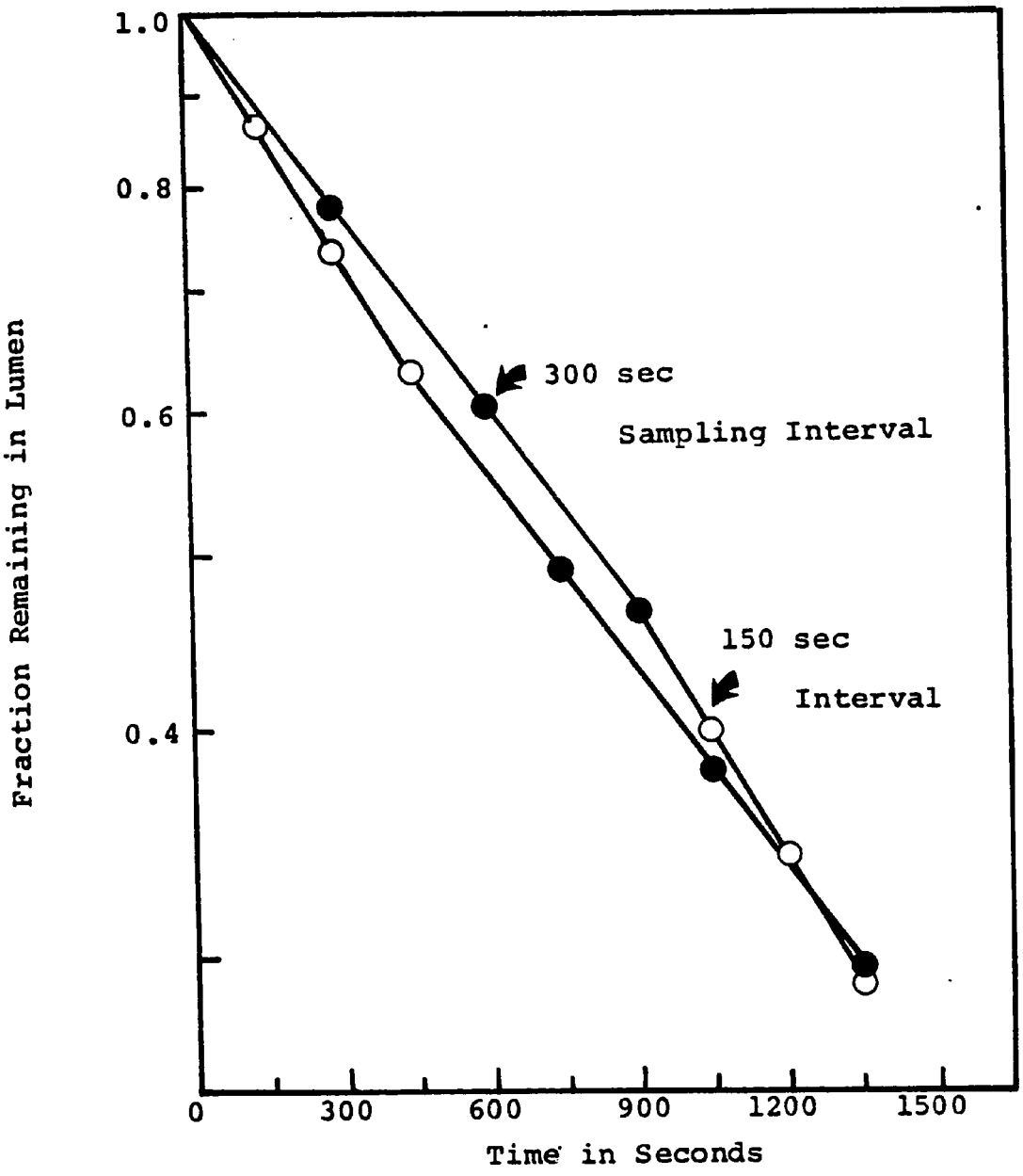


Figure 12. First order absorption of n-butanol at 37°C and pH 6.0. Biexponential character is not as apparent as that with n-octanol since n-butanol is less aqueous diffusion-controlled and more membrane-controlled as compared to the more lipophilic n-octanol.

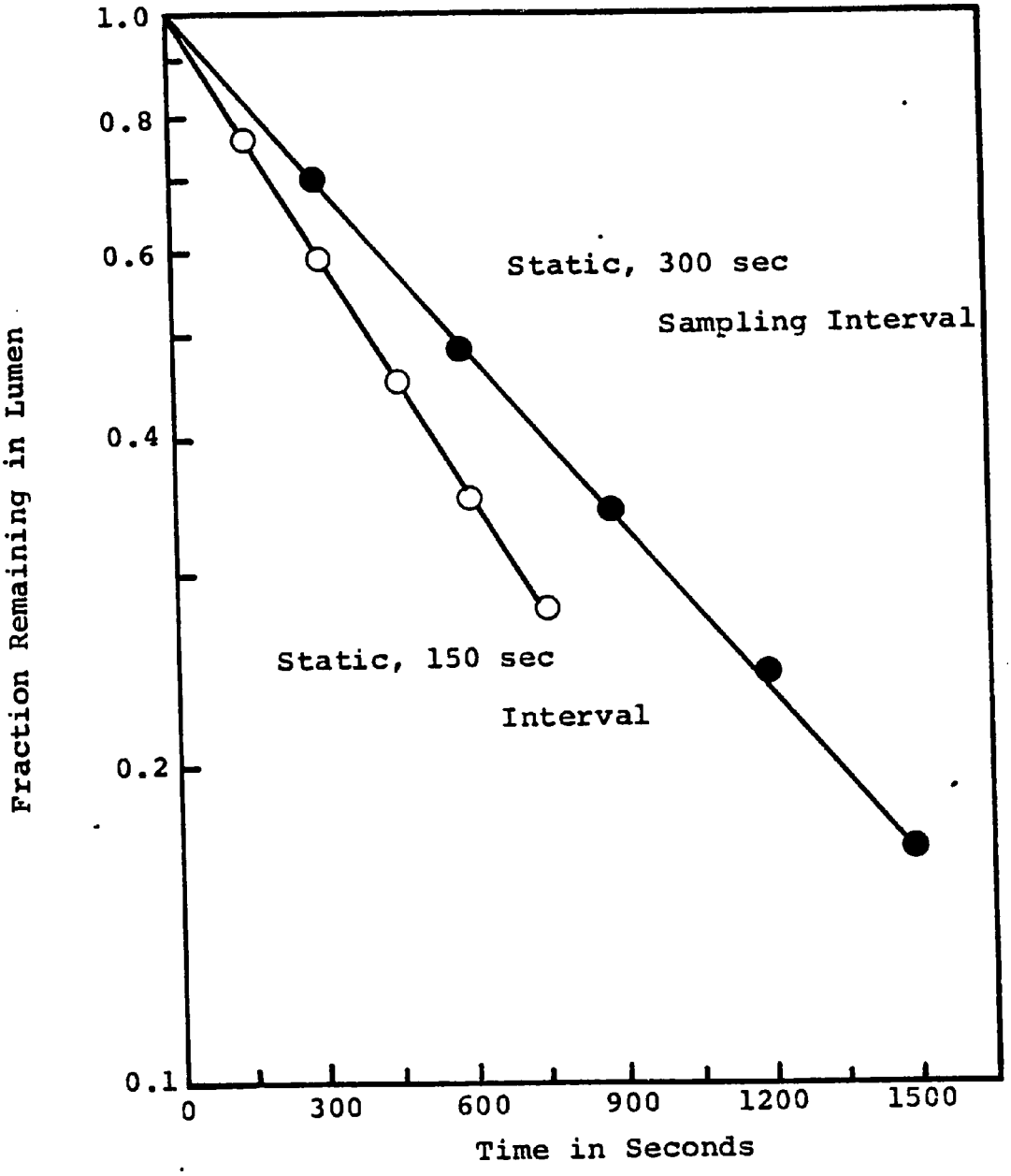


Figure 13. Absorption of salicylic acid at 37°C and pH 6.0 under constant hydrodynamic conditions.

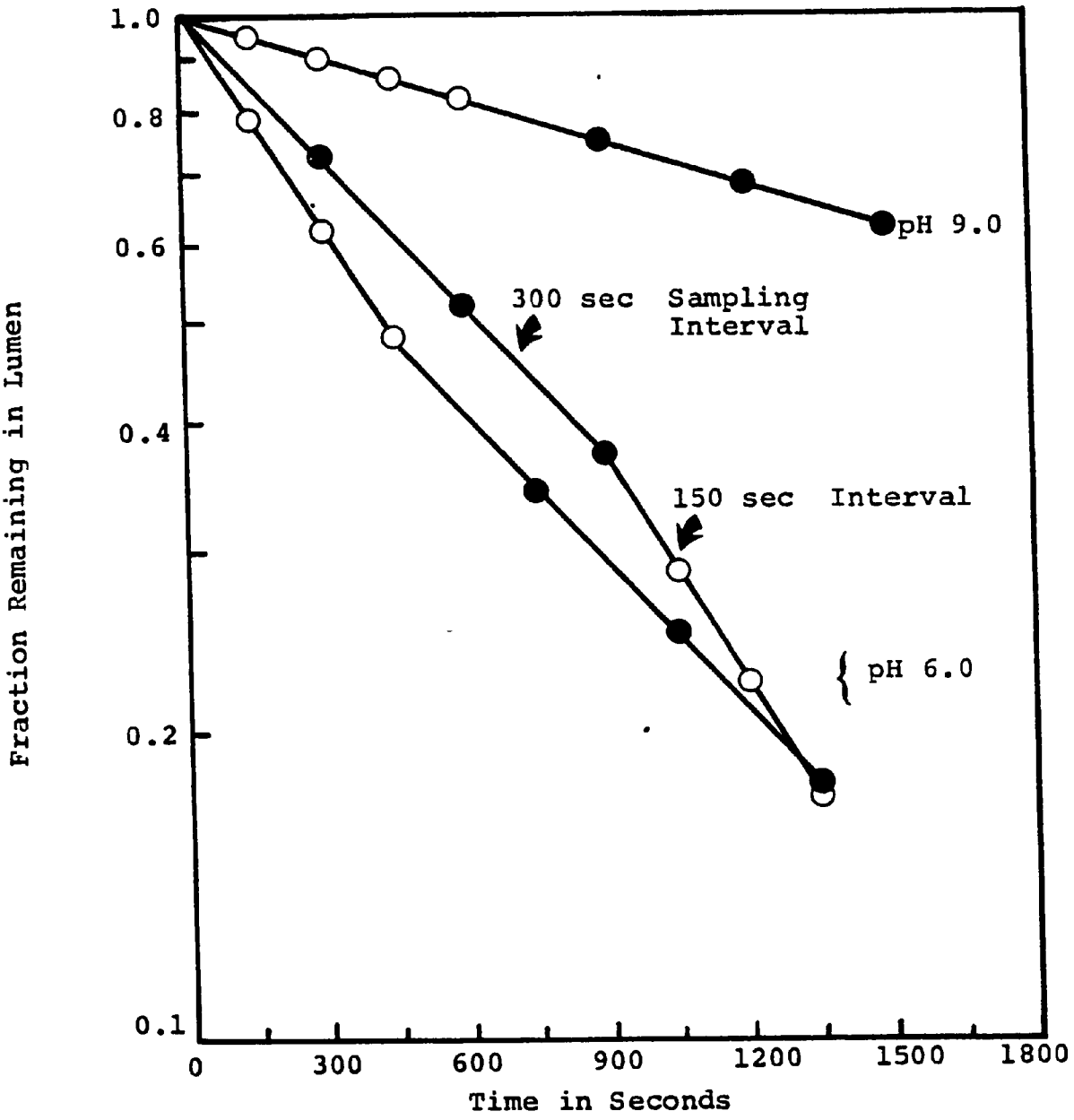


Figure 14. Absorption of salicylic acid at 37°C and pH 6.0. Biexponential curves at pH 6.0 produced by changing the sequence of 150 and 300 seconds sampling interval periods. Monoexponential decrease at pH 9.0 is independent of sampling intervals.

the pK_a is 3.0 is given in the general discussion.

4. The Permeability Coefficients: To determine the permeability coefficients of the aqueous boundary layer and the intestinal membrane, the following method is used. Although the ensuing mathematical descriptions are specifically written for the steroids, similar descriptions can be readily made for the other solutes.

Taking into consideration the different rates of absorption under different hydrodynamic conditions and, subsequently, the expression of the rate constant in Eq. 8, one can write a set of linear algebraic equations:

$$\frac{1}{P_{aq}} + \frac{1}{P_o} = \frac{A}{V K_u} \qquad \text{(Eq. 21)}$$

$$\frac{1}{P'_{aq}} + \frac{1}{P_o} = \frac{A}{V K'_u} \qquad \text{(Eq. 22)}$$

It is noted here that the first order rate constant (K_u) and the permeability coefficient of the unstirred aqueous layer (P_{aq}) are different from K'_u and P'_{aq} because of the differences in the hydrodynamic conditions. In contrast, the permeability coefficient of intestinal membrane (P_o) is independent of the hydrodynamics in the lumenal solution. If one knows the value of the ratio $\underline{r}^*$ between P_{aq} and P'_{aq}, i.e.,

$$\frac{P'_{aq}}{P_{aq}} = r^* \qquad (P'_{aq} > P_{aq};\ r^* > 1.0) \qquad \text{(Eq. 23)}$$

it follows that

$$\frac{1}{P_{aq}} + \frac{1}{P_o} = \frac{A}{V K_u}$$

$$\frac{1}{r^*} \cdot \frac{1}{P_{aq}} + \frac{1}{P_o} = \frac{A}{V K'_u} \qquad \text{(Eq. 25)}$$

Thus, one has two equations in two unknowns, P_{aq} and P_o, that can be solved by the usual methods.

As shown in Figure 15, the absorption rate constants generally increases with increasing carbon numbers in the n-alkanol series until it reaches a maximum asymptotic value independent of the homologous series. With increasing degree in the stirring of the system, the rate constants reach a maximum plateau value with n-alkanol, always larger in carbon number. For example, with the static hydrodynamic situation involving the 300 and 150 second sampling intervals, the maximum rate constant occurs with n-hexanol and n-octanol, respectively. With the continuous oscillation situation, the maximum is observed from n-decanol on. These maximum values are indicative of the aqueous boundary layer being the rate-controlling transport barrier and is equal to

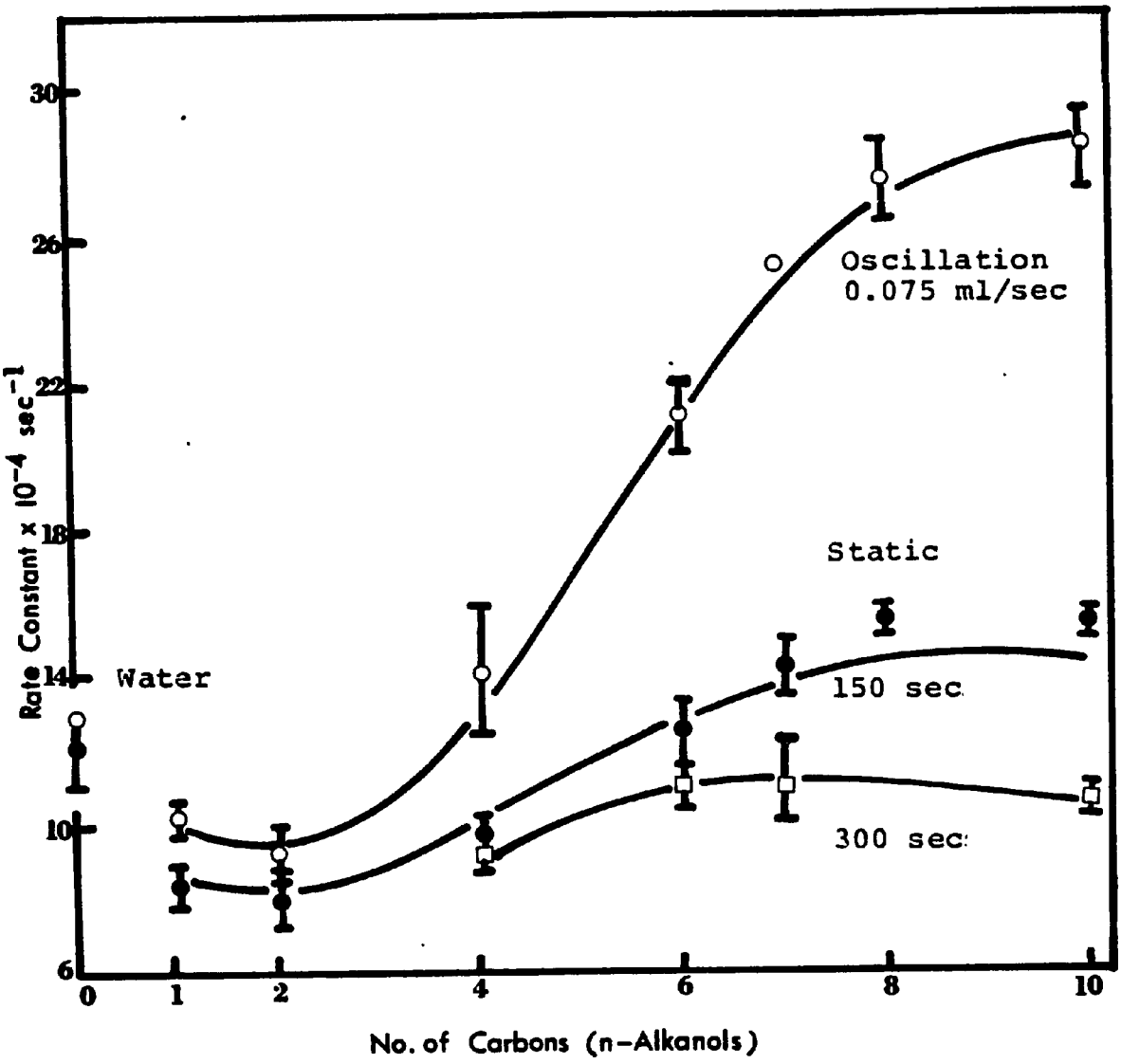


Figure 15. First order absorption rate constants versus number of carbons in the n-alkanol series under various hydrodynamic situations. The solid lines are theoretically derived.

$$K_u(\text{aqueous diffusion-control}) = \frac{AP_{aq}}{V} \qquad \text{(Eq. 26)}$$

All of these observations including the family of curves in Figure 15 are consistent with the predictions of Eq. 3 and are analyzed more in detail elsewhere.[7,76] For the purpose of this thesis, the significance is in its application in the determination of r* as given in Table V.

Table V. Estimation of r* Between the Permeability Coefficients of the Unstirred Aqueous Layer under Various Hydrodynamic Conditions. Data taken from the Maximum Asymptotic Rate Constants of the n-Alkanols in the Rat Jejunum in Figure 15.

Hydrodynamic Condition	Aqueous Diffusion - Controlled K_u sec^{-1}	r*
Oscillation: 0.075 ml sec^{-1}	32.68×10^{-4}	2.12
Static: 150 sec interval	15.45×10^{-4}	1.40
Static: 300 sec interval	11.05×10^{-4}	
Between Oscillation and Static (300 sec interval)		2.96

The rate constants and permeability coefficients of the aqueous boundary layer (P_{aq}) and the jejunal membrane (P_o)

of hydrocortisone and prednisolone are found in Table VI. The P_{aq} of hydrocortisone ranges from 0.35-1.03 x 10^{-4} cm sec^{-1} and increases with increasing degree of agitation of the solution in the lumen. The P_o is 0.95 x 10^{-4} cm sec^{-1} and, as one expects, is found to be independent of the degree of agitation. The P_o of prednisolone is somewhat larger than that of hydrocortisone but is not significantly different at the 5 percent statistical confidence level. The P_{aq} of prednisolone is also not significantly different from the P_{aq} of hydrocortisone at identical hydrodynamic conditions. Considering any one drug in Tables VI and VII, the permeability coefficients of the aqueous diffusion layer (P_{aq}) and the intestinal membrane (P_o for the steroids and $P_{e,membr.}$ for n-butanol, n-octanol, salicylic acid) become increasingly comparable to each other as the degree of agitation of the solution in the intestinal lumen increases, i.e., static 300 seconds sampling interval to continuous oscillation 0.075 ml sec^{-1}. The P_{aq} differs among the solutes in decreasing order comparable to their diffusion coefficients in water: n-butanol>salicylic acid>n-octanol>hydrocortisone and prednisolone.

5. General Discussion: The extent to which the aqueous boundary layer plays an important role in the total transport rate can now be generally assessed. Let us consider initially the simplest physical model embodied in Eq. 8 that has been applied to the steroids

Table VI. Rate Constants and Permeability Coefficients of Steroids in the Jejunum at 37°C and pH 6.0.

Steroids	Hydrodynamic Conditions	Rate Constants $K_u \times 10^4$ sec^{-1} (± s.d.)	Permeability Coefficients $\times 10^4$ cm sec^{-1}		
			P_{aq}	P_o	P_{aq}/P_o
Hydrocortisone	Static (300 sec)	2.83 (0.11)	0.35	0.96	0.36
	Static (150 sec)	3.59 (0.13)	0.48	0.96	0.50
	Oscillation	5.52 (0.20)	1.03	0.94	1.10
Prednisolone	Static (300 sec)	2.77 (0.17)	0.32	1.09	0.29
	Static (150 sec)	3.56 (0.18)	0.45	1.10	0.41
	Oscillation	5.68 (0.14)	0.96	1.02	0.94

Table VII. Rate Constants and Permeability Coefficients of n-Alkanols and Salicylic Acid in Jejunum at 37°C.

Solutes	Hydrodynamic Conditions	Rate Constants $K_u \times 10^4$ sec^{-1} (± s.d.)	Permeability Coefficients $\times 10^4$ cm sec^{-1}		$P_{aq}/P_{e,membrane}$
			P_{aq}	$P_{e,membrane}$	
n-Butanol (pH 6.0)	Static (300 sec)	9.06 (0.49)	1.51	1.5	1.01
	Static (150 sec)	9.82 (0.31)	2.13		1.43
n-Octanol (pH 6.0)	Static (300 sec)	11.10 (0.93)	1.03	12.5	0.08
	Static (150 sec)	15.45 (1.11)	1.46		0.11
Salicylic Acid (pH 6.0)	Static (300 sec)	11.91 (0.47)	1.31	5.7	0.23
	Static (150 sec)	15.50 (1.44)	1.83		0.32
Salicylic Acid (pH 9.0)	Static (300 sec)	2.52 (0.37)	1.78	0.3	6.85
	Static (150 sec)	2.52 (0.37)	1.78		6.85

n-Butanol and n-octanol: $P_{e,membrane} = P_o + P_p$

Salicylic acid: $P_{e,membrane} = P_o X_s + P_p$

$$K_u = \frac{A}{V} P_{aq} \cdot \frac{1}{1 + \frac{P_{aq}}{P_o}} \qquad \text{(Eq. 8)}$$

When $P_{aq} << P_o$, K_u attains a maximum value equivalent to

$$K_u = \frac{A}{V} P_{aq} \qquad \text{(Eq. 9)}$$

for the aqueous diffusion-controlled situation. For example, using the P_{aq} values found in Table VI, the maximum rate constants of both hydrocortisone and prednisolone are 3.73×10^{-4} and 5.23×10^{-4} sec^{-} for the 150 and 300 seconds sampling interval, static hydrodynamic cases, respectively, and about 11×10^{-4} for the continuous oscillation case.

As one observes in Eq. 8, when P_{aq} is somewhat comparable to or greater than P_o, the rate constant is less controlled by the unstirred layer by a factor of $1/(1 + P_{aq}/P_o)$. Stated in another way, the fraction by which the experimental rate constant is affected by the unstirred layer is measured by taking the ratio of the experimental K_u and the aqueous diffusion-controlled K_u (see Eq. 26). As an example, let us consider hydrocortisone in Table VIII in the static hydrodynamic case involving the 300 and 150 seconds sampling interval, the rate is 75 and 65 percent controlled by the aqueous diffusion layer, respectively; while by the continuous oscillation of the lumenal solution, the rate is 50 percent aqueous diffusion-controlled.

Table VIII. Influence of the Unstirred Aqueous Layer on the Experimental Rate Constants

Hydrodynamic Conditions	Solutes	Rate Constants x 10^4 sec^{-1} K_u (expt)	K_u (aqueous diffusion controlled)	Percent of Rate Constant Controlled by Unstirred Layer
Static (300 sec intervals)	Hydrocortisone	2.83	3.86	73.3
	Prednisolone	2.77	3.60	77.0
	n-Butanol	9.06	16.90	53.6
	n-Octanol	11.10	11.55	96.0
	Salicylic Acid (pH 6.0)	11.91	14.67	81.2
	Salicylic Acid (pH 9.0)	2.52	19.94	12.4
Static (150 sec intervals)	Hydrocortisone	3.59	5.41	66.4
	Prednisolone	3.56	5.05	70.5
	n-Butanol	9.72	24.10	41.0
	n-Octanol	15.45	16.35	94.5
	Salicylic Acid (pH 6.0)	15.50	20.54	75.6
	Salicylic Acid (pH 9.0)	2.52	19.94	12.4
Oscillation (0.075 ml sec^{-1})	Hydrocortisone	5.52	11.54	47.8
	Prednisolone	5.68	10.72	53.0
	n-Butanol	14.16	41.00	34.5
	n-Octanol	29.50	31.82	92.7

The influence of the unstirred aqueous layer on n-butanol and n-octanol absorption provides an interesting situation. Since P_o of n-octanol is about 9 times greater than P_o of n-butanol(the incremental partition constant per CH_2 group[7] being 1.78), it is evident by Eq. 7 that the transport rate of n-octanol will be more aqueous diffusion-controlled than the rate of n-butanol at corresponding hydrodynamic conditions imposed (Table VIII).

The importance of the unstirred layer to the passive transport of weak acids can be more clearly analyzed with aid of Eq. 6, which is again shown below

$$K_u = \frac{A}{V} P_{aq} \cdot \frac{1}{1 + \frac{P_{aq}}{P_o X_s + P_p}} \qquad \text{(Eq. 6)}$$

One is reminded that X_s is the fraction of nondissociated acid species at the membrane surface and the surface pH is not necessarily equal to the bulk buffer pH.[7] When the lipoidal pathway is intrinsically the dominant route of transport in the membrane and P_o is much larger than P_{aq} and P_p, the total transport rate can yet be predominantly aqueous diffusion-controlled although the surface pH is a few units larger than the pK_a of the weak acid. This is the case of the intestinal transport of salicylic acid (pK_a 3.0) at buffer pH 6.0, where the rate is about 80 percent aqueous diffusion-controlled at comparable hydrodynamic conditions. It also follows that at much higher

surface pH the transport will be rate-limited by the aqueous pores of the membrane, i.e.

$$K_u = \frac{A}{V} P_{aq} \cdot \frac{1}{1 + \frac{P_{aq}}{P_p}} \simeq \frac{A}{V} P_p \qquad \text{(Eq. 27)}$$

C. Intestinal Absorption of n-Alkanoic Acids.

1. General Absorption Studies: The absorption of n-alkanoic acid homologs (^{14}C-labeled n-butyric to n-decanoic acids) was carried out in the jejunal segment at various isotonic, high capacity buffer pH and stirring conditions of the solution in the lumen. The absorption of the alkanoic acids at pH 6.0 and under the oscillation procedure is shown in Figure 16. The first order slopes increase with increasing carbon chain length. As seen in the absorption rates of n-butyric and n-octanoic acids in Figure 17, the influence of the aqueous boundary layer on the transport kinetics is significant. Table IX gives the summary of the first order rate constants of the n-alkanoic acids at various pH and two hydrodynamic conditions. These results are dramatically illustrated in Figure 18. Here, the in situ rat intestinal absorption rate constant versus bulk lumenal pH profiles on the n-alkanoic acid series shows the interplay of pH, lipophilicity and hydrodynamics on intestinal transport. The shape of the profile of any one acid is sigmoidal which is expected of the passive

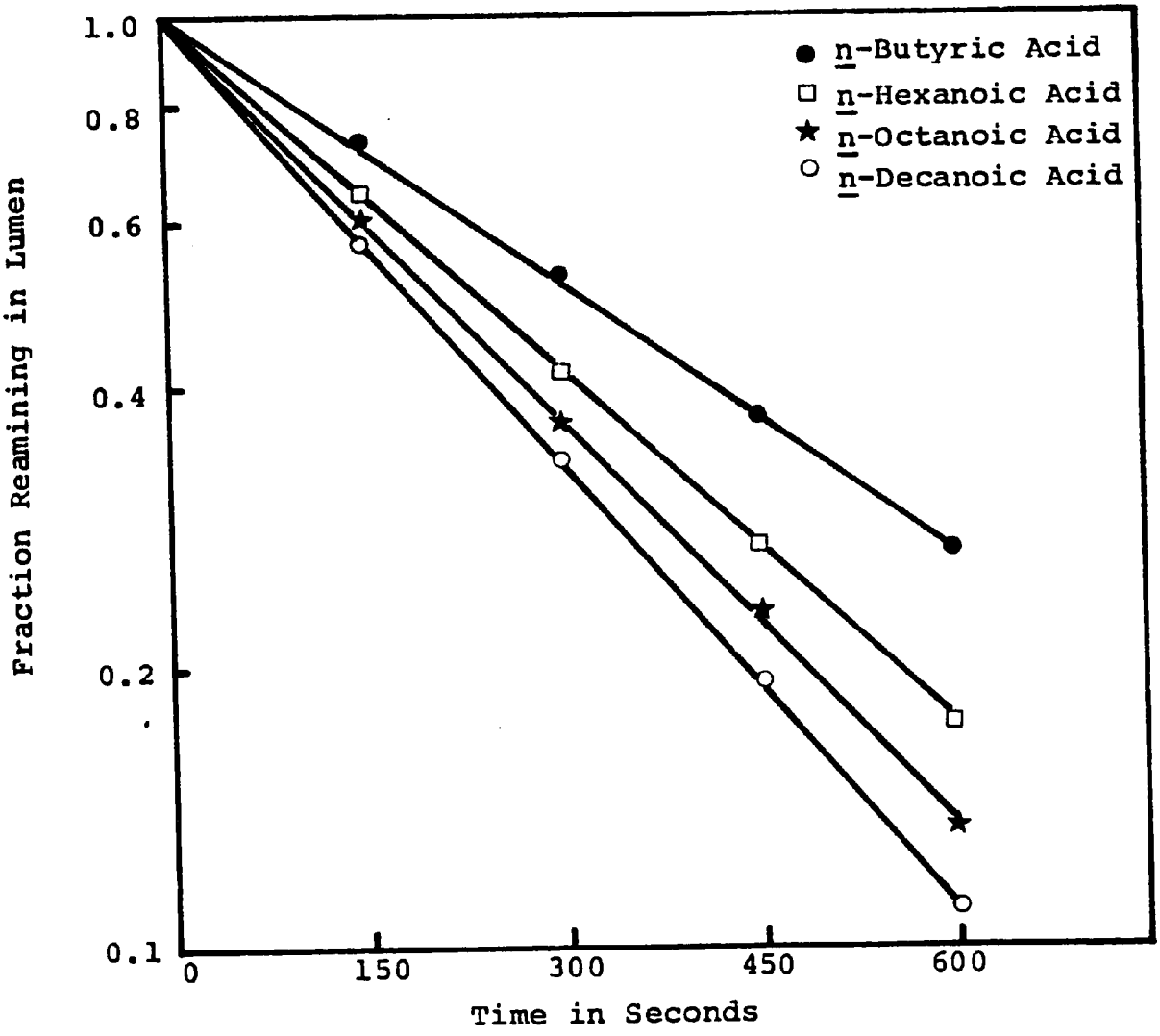


Figure 16. Semilogarithmic plots in the fraction of n-alkanoic acids remaining in the lumen with time at pH 6.0 and oscillation hydrodynamic condition.

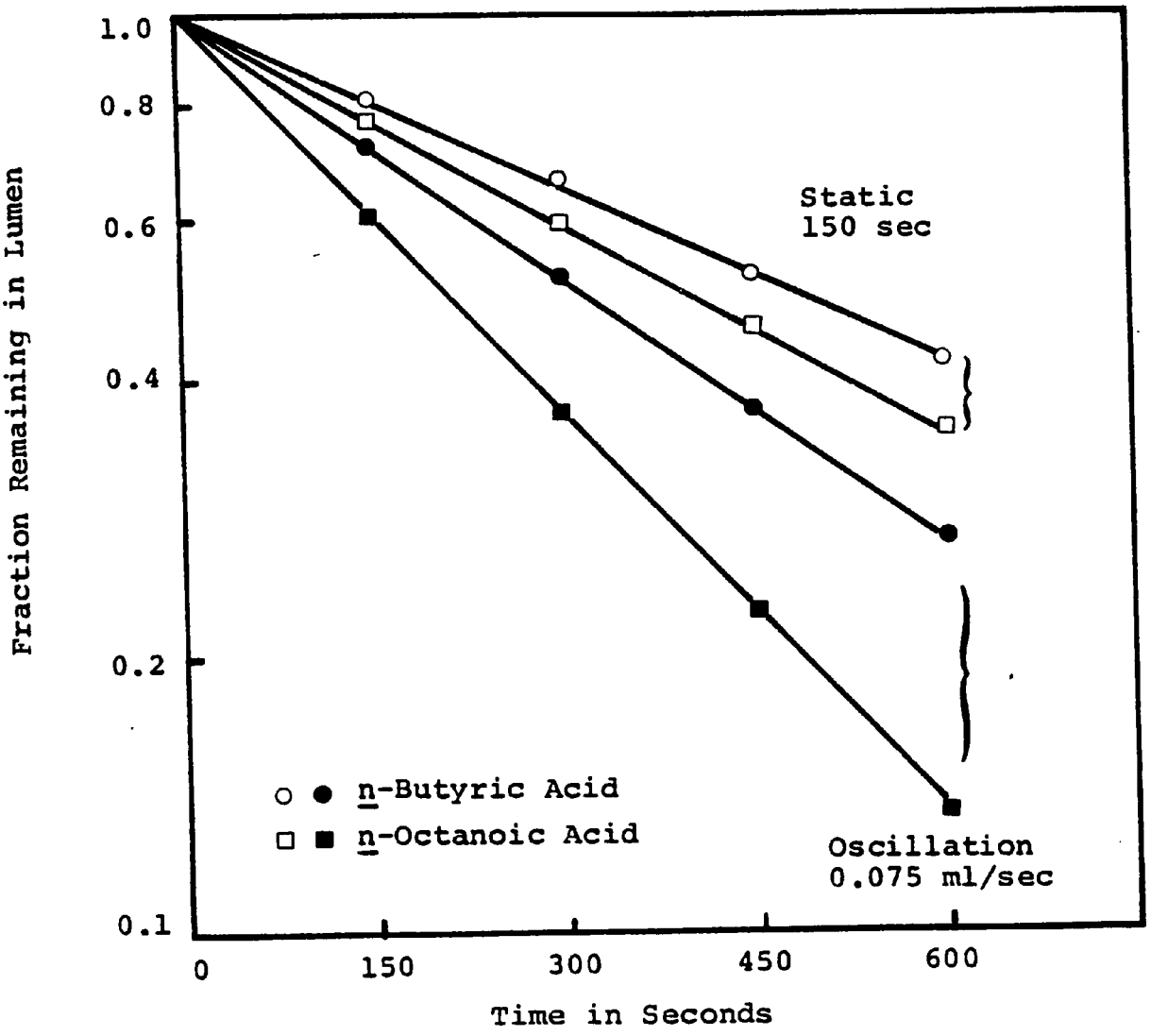


Figure 17. Absorption of n-butyric and n-octanoic acids in the rat jejunum at two different hydrodynamic situations.

Table IX. The First Order Rate Constants of the n-Alkanoic Acids at Various pH and Two Hydrodynamic Conditions.

n-Alkanoic Acid	Buffer pH	$K_u \times 10^3$ sec^{-1} Static 150 sec (± s.d.)	$K_u \times 10^3$ sec^{-1} Oscillation 0.075 ml/sec (± s.d.)
n-Butyric	3.5	1.54 (0.04)	2.39 (0.12)
	4.5		2.30 (0.10)
	6.0	1.36 (0.12)	2.10 (0.09)
	7.5	1.00 (0.08)	1.44 (0.18)
	8.5	0.45 (0.04)	
	9.5	0.40 (0.02)	0.40 (0.01)
n-Hexanoic	3.5	1.75 (0.08)	3.20 (0.20)
	6.0	1.59 (0.11)	2.95 (0.10)
	7.5	1.12 (0.20)	2.40 (0.24)
	8.5		1.27 (0.25)
	9.5	0.35 (0.05)	0.51 (0.03)
n-Octanoic	3.5	1.74 (0.07)	3.55 (0.14)
	6.0	1.62 (0.08)	3.30 (0.16)
	7.5	1.24 (0.01)	3.09 (0.13)
	8.5	0.86 (0.06)	1.73 (0.10)
	10.5	0.35	0.45
n-Decanoic	3.5	1.75 (0.03)	3.54 (0.05
	6.0	1.70 (0.02)	3.50 (0.10)
	7.5	1.40	3.33 (0.13)

transport of weak acids across a membrane, operationally consisting of lipoidal and aqueous pore pathways of intestinal membrane of the jejunum. The essence of the pH-partition phenomenon is present.

Focusing attention at the moment at the high stirring hydrodynamic situation (0.075 ml/sec oscillation), one observes that the absorption rate constant generally increases with alkyl chain length. However, at the pH 3.5-

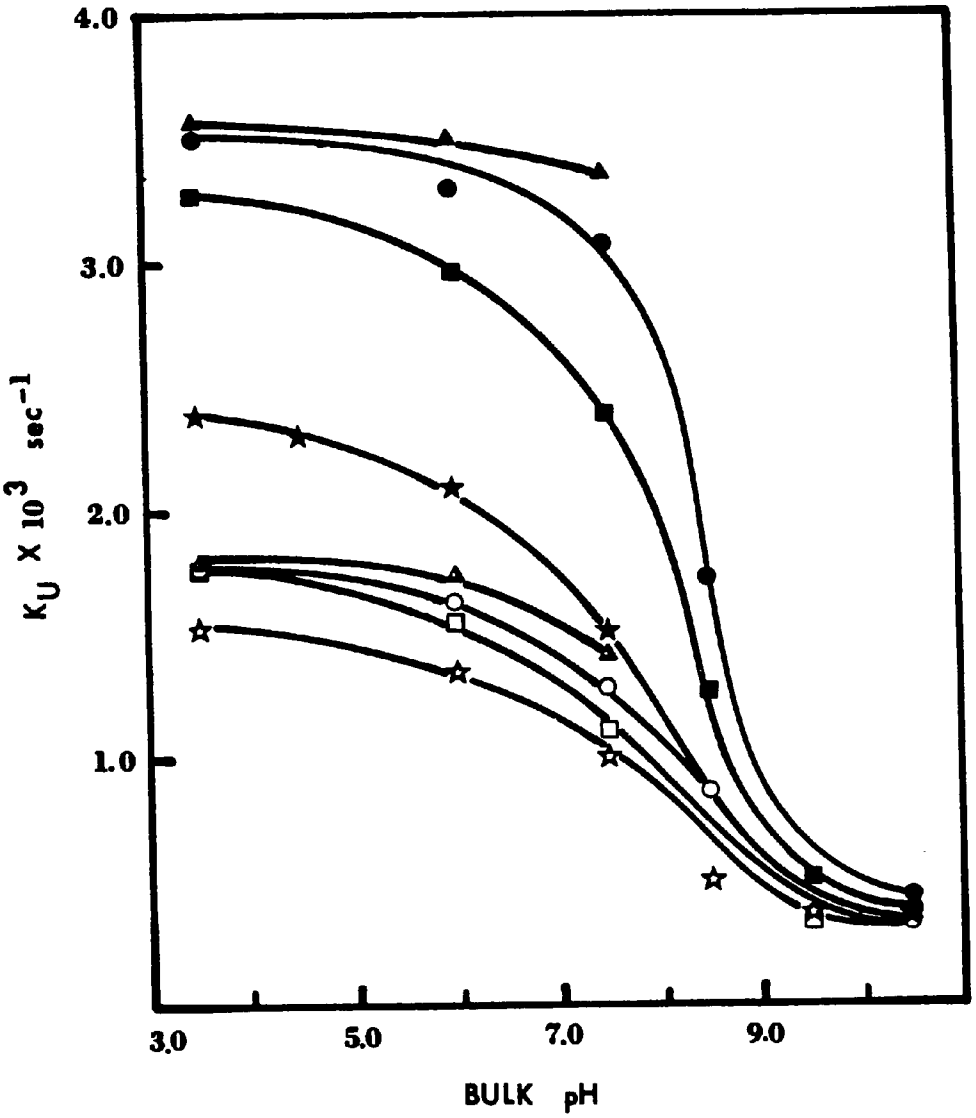


Figure 18. First order absorption rate constant-buffer pH profiles of n-alkanoic acid homologs. In situ studies carried out in 22 cm rat jejunum at 37°C by the modified Doluisio method for two hydrodynamic conditions. Legend: Open symbols; static, 150 secs. Closed symbols; oscillation, 0.075 ml/sec. ☆,★ n-butyric acid; □,■ n-hexanoic acid; ○,● n-octanoic acid; △,▲ n-decanoic acid.

6.0 range the rate constant tends to reach a maximum value independent of chain length. Here, as in the case of the n-alkanols, the rate-determining factor is not the permeability of the membrane but that of the aqueous diffusion layer. There is also a progressive rightward shift in the curves with increasing chain length due to the increasing significance of the aqueous diffusion layer. For each weak acid the $K_u = 0.5\ K_{u,max}$ at $pH > pK_a = 5.0$; for example, 0.5 $K_{u,max}$ for n-butyric acid occurs at bulk pH 7.5 and for hexanoic acid at pH 8.2. In the high pH region all of the acids have the same identical absorption rate constant.

In the lower stirring situation the family of curves are likened to that at higher stirring condition and the absorption rates are correspondingly smaller. Because the transport of the alkanoate anions is controlled by the aqueous pores of the membrane at relatively high pH, the absorption rates are effectively independent of stirring conditions in the intestinal lumen. The general character of these profiles is consistent with the physical model for the simple passive absorption of weak acids as described in Eq. 3.

In considering the data in Figure 18 in another way it is seen that maximum absorption rates at pH 3.5 and low stirring in the lumen are achieved beyond n-heptanoic acid within the homologous series and at higher stirring from n-nonanoic acid (Figure 19). Furthermore, maximum rates at pH 6.0 are attained with nonanoic and undecanoic acids

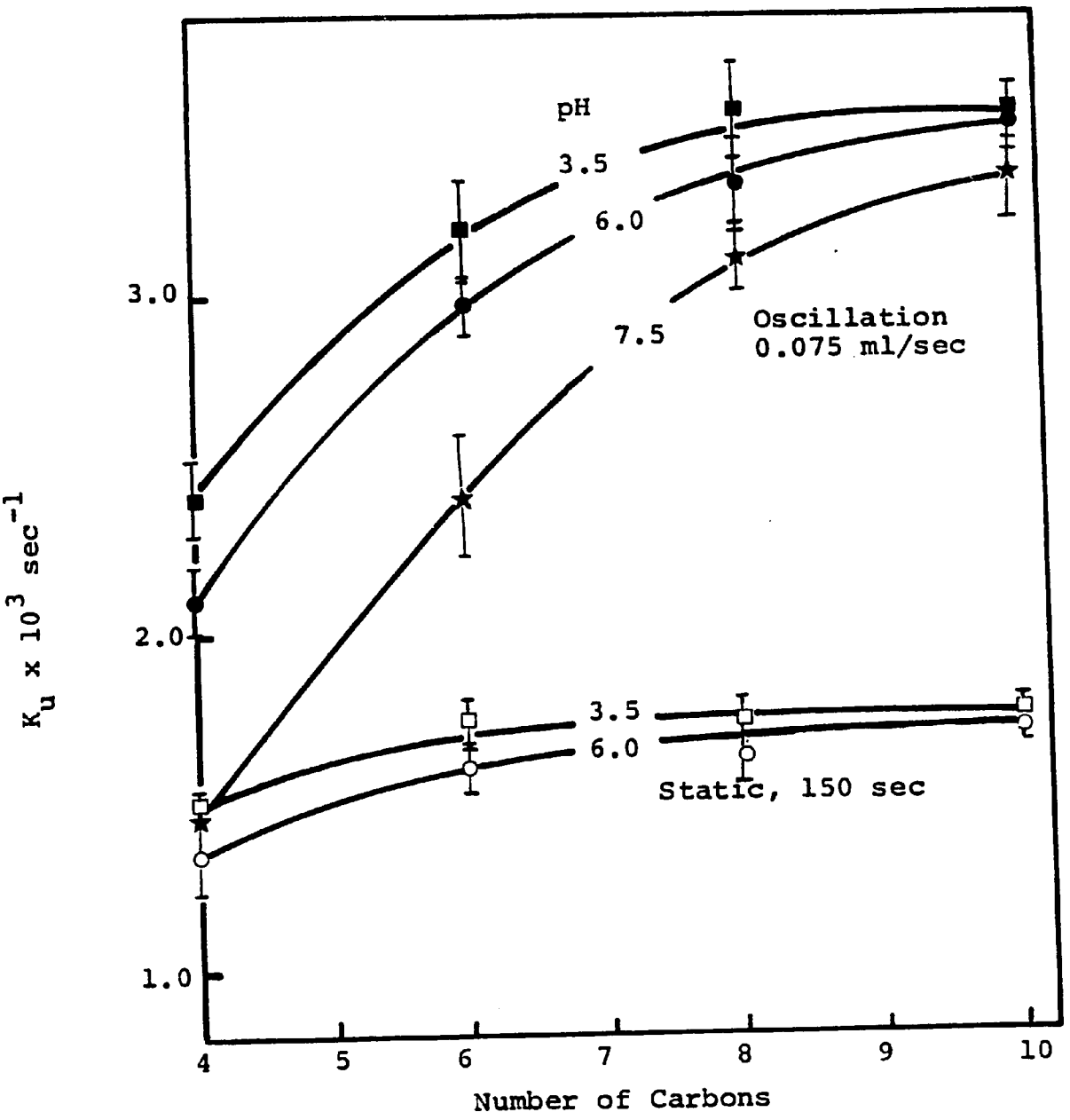


Figure 19. Profiles of absorption rate constant versus carbon number in n-alkanoic acid series as a function of buffer pH and hydrodynamic conditions. Brackets refer to the standard deviation.

for the low and high stirring conditions, respectively.

2. Permeability Coefficients and Incremental Partition Constant per CH_2 Group: Using the absorption data at pH 3.5 at which the rate constant becomes independent of chain length at each corresponding hydrodynamic situation (Figure 18), the permeability coefficients of the aqueous boundary layer were calculated with the aid of Eq. 9. As seen in Table X, the P_{aq} for the static and oscillation cases are 1.56×10^{-4} and 3.17×10^{-4} cm/sec, respectively. The effective thickness of the aqueous boundary layer are, correspondingly, 487 and 209 microns. To

Table X. Estimation of the Permeability Coefficients and Effective Thickness of the Aqueous Boundary Layer*

Hydrodynamic Condition	$K_{u,max} \times 10^4$ sec^{-1} at pH 3.5	$P_{aq} \times 10^4$ cm sec^{-1}	L_{aq} microns
Static, 150 sec interval	17.5 (n-hexanoic acid)	1.56	487
Oscillation 0.075 ml sec^{-1}	35.5 (n-octanoic acid)	3.17	209

*The permeability coefficient, P_{aq}, and the aqueous boundary layer, L_{aq}, are determined with Eqs. 9 and 11 using the surface area to volume ratio equal to 11.2. Aqueous diffusion coefficients: n-octanoic acid, 6.6×10^{-6} cm^2 sec^{-1}: n-hexanoic acid, 7.6×10^{-6} cm^2 sec^{-1}.

account for the difference in the aqueous diffusion coefficients among the n-alkanoic acids, the permeability coefficient of each weak acid across the aqueous boundary layer was calculated in the following manners using n-butyric acid as an example. For the static 150 sec hydrodynamic case,

$$P_{aq,butyric} = P_{aq,hexanoic} \left(\frac{MW_{hexanoic}}{MW_{butyric}}\right)^{2/9} \qquad \text{(Eq. 28)}$$

and in the oscillation hydrodynamic case,

$$P_{aq,butyric} = P_{aq,octanoic} \left(\frac{MW_{octanoic}}{MW_{butyric}}\right)^{2/9} \qquad \text{(Eq. 29)}$$

where MW is the molecular weight and the $P_{aq,hexanoic}$ and $P_{aq,octanoic}$ are known (Table X) and used as the reference. A tabulation of these P_{aq} values is found in Table XI. Derivations of Eqs. 28 and 29 are found in the Appendix.

The permeability coefficients of the n-alkanoic acid anions were determined by applying Eq. 12 to the absorption data at pH 8.5 to 10.5. The P_p is 0.43×10^{-4} cm/sec for all alkanoic acids from n-butyric to n-decanoic acids. Now that the values of the permeability coefficient of the aqueous boundary layer and the aqueous pores of the membrane are known, the effective permeability coefficients of the membrane lipoidal pathway ($P_{e,lipid}$) are readily quantified and, in turn, lead to the estimation of the incremental lipoidal biophase-water partition constant per CH_2 group. For this purpose, the absorption studies at pH 6.0 and 7.5 were selected since the alkanoic acid transport at this pH from

Table XI. *In Situ* Permeability Coefficients of n-Alkanoic Acids for the Rat Jejunum.

pH	n-Alkanoic Acid	$P_{app} \times 10^4$ cm/sec	$P_{aq} \times 10^4$ cm/sec	$P_{e,membrane} \times 10^4$ cm/sec		n_{CH_2}
				P_p	$P_{e,lipid}$*	
6.0	Butyric	1.88	3.54	0.43	4.1	1.76
	Hexanoic	2.64	3.30	0.43	12.7	1.80
	Octanoic	2.95	3.17	0.43	41.0	
	Decanoic	3.12	3.05	0.43	132.1**	
7.5	Butyric	1.28	3.54	0.43	2.0	1.75
	Hexanoic	2.14	3.30	0.43	6.1	1.87
	Octanoic	2.76	3.17	0.43	21.3	
	Decanoic	2.95	3.05	0.43	68.8**	

* $P_{e,lipid} = P_o X_s$ where P_o is the intrinsic permeability coefficient of the lipoidal pathway and X_s is the fraction of nondissociated weak acid species at the membrane surface.

** $P_{e,lipid}$ for n-decanoic acid at pH 6.0 and 7.5 was not determined from the raw data since the absorption of this weak acid is aqueous diffusion-controlled. Instead, it was calculated using the $P_{e,lipid}$ of n-octanoic acid and the average n_{CH_2} being 1.80.

n-butyric to n-octanoic acids is effectively controlled by the lipoidal pathway. Thus, as shown in Table XI, $P_{e,lipid}$ at pH 6.0 ranges from 4.1×10^{-4} for n-butyric acid to 132×10^{-4} cm/sec for n-decanoic acid. The incremental partition constant per CH_2 group (n_{CH_2}) is 1.8 and the dimentionless incremental free energy (π_{CH_2}) is 0.255. These values for the methylene group are in excellent agreement with previous studies with n-alkanols and n-alkanoic acids in the rat jejunum[7] where n_{CH_2} and π_{CH_2} were 1.78 and 0.25, respectively.

3. General Discussion: The influence of the aqueous boundary layer adjacent to the mucosal surface upon intestinal absorption are made explicitly evident by unique baseline experiments on the in situ rat intestinal absorption of the n-alkanoic acid series. The inclusion of the aqueous layer is essential to the physically meaningful factorization and quantification of the permeability coefficients of the lipoidal and aqueous pore pathways of the membrane. The rate constants of the n-alkanoic acids increased with increasing alkyl chain length. However, in the pH range near the pK_a, the rate constants tend to reach maximum independent of chain length. At higher agitation rates of the solutions, the rate constants were larger than the corresponding alkanoic acids at less agitation conditions. As the degree of agitation increases, the permeability coefficient of the boundary layer increases.

The P_p of the alkanoic acids are the same. It is noteworthy that the pore transport of these linear molecules observed here are apparently not dependent upon molecular weight and, instead, related to their respective identical cross sectional area. The implications are also that the aqueous pore pathway is operationally in parallel with the lipoidal pathway of the membrane.

CHAPTER II: SIMULTANEOUS PASSIVE TRANSPORT AND BIOCONVERSION OF DRUGS

A. Theoretical Considerations.

1. General Description of the Physical Model: The physical model for the simultaneous transport and bioconversion of a drug, taken here as a weak acid, is shown in Figure 20. It consists of an aqueous diffusion layer (often referred to as the unstirred aqueous layer) in the lumen in series with the intestinal membrane barrier followed by the blood sink. Operationally, the membrane is comprised of two parallel pathways: the simultaneous diffusional transport-bioconversion pathway in the lipoidal fraction of the membrane and the aqueous pore pathway. It is assumed that (a) quasi-steady state conditions prevail, (b) metabolism in the lumenal solution, if it occurs, is insignificant, (c) only nondissociated drug species are able to partition into the lipoidal fraction of the membrane, (d) metabolism occurs homogeneously within the membrane and, consequently, no significant metabolism is assumed to occur with membrane surface enzymes, (e) the transport of nondissociated and anionic drug species across the aqueous pores occurs with equal facility, (f) isoosmotic conditions exist everywhere, and (g) the aqueous diffusion coefficients of nondissociated and anionic drug species are identical.

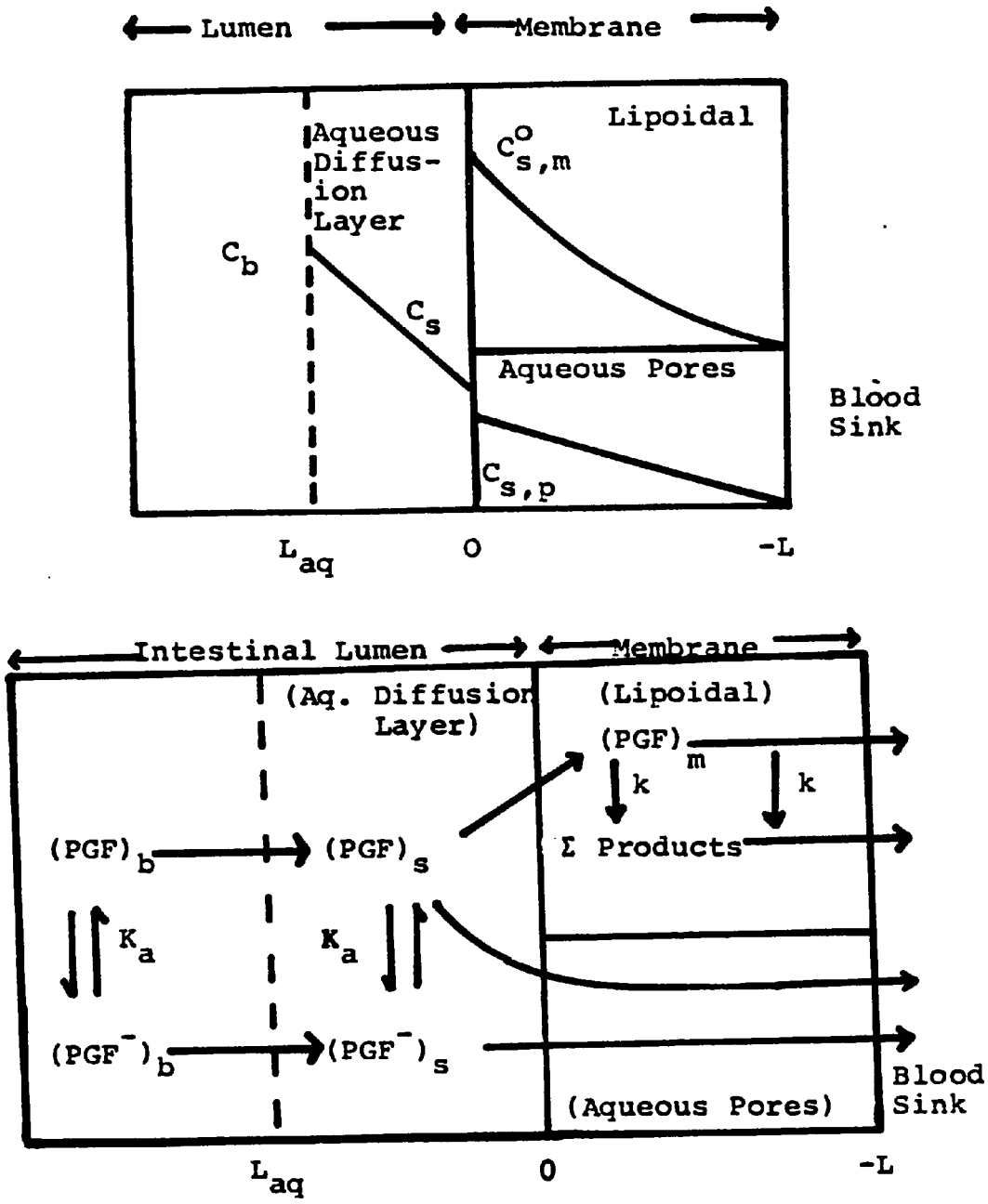


Figure 20. Physical model for the simultaneous intestinal membrane transport and bioconversion of a substrate drug. An aqueous diffusion layer in the intestinal lumen is in series with the membrane consisting of two parallel pathways: the diffusional transport-bioconversion pathway and the aqueous pore pathway. The model depicts the boundary concentrations and distances.

2. Steady-State Fluxes: The total flux of the drug (weak acid) across the aqueous diffusion layer is

$$J_{aq} = \frac{D_{aq}}{L_{aq}} (C_b - C_s) = P_{aq} (C_b - C_s) \qquad \text{(Eq. 30)}$$

J_{aq} = total flux in the aqueous boundary layer per unit area

D_{aq} = aqueous diffusion coefficient, $cm^2\ sec^{-1}$

L_{aq} = effective thickness of the aqueous diffusion layer

P_{aq} = permeability coefficient ($= D_{aq}/L_{aq}$), $cm\ sec^{-1}$

C_b, C_s = total concentration of nondissociated and anionic species in the bulk lumenal solution and at the membrane surface.

The quasi-steady state change in the concentration in the membrane with distance x is given by the following expression which describes the simultaneous diffusional transport and homogeneous metabolism.

$$D \frac{d^2C}{dx^2} - k C = 0 \qquad (0 \geq x \geq -L) \qquad \text{(Eq. 31)}$$

D = diffusion coefficient in the membrane, $cm^2\ sec^{-1}$

k = apparent first order enzyme rate constant, sec^{-1}

C = concentration in the membrane

With the boundary conditions,

$C = C^{o}_{s,m}$ at $x = 0$

$C = 0$ at $x = -L$

the solution is

$$C = \frac{C^{o}_{s,m}\sinh[\sqrt{k/D}\ (L+x)]}{\sinh(L\sqrt{k/D})} \qquad \text{(Eq. 32)}$$

Thus, the concentration of the intact drug in the membrane decreases exponentially with distance. The quasi-steady state flux is obtained by integrating Eq. 31 once; thus,

$$\text{Constant} = D\frac{dc}{dx} + k\int c\,dx \qquad \text{(Eq. 33)}$$

Using Eq. 32

$$J_m = \frac{\alpha C^{o}_{s,m}\sqrt{kD}\cosh[\sqrt{k/D}\ (L+x)]}{\sinh(L\sqrt{k/D})} \qquad \text{(Eq. 34)}$$

J_m = flux in the membrane per unit apparent surface area

$C^{o}_{s,m}$ = concentration of nondissociated species at the surface on the membrane side

α = volume fraction of lipoidal phase of the membrane

The flux of the total concentration of drug per unit area across the aqueous pores of the membrane into the blood sink is

$$J_p = \frac{(1-\alpha)D_pC_s}{L} = P_pC_s \qquad \text{(Eq. 35)}$$

J_p = flux per unit apparent surface area across the pores

$(1-\alpha)$ = volume fraction of aqueous pores of the membrane

D_p = diffusion coefficient in the pores, $cm^2\ sec^{-1}$

L = thickness of the membrane

P_p = permeability coefficient of the pores
$= (1-\alpha)D_p/L$ cm sec^{-1}

Here, it is taken that there is no metabolism occurring in the aqueous pore pathway.

The continuity of flow across the membrane interface is

$$J_{aq} = (J_m)_{x=0} + J_p \qquad \text{(Eq. 36)}$$

The aqueous lipoidal membrane partition coefficient is

$$K = \frac{C^o_{s,m}}{C^o_s} = \frac{C^o_{s,m}}{C^o_p} \qquad \text{(Eq. 37)}$$

K = partition coefficient

C^o_s = concentration of nondissociated species at the membrane surface on the lumen side

C^o_p = concentration of nondissociated species in the aqueous pores

The fraction of nondissociated species[a] of the weak acid is given by

---

[a] For a weak base, $X_s = 1/(1 + (H^+)_s/K_a)$ and for a neutral molecule, $X_s = 1$.

$$X_s = \frac{C_s^o}{C_s} = \frac{1}{1+K_a/(H^+)_s} \qquad \text{(Eq. 38)}$$

X_s = fraction of nondissociated species at the membrane surface

K_a = dissociation constant

$(H^+)_s$ = hydrogen ion concentration at membrane surface

After combining Eqs. 30 and 34-38 and algebraic rearrangement, the total concentration at the membrane surface on the lumen side is explicitly related to the total concentration of drug in the bulk lumenal solution by

$$C_s = \frac{P_{aq}C_b}{P_{aq} + \dfrac{\alpha K X_s \sqrt{kD}}{\tanh(L\sqrt{k/D})} + P_p} \qquad \text{(Eq. 39)}$$

whereupon Eq. 30 becomes

$$J_{aq} = \frac{C_b}{\dfrac{1}{P_{aq}} + \dfrac{1}{\dfrac{\alpha K X_s \sqrt{kD}}{\tanh(L\sqrt{k/D})} + P_p}} \qquad \text{(Eq. 40)}$$

Since

$$J_{aq} = -\frac{V}{A}\frac{dC_b}{dt} \qquad \text{(Eq. 41)}$$

V = volume of solution

A = apparent surface area

t = time

then

$$\frac{dC_b}{dt} = - K_u C_b \qquad \text{(Eq. 42)}$$

where

$$K_u = \frac{A}{V} \cdot \frac{1}{\frac{1}{P_{aq}} + \frac{1}{\frac{\alpha K X_s \sqrt{kD}}{\tanh(L\sqrt{k/D})} + P_p}} \qquad \text{(Eq. 43)}$$

Integrating between the initial total concentration C_b (O) and C (t), one obtains the semi-logarithmic expression:

$$\ln C_b = \ln C_b (O) - K_u t \qquad \text{(Eq. 44)}$$

3. Special Case of Simple Passive Transport: In the special case when there is an insignificant occurrence or absence of bioconversion during the passive transport across the membrane, i.e., k<<D, the $\tanh(L\sqrt{k/D})$ term in Eq. 43 converges to zero, and consequently, gives an apparent impression that there is no passive membrane transport. Physically, this is inconsistent. However, letting $u = L\sqrt{k/D} << 1.0$, the series expansion leads to

$$\tanh u = u + \ldots\ldots \qquad (u << 1.0) \qquad \text{(Eq. 45)}$$

in which the higher terms are small and inconsequential. It follows that

$$\frac{\underset{u\to 0}{\text{Lim}}\ \tanh u}{\sqrt{kD}} = \frac{L}{D} \qquad \text{(Eq. 46)}$$

which yields when introduced into Eq. 43 the familiar expression:[76]

$$K_u = \frac{A}{V} \cdot \frac{1}{\frac{1}{P_{aq}} + \frac{1}{\frac{\alpha K X_s D}{L} + P_p}} \qquad \text{(Eq. 47)}$$

4. Factorization of the Effective Transport-Bioconversion Permeability Coefficient: The effective permeability coefficient of the lipoidal membrane diffusional-bioconversion pathway ($P_{e,m}$) is given by

$$P_{e,m} = \frac{\alpha K X_s \sqrt{kD}}{\tanh(L\sqrt{k/D})} \qquad \text{(Eq. 48)}$$

where k = apparent first order enzyme rate constant and the other terms have been previously defined. For a neutral drug undergoing membrane metabolism, the X_s term is unity.

The corresponding lipoidal membrane permeability coefficient of the molecular modified drug for the general case is expressed by

$$P^*_{e,m} = \frac{\alpha K^* X^*_s \sqrt{k^* D^*}}{\tanh(L\sqrt{k^*/D^*})} \qquad \text{(Eq. 49)}$$

In the limiting situation in which the modification protects the drug from enzymatic attack, i.e., $k^* = 0$, then Eq. 49

reduces to the permeability coefficient for simple passive diffusion:

$$P^*_{e,m} = \frac{\alpha K^* X^*_s D^*}{L} = P^*_o X^*_s \qquad \text{(Eq. 50)}$$

5. The π* Concept: The influence of a substituent group on simultaneous passive membrane transport and metabolism is a function of the relative lipophilicity and relative bioconversion rates of the modified drug compared to the parent drug. Thus,

$$n^* = \frac{P^*_{e,m}}{P_{e,m}} = \frac{K^* X^*_s \sqrt{k^* D^*}}{K X_s \sqrt{kD}} \cdot \frac{\tanh(L\sqrt{k/D})}{\tanh(L\sqrt{k^*/D^*})} \qquad \text{(Eq. 51)}$$

Where n^* = overall transport-bioconversion incremental constant of the substituent group and its position

$*$ = superscript denoting the substituted drug

Taking the logarithm of both sides of the equation and letting $D \simeq D^*$, we get the following linear expression:

$$\log n^* = \log \frac{K^*}{K} + \log\left(\sqrt{\frac{k^*}{k}} \frac{\tanh(L\sqrt{k/D})}{\tanh(L\sqrt{k^*/D^*})}\right) + \log \frac{X^*_s}{X_s} \qquad \text{(Eq. 52)}$$

$$\pi^* = \pi_{PC} + \pi_k + \log \frac{X^*_s}{X_s} \qquad \text{(Eq. 53)}$$

Correspondingly,

$$P^*_{e,m} = P_{e,m} \cdot 10^{\pi^*} \qquad \text{(Eq. 54)}$$

Eqs. 52 and 53 are for the general case in evaluating the substituent effect on the passive diffusion-metabolism mechanism on membrane transport. There are two simplifying situations.

First condition: When there is no change in pK_a and k* is not too different from k, the log X_s^*/X_s and the logarithm of the hyperbolic function terms becomes inconsequential. Therefore,

$$\log n^* = \log \frac{K^*}{K} + 0.5 \log \frac{k^*}{k}$$

$$\pi^* = \pi_{PC} + \pi_k \qquad \text{(Eq. 55)}$$

Let us now consider this π^* and its component parameters in more detail. On one hand, if the substituent group leads to a decrease in the lipophilicity of the modified drug relative to the parent drug, π_{PC} will be a negative quantity. On the other hand, if there is a positive contribution to the lipophilicity, then π_{PC} will take a positive value. It is clearly understood that it is not sufficient to attribute π_{PC} to the substituent group itself; rather, it should also be taken in context with respect to the position of the substituent group since there are orientation and electrical induction effects resulting in a net lipophilic contribution. The value of π_k will be negative if the bioconversion rate constant of the substituted drug is smaller than that of the parent compound. In the opposite situation the π_k is a positive quantity. Since π^* is the sum of π_{PC} and π_k, it

is now readily observed that the net value of π^* may be negative or positive in sign for a variety of the above reasons. It can even be zero for the case when π_{PC} is exactly counter-balanced by π_k and vice versa.

Second condition: When there is no change in pK_a and the modified drug is not metabolized, then Eq. 52 reduces to:

$$\log n^* = \log \frac{K^*}{K} + \log \frac{\tanh(L\sqrt{k/D})}{L\sqrt{k/D}} \qquad \text{(Eq. 56)}$$

$$\pi^* = \pi_{PC} + \log \frac{\tanh(L\sqrt{k/D})}{L\sqrt{k/D}}$$

This case is exemplified by the structural modification of prostaglandin $F_{2\alpha}$ to the 15(S)-methyl-$PGF_{2\alpha}$ analog or $PGF_{2\alpha}$ C_1-carbamoylmethylamide derivative in which $PGF_{2\alpha}$ is a substrate to 15-OH prostaglandin dehydrogenase and the modified structures are non-substrates.

B. Intestinal Absorption of Prostaglandin $F_{2\alpha}$.

1. Introduction: Magee, Armour and Miller[48] showed that the absorption of the prostaglandin $F_{2\alpha}$ and E_2 acids and the 15-methyl-$PGF_{2\alpha}$ methyl ester is accompanied by extensive metabolism in the small intestines of the rat. Similar results were found in absorption experiments using intact intestinal loops of dogs.[49] Using ^{14}C-prostaglandin E_1, Parkinson and Schneider[47] found that only minute amounts of the intact weak acid survived the transport from the

mucosal to the serosal fluid of rat jejunum segments in vitro. They attributed the loss of the ^{14}C-label to an oxidative process leading to the formation of carbon dioxide. Prostaglandin E_1 is metabolized by homogenates of both rat and dog stomach and jejunum.[79] Intestinal absorption of PGE_1 and $PGF_{2\alpha}$ via the lymphatic system appear to be insignificant.[46,49] The absorption, distribution, excretion and metabolism of PGE_2 has been studied in female rats following oral administration.[80] Recently Bito[81] reviewed the literature and made postulations on the membrane carrier-mediated transport mechanism of the prostaglandins with respect to specific tissues and tissue functionality. Although the transport of $PGF_{2\alpha}$ across the rabbit vagina appears to be a saturable carrier-mediated process, there seems to be a lack of definitive mechanistic studies on intestinal transport in animals.

The purposes of this study are to provide a quantitative insight into some aspects of the absorption process of prostaglandin $F_{2\alpha}$ in the rat intestines and to identify and assess potential physiological reactions of the membrane and mesenteric circulatory system to the prostaglandin that may compromise the attainment of an unambiguous physical chemical interpretation of the absorption mechanism. These are only part of the larger objectives aim at the rational biopharmaceutical development of oral delivery systems of the prostaglandins and the molecular design of prostaglandin derivatives and analogs. To provide the conceptual

basis for the biopharmaceutical design, special emphasis is placed on the physical model approach to the design of *in situ* rat intestinal absorption experiments with selective prostaglandins and to the understanding of the transport processes and quantification of the transport and enzymatic kinetic parameters. The elucidation of the transport mechanism and quantitative parametization of physically meaningful constants obtained with these prostaglandins should establish the foundation to investigate and design other analogs and derivatives in a systematic and self-consistent manner.

2. General Absorption Studies: The absorption of $^{3}H\text{-}PGF_{2\alpha}$ at various isotonic buffer pH and high buffer capacities under the continuous oscillation procedure is shown in Figure 21. There is a logarithmic change in the concentration remaining in the lumen of the jejunum with time. The slopes decrease with increasing pH. At pH 7.5 and 9.5 the finite rate constants of the anionic species are about the same. It is observed that the absorption at pH 3.5 and 4.5 tend to depart from linearity at later times. As will be shown, this is most likely due to the flow of intestinal secretions changing the surface and bulk pH with time.

The marked influence of the aqueous boundary layer on the transport kinetics is observed in the first order plots in Figure 22. All other factors being constant, the hydro-

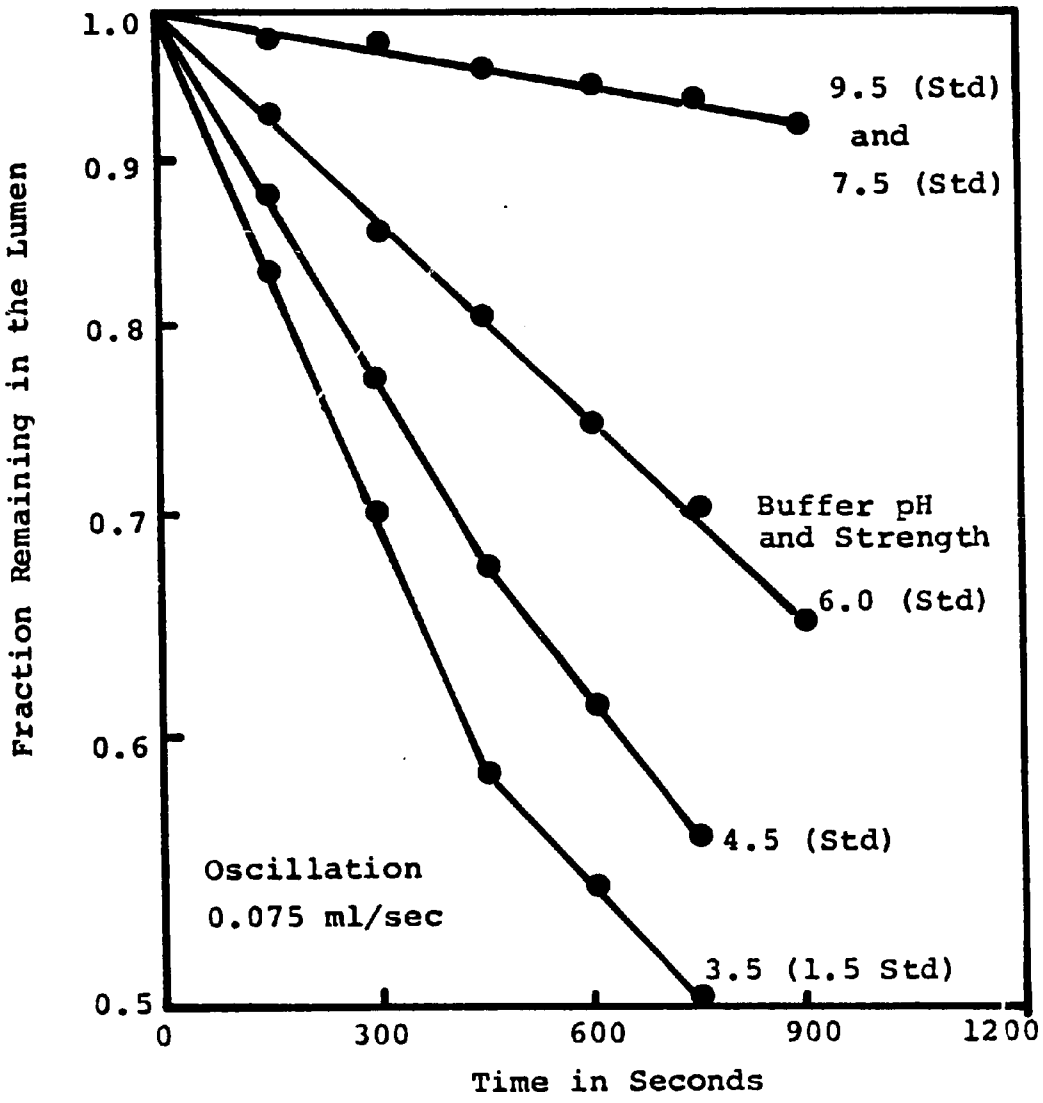


Figure 21. Semilogarithmic change in the fraction of $^{3}H\text{-}PGF_{2\alpha}$ remaining in the lumen with time.

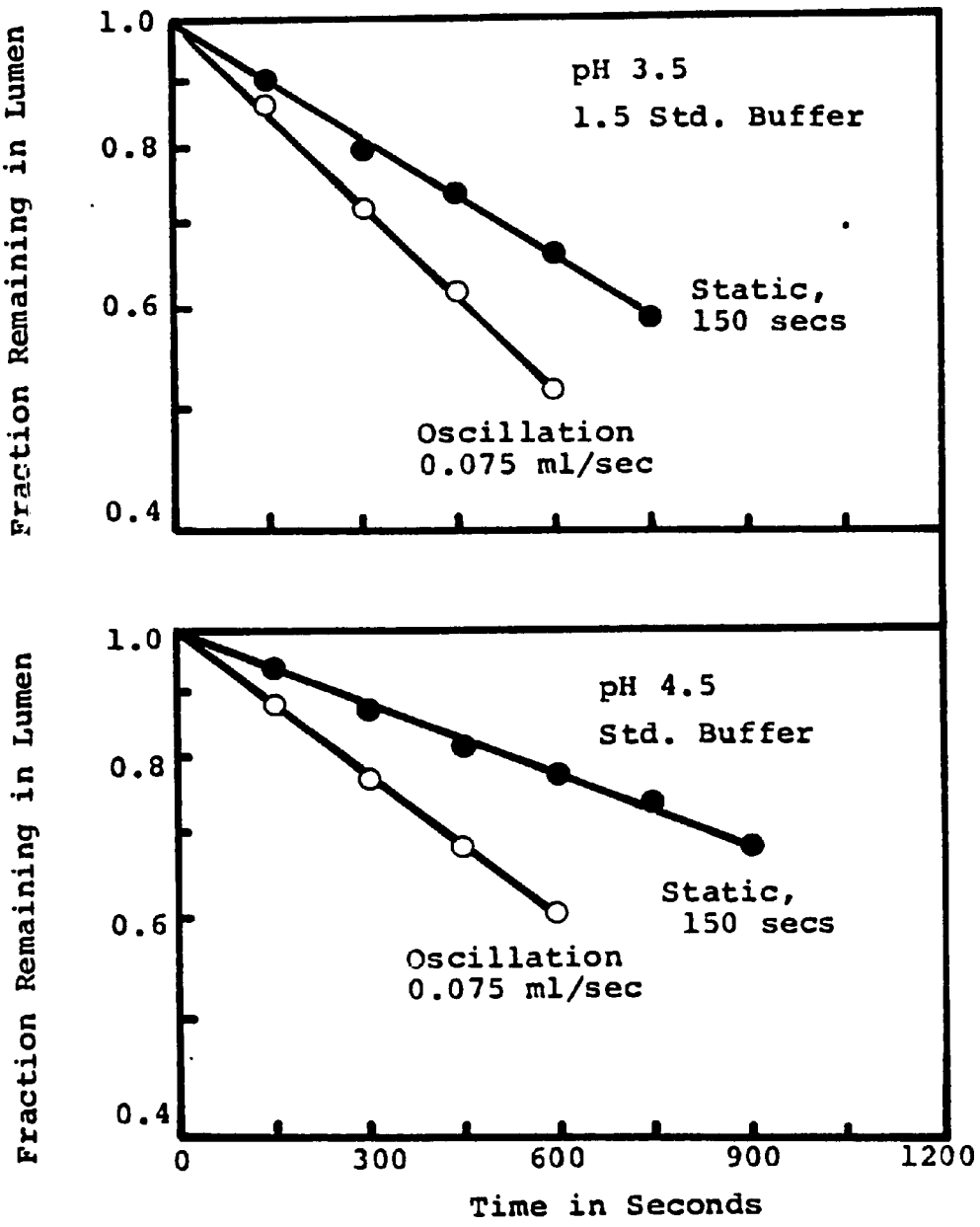


Figure 22. Comparison of the <u>in situ</u> absorption of $PGF_{2\alpha}$ at buffer pH 3.5 and 4.5 under two hydrodynamic conditions.

dynamics produced by the oscillation of the lumenal solution have a larger effect on the slope than the hydrodynamics produced by the static method with 150 seconds sampling intervals. The higher the degree of agitation, the thinner will be the aqueous diffusion layer on the mucosal side of the intestinal membrane.

Table XII is a summary of the absorption experiments

Table XII. In Situ Absorption of ^{3}H-$PGF_{2\alpha}$ (5×10^{-3} µg/ml) in Rat Jejunum at 37°C: Apparent Rate Constants*

Hydrodynamic Condition	Buffer pH	Buffer Capacity	No. of Expts.	$K_u \times 10^4$ sec^{-1}	(± S.D.)
Oscillation 0.075 ml/sec	3.5	Std	3	11.49	(0.05)
		1.5 Std	1	11.1	
	4.5	Std	4	9.24	(0.70)
	6.0	Std	5	4.64	(0.14)
	7.5	Std	3	3.86	(0.18)
		1.5 Std	3	1.56	(0.15)
	8.5	1.5 Std	1	1.8	
	9.5	Std	2	1.51	(0.08)
Static, 150 sec intervals	3.5	1.5 Std	2	6.37	(0.35)
	4.5	Std	2	5.50	(0.22)
	6.0	Std	1	3.46	
	7.5	1.5 Std	2	1.48	(0.4)

*This table is a summary of all experiments with tracer concentrations of ^{3}H-$PGF_{2\alpha}$.

of ^{3}H-$PGF_{2\alpha}$ at tracer concentrations in the jejunum and the results are also illustrated in Figure 23. It is significant that the K_u *versus* pH profiles are similar to those expected for weak acids such as the *n*-alkanoic acids. At low pH the absorption under the higher degree of agitation of the solution is greater and less aqueous diffusion-controlled than absorption under less agitation. The differences in the absorption rate constants between the two hydrodynamic conditions become smaller with increasing pH. This is attributed to the increasing importance of the membrane as the rate-controlling transport barrier. From about pH 7.5 and higher, the K_u *versus* pH profiles for the two hydrodynamic situations converges to an asymptotic minimum. In an operation way this is indicative of the rate-limiting transport of the $PGF_{2\alpha}$ anions across the aqueous pores of the jejunal membrane.

3. Assessment of the Physiological Effects of $PGF_{2\alpha}$ on the Membrane System: The objectives of the following studies are to identify and assess potential physiological reactions of the membrane to $PGF_{2\alpha}$ that may compromise the attainment of an unambiguous biophysical interpretation and quantification of the absorption mechanism. This is accomplished by following the absorption of $PGF_{2\alpha}$ at varying concentrations repeatedly within the same intestinal segment of a rat and also between rats, and by absorption experiments with selective permeants in the

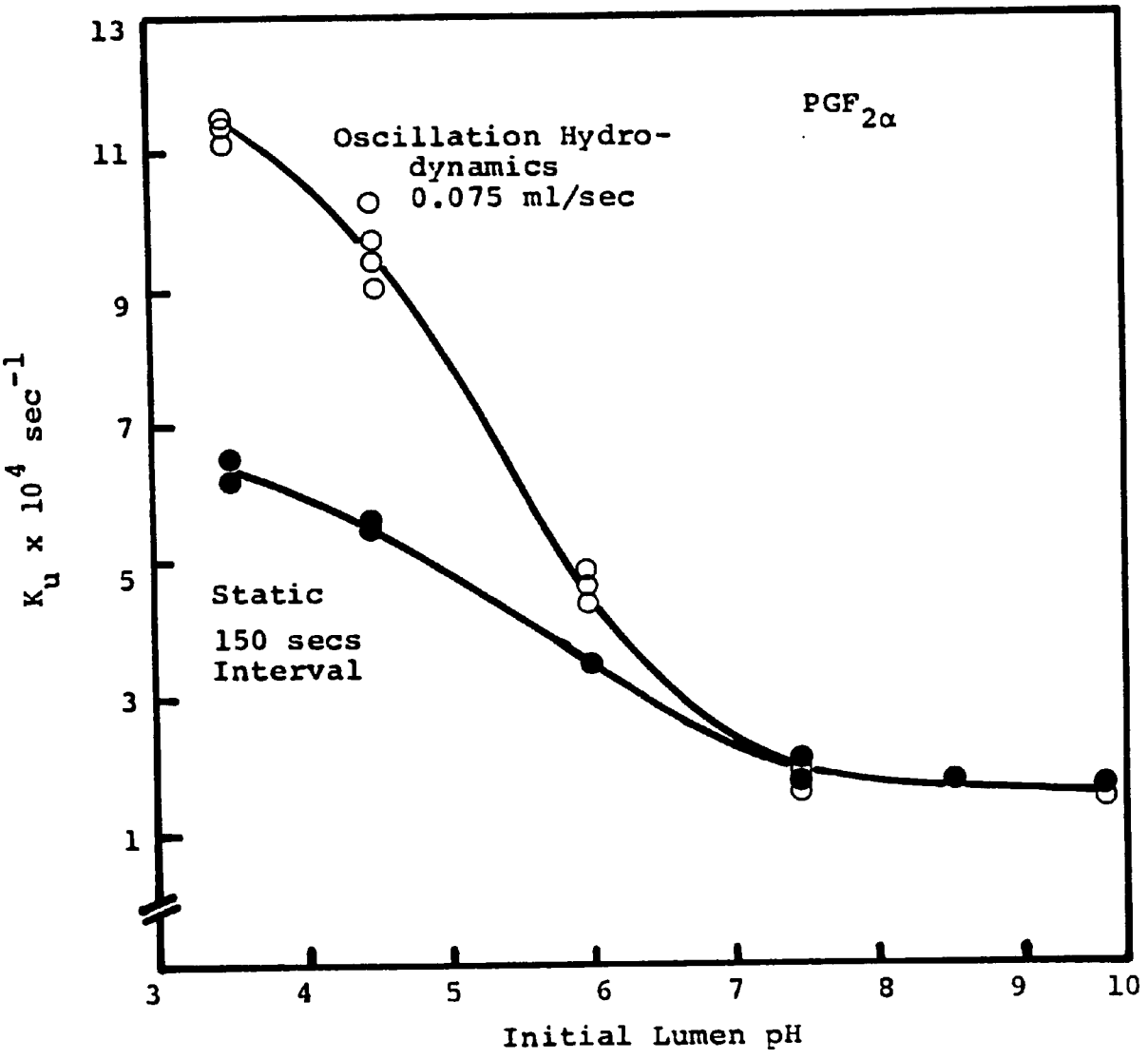


Figure 23. Apparent first order rate constants versus high buffer pH under two hydrodynamic conditions in the rat jejunum.

absence and presence of $PGF_{2\alpha}$.

Tables XIII and XIV show the results of successive absorption experiments in the same jejunal segment of a rat with various buffer pH combinations and with $PGF_{2\alpha}$ concentration combinations (up to 10 μg/ml) at pH 6. Taken together, the results indicate that pH and $PGF_{2\alpha}$ do not have adverse effects on the membrane under the experimental conditions. The within-rat variation is small. It is significant that a 1.5×10^4 fold increase in the concentration, corresponding to 0.014 and 210 mM, respectively, did not influence the absorption rate constant.

To provide an independent support of the observations inferred in Tables XIII and XIV that $PGF_{2\alpha}$ has no significant adverse membrane and vascular effects to transport, it is found that the absorption rates of ^{14}C-n-butanol in the

Table XIII. Successive Absorption Experiments of ^3H-$PGF_{2\alpha}$ in Same Jejunum Segment at Various Buffer pH Combinations.*

Order of exp't in same jejunum segment, 22 cm	Rat A		Rat B		Rat C	
	Buffer pH	$K_u \times 10^4$ sec^{-1}	Buffer pH	$K_u \times 10^4$ sec^{-1}	Buffer pH	$K_u \times 10^4$ sec^{-1}
1	3.5	11.51	4.5	10.42	7.5	4.08
2	9.5	1.43	7.5	3.65	4.5	9.1
3	3.5	11.43	4.5	8.8	7.5	3.86

*All buffers are of standard buffer capacities. The concentration of ^3H-$PGF_{2\alpha}$ is 5×10^{-3} μg/ml.

Table XIV. Successive Absorption Experiments at pH 6.0 in Same Jejunum Segment at Various $PGF_{2\alpha}$ Concentration Combinations.

Order of exp't in same jejunum segment, 22 cm	Rat A		Rat B		Rat C		Rat D	
	Conc. µg/ml	$K_u x10^4$ sec^{-1}	Conc. µg/ml	$K_u x10^4$ sec^{-1}	Conc. µg/ml	$K_u x10^4$ sec^{-1}	Conc. µg/ml	$K_u x10^4$ sec^{-1}
1	$5x10^{-3}$	4.28	1	4.79	10	5.1	100	4.37
2	1	4.57	$5x10^{-3}$	4.64	10	5.0	100	4.41
3	$5x10^{-3}$	4.44	1	5.96	--	---	100	4.86

Concentration of 1, 10 and 100 µg/ml refers to $PGF_{2\alpha}$ tromethamine salts. Tracer ^3H-$PGF_{2\alpha}$ concentrations of 5×10^{-3} µg/ml were added.

jejunum in the absence and presence of $PGF_{2\alpha}$ are not statistically different (Table XV). There is also no effect of $PGF_{2\alpha}$ on the transport of ^{14}C-n-octanol at pH 4.5 (Figure 24). As shown in Table XVI, the fact that the absorption of

Table XV. Absorption of ^{14}C-n-Butanol in the Jejunum at pH 6.0 in the Absence and Presence of $PGF_{2\alpha}$*

Concentration of non-radiolabeled $PGF_{2\alpha}$-tham salt	No. of Expts	$K_u \times 10^3$ sec^{-1} for n-Butanol
0	4	1.59 (0.16)
10 µg/ml	2	1.51 (0.2)
100 µg/ml	3	1.61 (0.13)

*Oscillation 0.075 ml/sec procedures were used. 10 and 100 µg/ml is equivalent to 21 and 210 µM, respectively.

Table XVI. In Situ Absorption of ^{14}C Benzoate at pH 8.5 in the Absence and Presence of $PGF_{2\alpha}$ in the Jejunum*

Order of Exp't	Rat A		Rat B		Rat C	
in same jejunal segment, 22 cm	$PGF_{2\alpha}$ µg/ml	$K_u \times 10^4$ sec^{-1}	$PGF_{2\alpha}$ µg/ml	$K_u \times 10^4$ sec^{-1}	$PGF_{2\alpha}$ µg/ml	$K_u \times 10^4$ sec^{-1}
1	0	6.36	0	5.32	1	5.85
2	1	6.80	1	4.74	0	4.22
3	0	6.45	0	5.29	1	5.22

* Oscillation 0.075 ml/sec hydrodynamics, pH 8.5 (1.5 standard buffer capacity), $PGF_{2\alpha}$ as tham-salt.

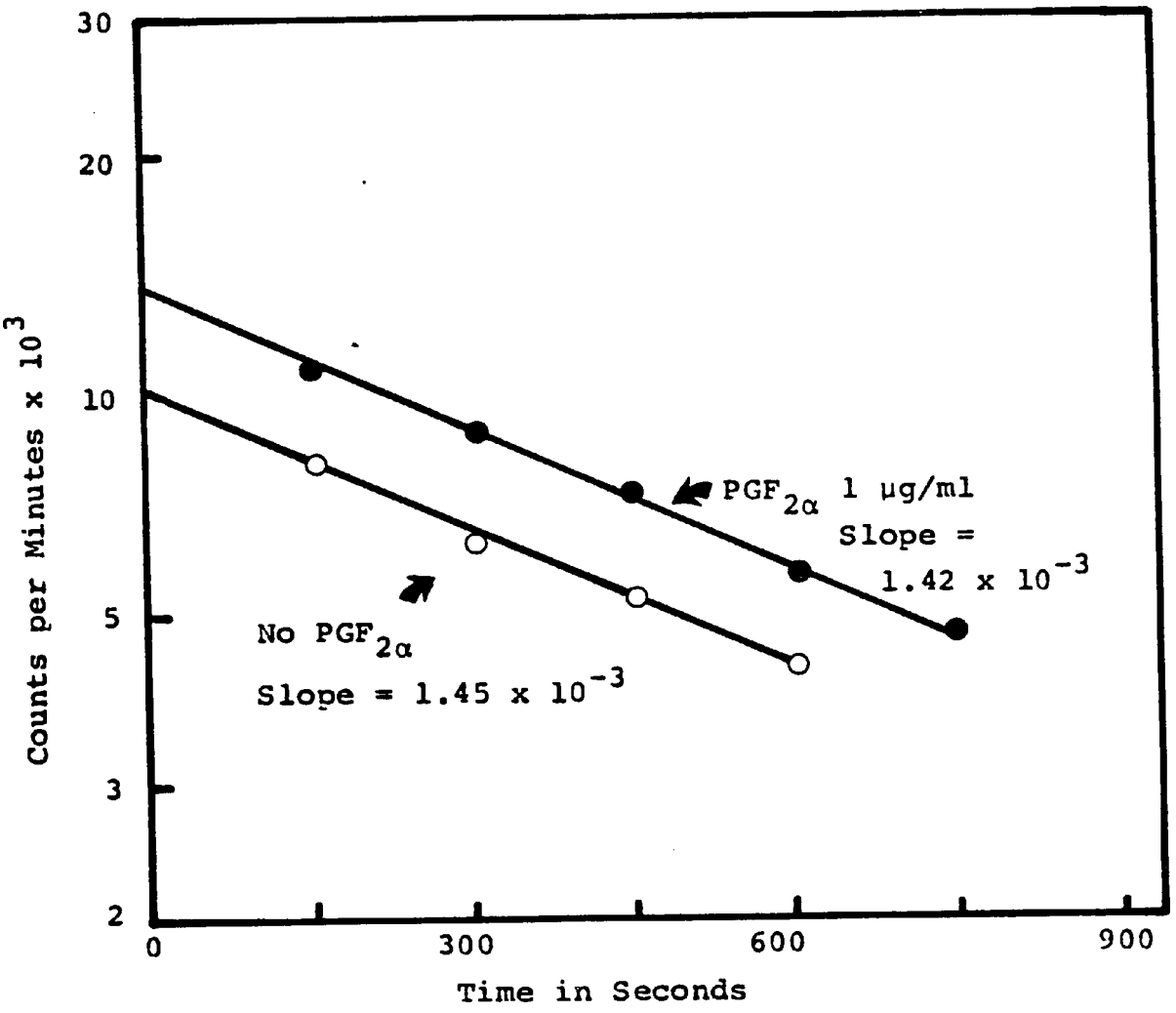


Figure 24. Semilogarithmic plots of the concentration of ^{14}C-n-octanol remaining in the lumen of the jejunum with time in the presence and absence of $PGF_{2\alpha}$ under static, 150 seconds sampling interval, hydrodynamics.

^{14}C benzoate anions at pH 8.5 was not apparently influenced by the presence of $PGF_{2\alpha}$ is an indication that the prostaglandin did not significantly affect the aqueous pore pathway of the jejunal membrane.

It is concluded from the results of the foregoing studies that $PGF_{2\alpha}$ does not have apparent adverse membrane and vascular effects under the experimental conditions employed.

4. Mechanism of Membrane Transport: It was postulated in the theoretical section that the absorption of $PGF_{2\alpha}$ in the rat occurs by passive transport across the aqueous diffusion layer and then by the simultaneous passive membrane transport and bioconversion mechanism. The nature of the K_u versus pH plots in Figure 23, which are of the kind predicted by the pH-partition-aqueous diffusion layer hypothesis for the passive absorption of weak acids, serves as one of the bases for the postulation of the passive mechanism element of the total transport process of $PGF_{2\alpha}$ across the jejunal membrane. As an illustration of this point, the absorption pH profile of $PGF_{2\alpha}$ are similar to that of n-butyric acid in Figure 25.

The following results provide additional evidence that the absorption does not involve a membrane saturable process. As shown in Table XVII and Figure 26, the rate constant of $PGF_{2\alpha}$ at pH 6 and 7.5 is not concentration dependent with concentrations from 1.4×10^{-2} to 200 μM

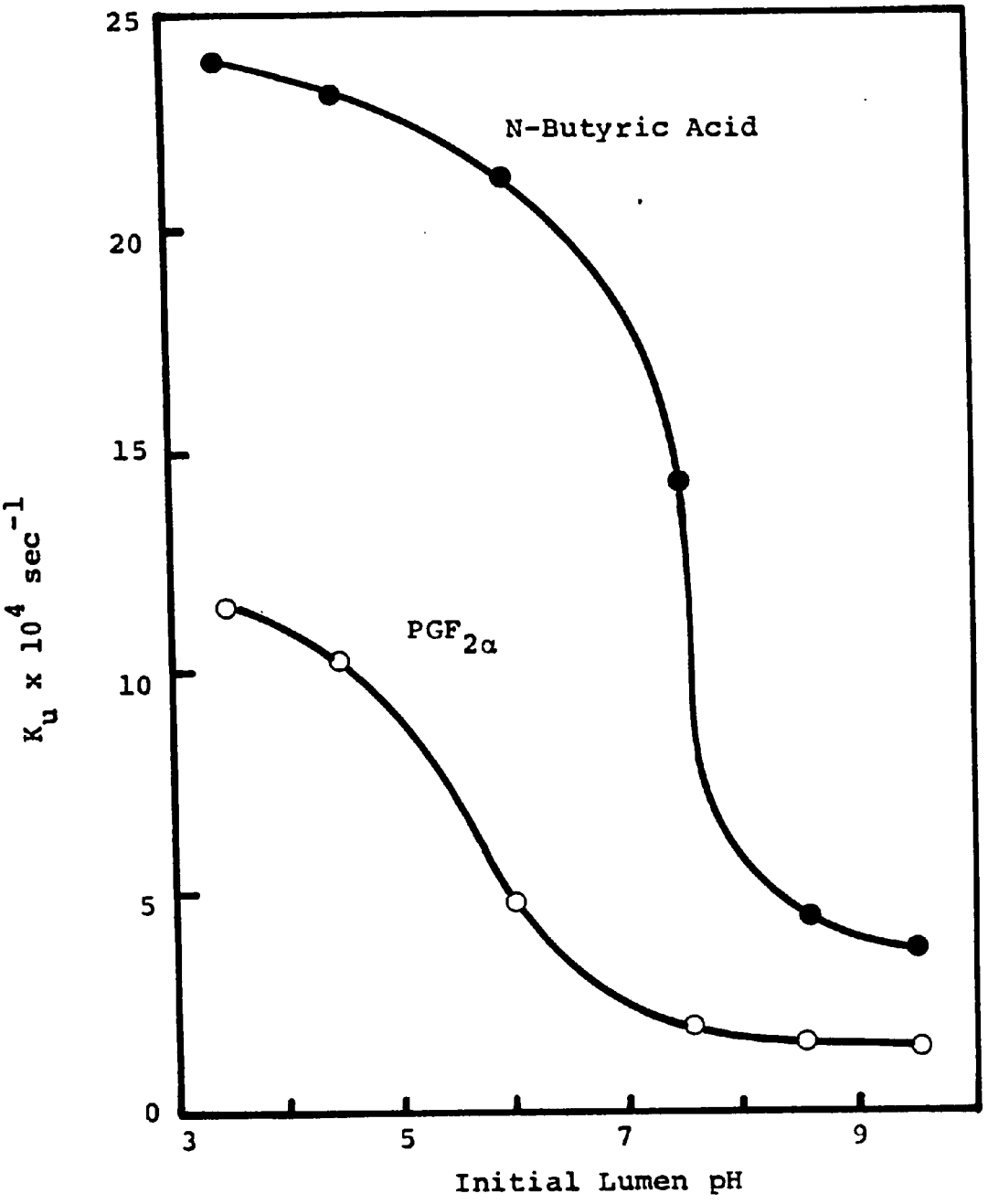


Figure 25. Comparison of the absorption-pH profiles of $PGF_{2\alpha}$ and n-butyric acid under oscillation 0.075 ml/sec hydrodynamics in the rat jejunum. $PGF_{2\alpha}$ undergoes simultaneous diffusional transport-bioconversion kinetics in the membrane while n-butyric acid is passively absorbed.

(a 1.5 x 10^4 fold range). Furthermore, the data in Tables XVIII and XIX indicate that the absorption is not affected by iodoacetic acid and indomethacin, substances found to inhibit the carrier-mediated transport of $PGF_{2\alpha}$ and other

Table XVII. In Situ Absorption of ^3H-$PGF_{2\alpha}$ at Various Concentrations and Buffer pH*

Buffer pH	Buffer Capacity	No. of Expts.	Conc $PGF_{2\alpha}$ µg/ml	$K_u x10^4$ (s.d.) sec^{-1}
6.0	Std	3	5 x 10^{-3}	4.45 (0.18)
		2	1	5.11 (0.75)
		2	10	5.05 (0.07)
		3	100	4.61 (0.26)
7.5	1.5 Std	3	5 x 10^{-3}	1.56 (0.15)
		3	1	1.81 (0.17)

*Oscillation hydrodynamics (0.075 ml/sec) employed $PGF_{2\alpha}$ concentrations at 1-100 µg/ml involved the $PGF_{2\alpha}$-tham salt with 5 x 10^{-3} µg/ml ^3H-$PGF_{2\alpha}$ added.

Table XVIII. Absorption of ^3H-$PGF_{2\alpha}$ in the Absence and Presence of Indomethacin at Buffer pH 7.5*

Order of Exp't in same jejunal segment, 22 cm	Rat A		Rat B	
	Conc Indomethacin	$K_u x10^4$ sec^{-1}	Conc Indomethacin	$K_u x10^4$ sec^{-1}
1	0	1.99	10^{-5}M	1.71
2	10^{-5}M	1.83	0	1.74
3	0	1.71	10^{-5}M	1.61

*Oscillation hydrodynamics, 0.075 ml/sec. Buffer capacity is 1.5 Std. $PGF_{2\alpha}$ concentration is 1 µg/ml $PGF_{2\alpha}$-tham with 5 x 10^{-3} g/ml ^3H-$PGF_{2\alpha}$.

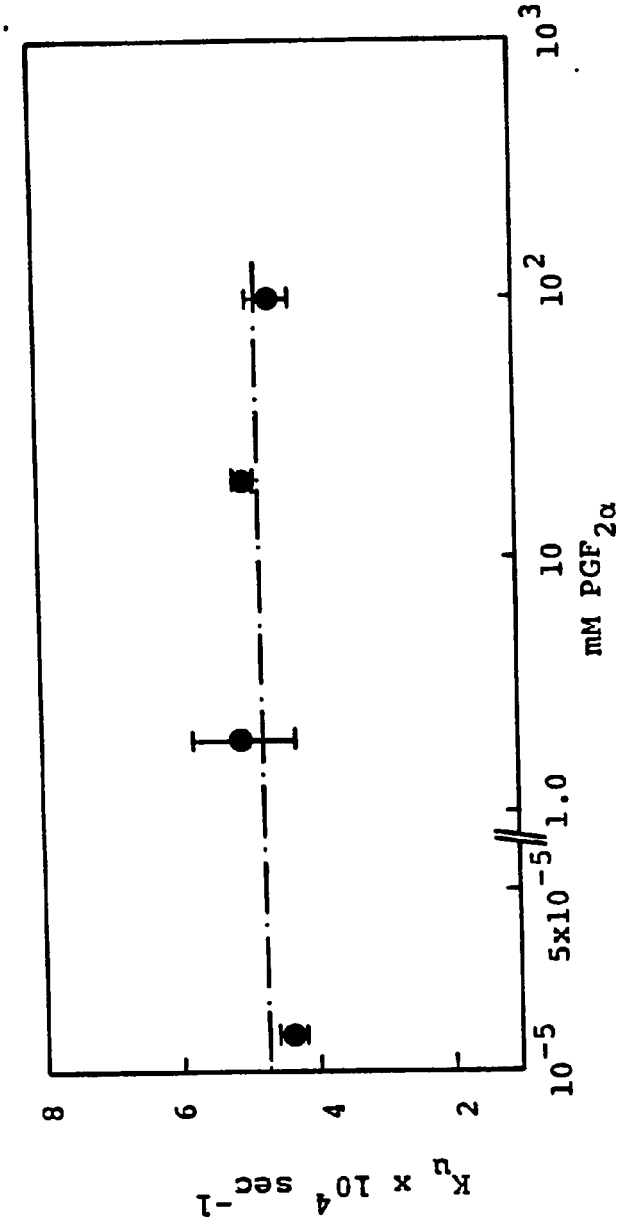


Figure 26. Effect of $PGF_{2\alpha}$ concentration on the intestinal absorption rate constant at pH 6.0 and oscillation hydrodynamics. The bars represent the standard deviation; the dash line is the mean rate constant for all concentrations which is equal to 4.8×10^{-4} sec^{-1}.

prostaglandins.[69] Indomethacin is also known to be a prostaglandin synthetase inhibitor.

Table XIX. In Situ Absorption of ^{3}H-$PGF_{2\alpha}$ in the Absence and Presence of Iodoacetic Acid at Buffer pH 6.0.

Order of exp't in same jejunal segment, 22 cm	Rat A		Rat B		Rat C	
	Iodo-acetic Acid, mM	$K_u x 10^4$ sec^{-1}	Iodo-acetic Acid, mM	$K_u x 10^4$ sec^{-1}	Iodo-acetic Acid, mM	$K_u x 10^4$ sec^{-1}
1	0	4.50	2	4.83	10	4.64
2	2	4.77	0	4.81	--	- -
3	0	4.80	2	4.73	--	- -

Oscillation hydrodynamics, 0.075 ml/sec. Buffer capacity is 1.5 Std. ^{3}H-$PGF_{2\alpha}$ concentrations are 5×10^{-3} µg/ml for rats A and B and 0.1 µg/ml for rat C.

5. Metabolism Studies: These studies were carried out to generally characterize the metabolism of $PGF_{2\alpha}$ in the first 20 minutes of the in situ rat intestinal absorption experiments at buffer pH 6.0. The results in Figure 27 show that the first 5 minutes there is less than 1.0 percent of 15-keto-$PGF_{2\alpha}$ and 13, 14-dihydro-15-keto-$PGF_{2\alpha}$ appearing in the lumenal solution and in 20 minutes there are about 10 percent of these major metabolites present. $PGF_{2\alpha}$ was not metabolized in vitro in rat blood and the lumenal secretion solution (Figure 28). How-

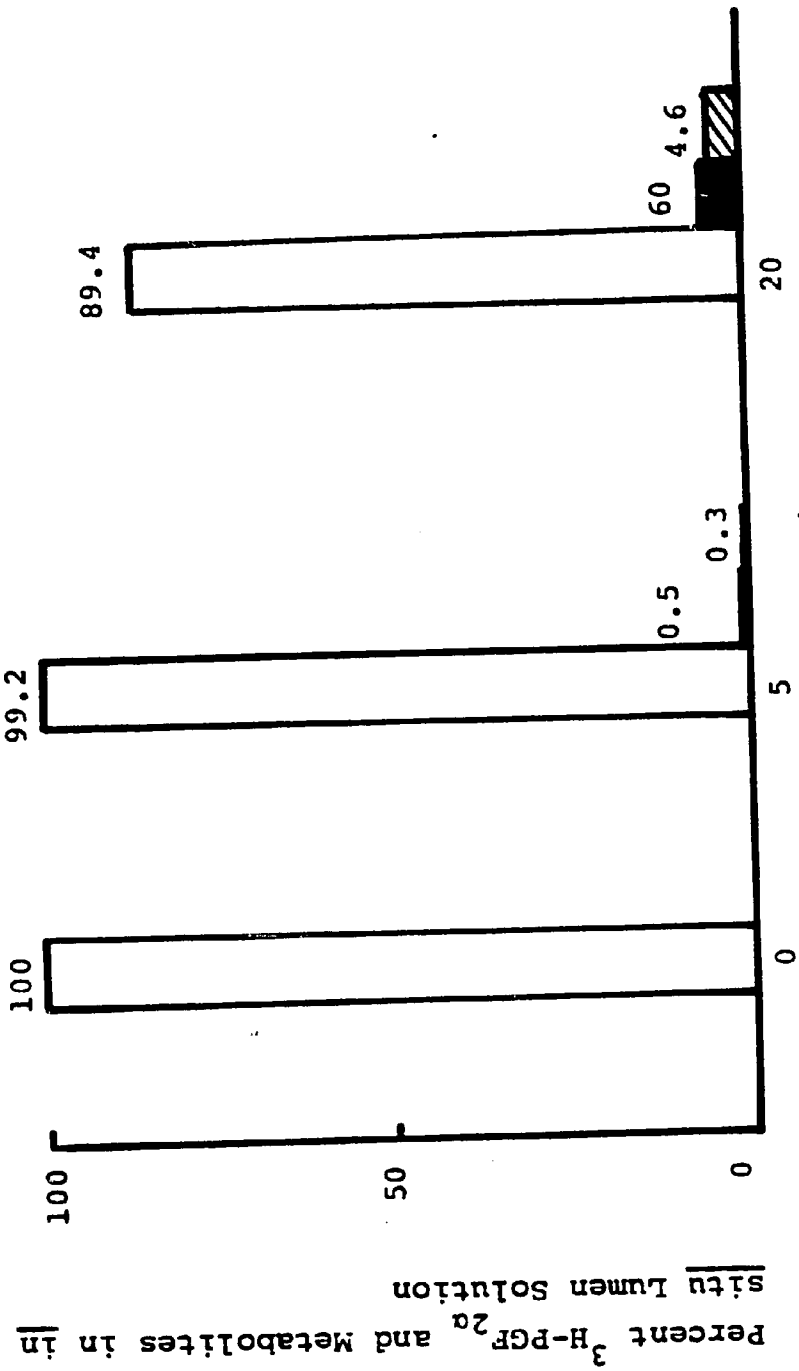


Figure 27. Percent of radiolabeled PGF$_{2\alpha}$ and metabolites found in the lumen of the rat jejunum in situ with time.

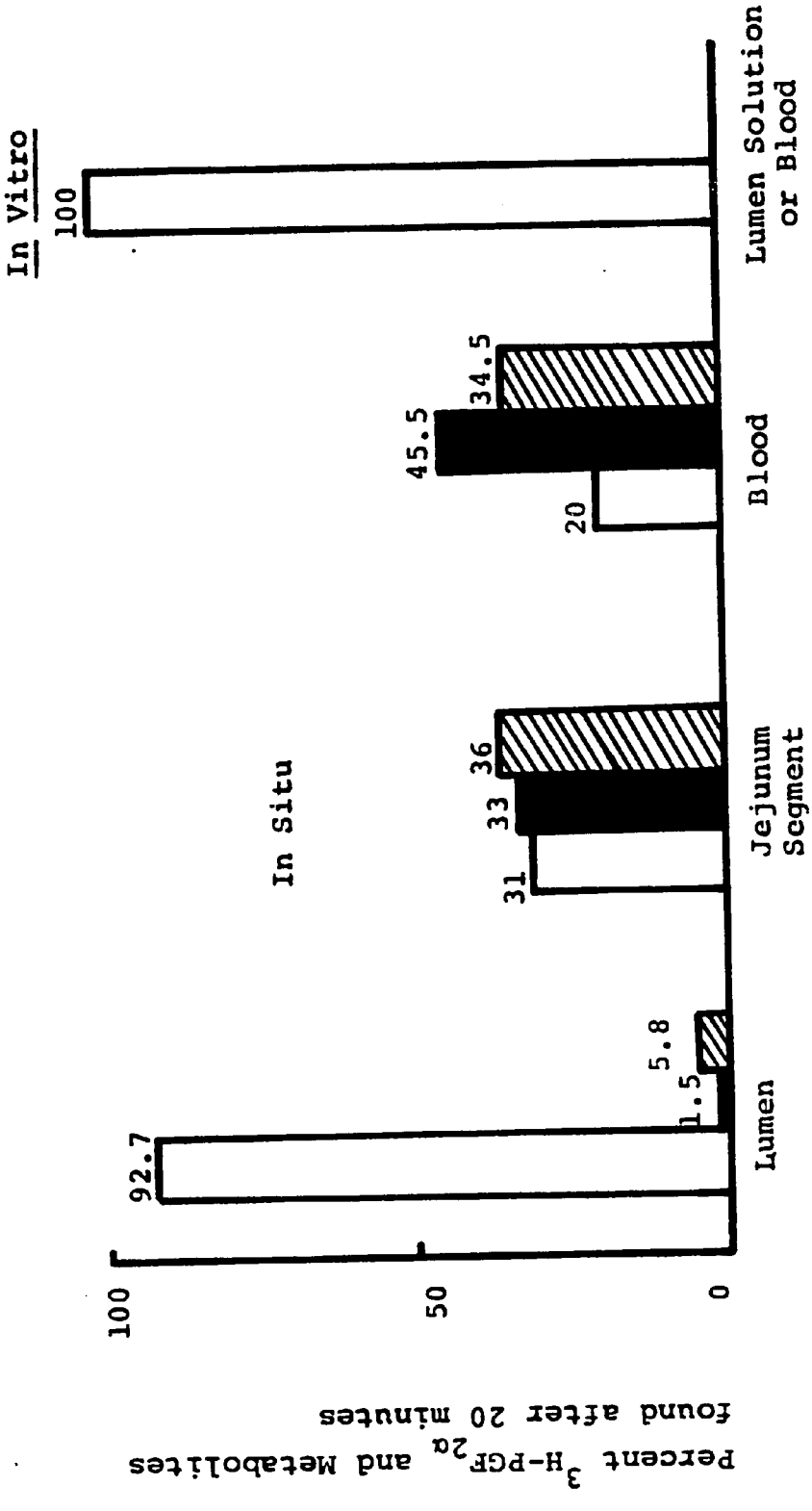


Figure 28. Percent of radiolabeled $PGF_{2\alpha}$ and metabolites found in the lumenal solution, jejunal gut segment and blood after 20 minutes from in situ absorption experiments and in the lumenal solution and blood after 20 minutes exposure from in vitro experiments. Legend: $PGF_{2\alpha}$, 15-keto-$PGF_{2\alpha}$, 13,14-dihydro-15-keto-$PGF_{2\alpha}$.

ever, $PGF_{2\alpha}$ and its major metabolites (15-keto- and 13,14-dihydro-15-keto-$PGF_{2\alpha}$) were found in the intestinal segments and the blood in the in situ absorption studies. If ß-oxidation products were present, it could not be detected by the chromatographic techniques employed.

Taking the preliminary in vitro and in situ studies together, the results infer that there is no metabolism of $PGF_{2\alpha}$ in the lumen, metabolism by 15-OH prostaglandin dehydrogenase and Δ^{13}-reductase occurs in the membrane and there is a back diffusion of metabolites into the lumen. Although the possibility of membrane contact metabolism of $PGF_{2\alpha}$remains, it seems unlikely since the enzyme systems usually associated with the membrane surface include the carbohydrases, peptidases, lipases, hydrolases and iso-enzymes of alkaline phosphatase.[8] As shown in Table XX and Figure 29, the absorption is not affected by furosemide

Table XX. Absorption of ^{3}H-$PGF_{2\alpha}$ in the Absence and Presence of Furosemide at Buffer pH 4.5, 6.0 and 7.5

	Rat A		Rat B	
Buffer pH	Concentration of Furosemide	$K_u x10^4$ sec^{-1}	Concentration of Furosemide	$K_u x10^4$ sec^{-1}
4.5	0	8.57	0	9.39
	10^{-2} mM	7.95	10^{-2} mM	9.56
6.0	0	4.98	0	- -
	10^{-2} mM	4.87	2 mM	4.85
7.5	0	2.41		
	10^{-2} mM	2.20		

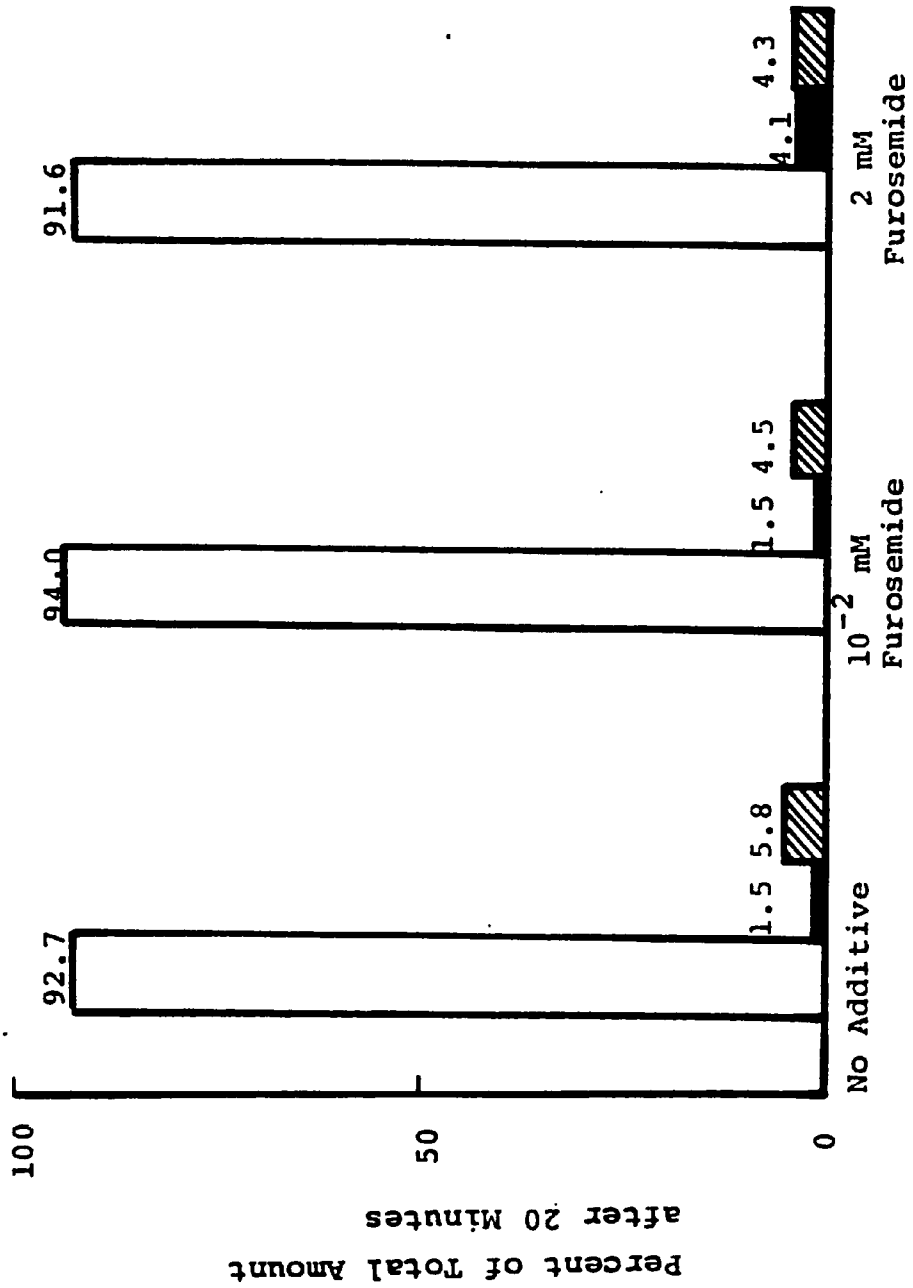


Figure 29. Percent of radiolabeled $PGF_{2\alpha}$ and metabolites found in the lumen of the rat jejunum after 20 minutes in situ experiments in the presence and absence of furosemide at pH 6.0. Legend: $PGF_{2\alpha}$ 15-keto-$PGF_{2\alpha}$ 13,14-dihydro-15-keto-$PGF_{2\alpha}$.

which is known to be a 15-hydroxy prostaglandin dehydrogenase inhibitor. Furthermore, Figure 30 indicates that the furosemide (10^{-2} mM) does not have adverse effects on the membrane under the experimental conditions.

6. Permeability Coefficients: The theoretical physical model described above is operationally consistent with the experimental evidence. Consequently, the permeability coefficients of the aqueous diffusion layer, the diffusional transport-bioconversion and aqueous pore pathways of the jejunal membrane may be estimated from the derived modelistic statements.

As previously discussed in Chapter I of the theoretical section, the following relations hold between two absorption rate constants obtained at the same buffer pH but under different hydrodynamics in the lumen.

$$\frac{1}{P_{aq}} + \frac{1}{P_{e,m}} = \frac{A}{VK_u} \qquad \text{(Eq. 21)}$$

$$\frac{1}{P'_{aq}} + \frac{1}{P_{e,m}} = \frac{A}{VK'_u} \qquad \text{(Eq. 22)}$$

$$r^* = P'_{aq}/P_{aq} \qquad \text{(Eq. 23)}$$

The ratio r^* has already been determined for a number of hydrodynamic situations in the rat intestinal tract using the n-alkanol series (Table V). Between the continuous oscillation 0.075 ml/sec and the static 150 sec sampling interval cases, r* is 2.12. As shown in Table XXI, the

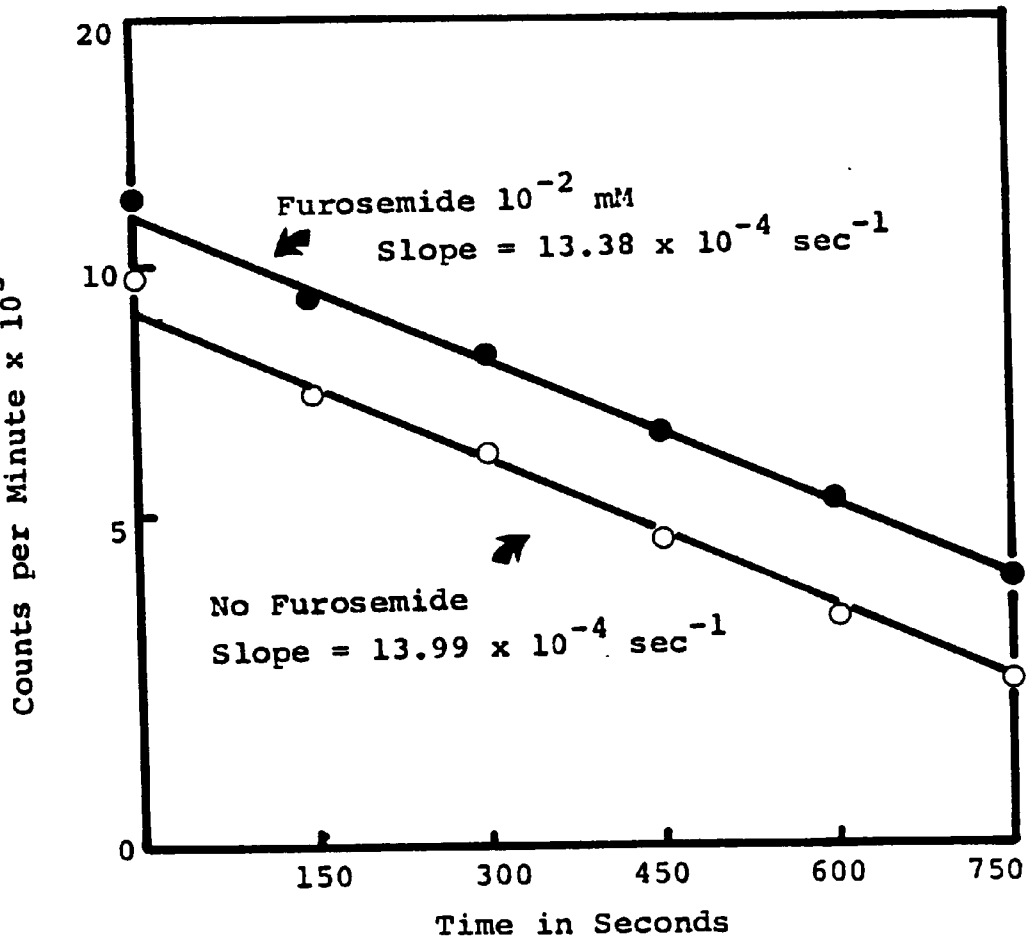


Figure 30. Semilogarithmic plots of the concentration of ^{14}C-n-butanol remaining in the lumen of the jejunum with in the absence and presence of furosemide to assess membrane damage at pH 6.0.

Table XXI. Permeability Coefficients of the Aqueous Diffusion Layer

Buffer pH	$K_u \times 10^4$ sec^{-1} Static 150 sec	$K_u \times 10^4$ sec^{-1} Oscillation 0.075 m/sec	Permeability Coefficient $\times 10^4$ cm/sec P_{aq} (Static)	Permeability Coefficient $\times 10^4$ cm/sec P_{aq} (Oscill)
3.5	6.61	11.09	0.8	1.64
4.5	5.66	8.65	0.8	1.64

P_{aq} for the static and oscillation situations and $P_{e,m}$ were calculated from the experimental rate constants with the use of Eqs. 21 and 22. The r* is 2.12 and A/V is 11.2.

permeability coefficients of the aqueous diffusion layer (P_{aq}) for the static and oscillation hydrodynamic situations are 0.8×10^{-4} and 1.7×10^{-4} cm sec^{-1}, respectively. The effective membrane permeability coefficients ($P_{e,m}$) are 2.57×10^{-4} cm sec^{-1} at buffer pH 3.5 and 1.46×10^{-4} at pH 4.5. Since the aqueous diffusion coefficient of $PGF_{2\alpha}$ is equal to 5.1×10^{-6} cm^2 sec^{-1}, the effective diffusion layer thickness is 310 microns for the oscillation hydrodynamics and 662 microns for the static situation.

The permeability coefficient of the aqueous pores (P_p) is determined from the experimental data in the limit of the buffer pH>>pK_a; thus

$$K_{u,min} = \frac{A/V}{\frac{1}{P_{aq}} + \frac{1}{P_p}} \qquad \text{(Eq. 57)}$$

Using Tables XII and XXI where the average $K_{u,min}$ is 1.51 x 10^{-4} sec^{-1} and P_{aq} (oscillation) is 1.7 x 10^{-4} cm sec^{-1}, one finds that P_p is 1.5 x 10^{-5} cm sec^{-1}. This may be compared to the P_p of the salicylate and p-aminobenzoate ions in the jejunum of 2.8 x 10^{-5} cm sec^{-1} and to that of taurocholate anion which is experimentally negligible.[80] It is reasonable to assume that the P_p of the nondissociated $PGF_{2\alpha}$ is at least equal to, if not slightly larger than the P_p of the anion. Consequently, the effective permeability coefficient of the principal transport-bioconversion pathway of the membrane, which is pH-dependent, can be readily found and completes the factorization of the effective permeability coefficient of the membrane (Table XXII).

Table XXII. Factorization of the Effective Permeability Coefficients of the Jejunal Membrane at Various Buffer pH into the Permeability Coefficients of the Aqueous Pores and Principal Membrane Pathway

Buffer pH	Buffer Capacity	Permeability Coefficient x 10^4 cm sec^{-1}		
		$P_{e,m}$	P_{pore}	$\frac{\alpha K X_s \sqrt{kD}}{\tanh(L\sqrt{k/D})}$
3.5	1.5 Std	2.59	0.15	2.44
4.5	Std	1.44	0.15	1.29
6.0	Std	0.53	0.15	0.38
7.5	1.5 Std	0.15	0.15	0
9.5	Std	0.15	0.15	0

The extent to which the transport rate is influenced by the aqueous diffusion layer barrier in front of the mucosal membrane is presented in Table XXIII. As one would expect, the rate constant is more aqueous diffusion-controlled at pH 3.5 than that at pH 4.5 and also the oscillation situation is less aqueous diffusion-controlled, as compared to the static situation. Although the degree of agitation of the lumenal solution at pH 3.5 produced by

Table XXIII. Influence of the Aqueous Diffusion Layer on the Transport Rate of $PGF_{2\alpha}$ in the Jejunum

Buffer pH	Hydrodynamic Condition	$K_{u,expt}$ $\times 10^{4} sec^{-1}$	$K_{u,max}$* $\times 10^{4} sec^{-1}$	Percent of Rate Constant Aqueous Diffusion-Controlled
3.5	Static, 150 sec	6.61	8.96	74
	Oscillation	11.09	19.0	58
4.5	Static, 150 sec	5.66	8.96	63
	Oscillation	8.65	19.0	46
6.0	Static 150 sec	3.56	8.96	40
	Oscillation	4.67	19.0	25
7.5 9.5	Oscillation	1.51	19.0	8

*Static case: $K_{u,max} = AP_{aq}/V = 11.2 \times 0.8 \times 10^{-4}$

$= 8.96 \times 10^{-4}$

Oscillation: $K_{u,max} = 11.2 \times 1.7 \times 10^{-4} = 19.0 \times 10^{-4}$

rapidly oscillating the solution is high, the rate is yet 60 percent diffusion-controlled. At higher pH values the rate is less aqueous diffusion-controlled.

7. General Observations of Buffer Capacity on In Situ $PGF_{2\alpha}$ Absorption: It was pointed out earlier in Figure 21 that the first order absorption-time profiles at pH 3.5 and 4.5 tend to depart from linearity with time. As also shown in Table XII for those cases where different buffer capacities at initial pH 3.5 and 7.5 were used, the rate constants varied with buffer capacity. Because of these observations and other intestinal absorption studies,[7] all $PGF_{2\alpha}$ absorption studies were carried out at sufficiently high buffer capacities such that the initial rate constants at all buffer pH were independent of buffer strength.

To complete the baseline studies, additional experiments were carried out wherein both the intestinal absorption and bulk lumenal pH changes with time were simultaneously followed at initial pH 3.5 and 7.5 and two buffer strengths. In Figure 31 one observes that the first order absorption curves for the pH 3.5 situation are linear for a short time period and then gradually decreases with time while the bulk lumenal pH increases with time toward pH 6.0. These changes occur more rapidly with the lower of the two buffer strengths employed. In both cases the initial slopes in the absorption curves are about the same. In

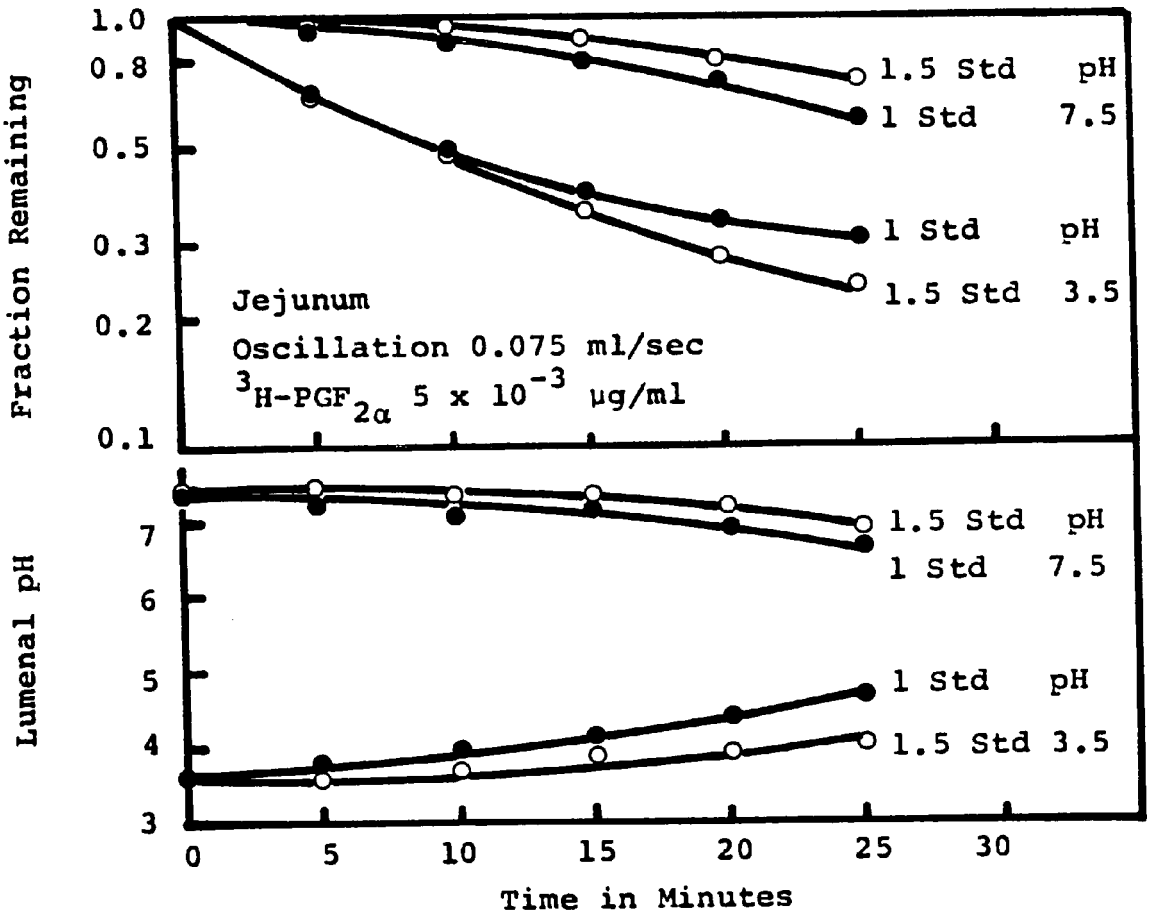


Figure 31. Semilogarithmic change in the lumenal concentration of $PGF_{2\alpha}$ and bulk pH change with time for the pH 3.5 and 7.5 cases under oscillation hydrodynamics and two buffer strengths.

contrast, the increase in the absorption with time at pH 7.5 is accompanied with a slow decrease in the bulk pH with time. These occur faster at lower buffer capacities.

All of these observations are consistent with the mechanistic studies on the rat intestinal absorption of n-butyric acid in which the factors influencing the dynamics of the surface pH, i.e., the pH at the aqueous-membrane interface, was quantitatively assessed. Because the surface pH depends upon the net effect of the fluxes of the intestinal buffer secretions and buffer species from the bulk solution, it becomes critical that sufficiently high buffer capacity solutions in the lumen should be used to have a baseline control of the surface pH relative to the initial bulk pH.

C. Quantitative Assessment of the Influence of Molecular Substituents Groups on the Intestinal Absorption Process of Prostaglandins.

1. Introduction: The purpose of this section is to demonstrate the quantitative assessment of molecular substituents of various prostaglandins, as model solutes, on the overall small intestinal absorption process. In situ rat intestinal absorption are interfaced with in vitro enzyme kinetic studies whereby the combination of the in situ permeability coefficients for the membrane passive diffusional-bioconversion pathway and the in vitro V_{max} and Michaelis K_M enzyme kinetic parameters has yielded specific

quantitative assignment of substituent groups to membrane partitioning and bioconversion by the physical model approach.

2. General Results: The rat intestinal absorption of prostaglandins $F_{2\alpha}$ and E_2 at various buffer pH and hydrodynamic conditions is illustrative of the physical model predictions (Figures 23, 32). The effect of stirring on the hydrodynamic boundary layer in front of the mucosal membrane is evident. Although $PGF_{2\alpha}$ is absorbed slower than PGE_2 at relatively low pH, the absorption of the anions of these weak acids at high pH are the same. There is much similarity in the shapes of the absorption curves to those of the n-alkanoic acids. The absorption versus chain length profiles of the $PGF_{2\alpha}$ C_1-n-alkylamide homologs is shown in Figure 33. The absorption of the C_1-amides are independent of pH. Both the weak acids and the $PGF_{2\alpha}$ C_1-amides are metabolized consecutively by 15-OH prostaglandin dehydrogenase and Δ^{13}-reductase to their respective 15-keto- and 13,14-dihydro, 15-keto-prostaglandins in the biomembrane. These absorption studies were derived from in situ experiments in the rat jejunum by a modified Doluisio method. An analytical breakdown of the first order absorption rate constants into their component permeability coefficients are found in Table XXIV.

In vitro enzyme kinetic studies show that PGE_2, $PGF_{2\alpha}$, $PGF_{2\alpha}$ C_1-n-alkylamide derivatives are substrates to monkey

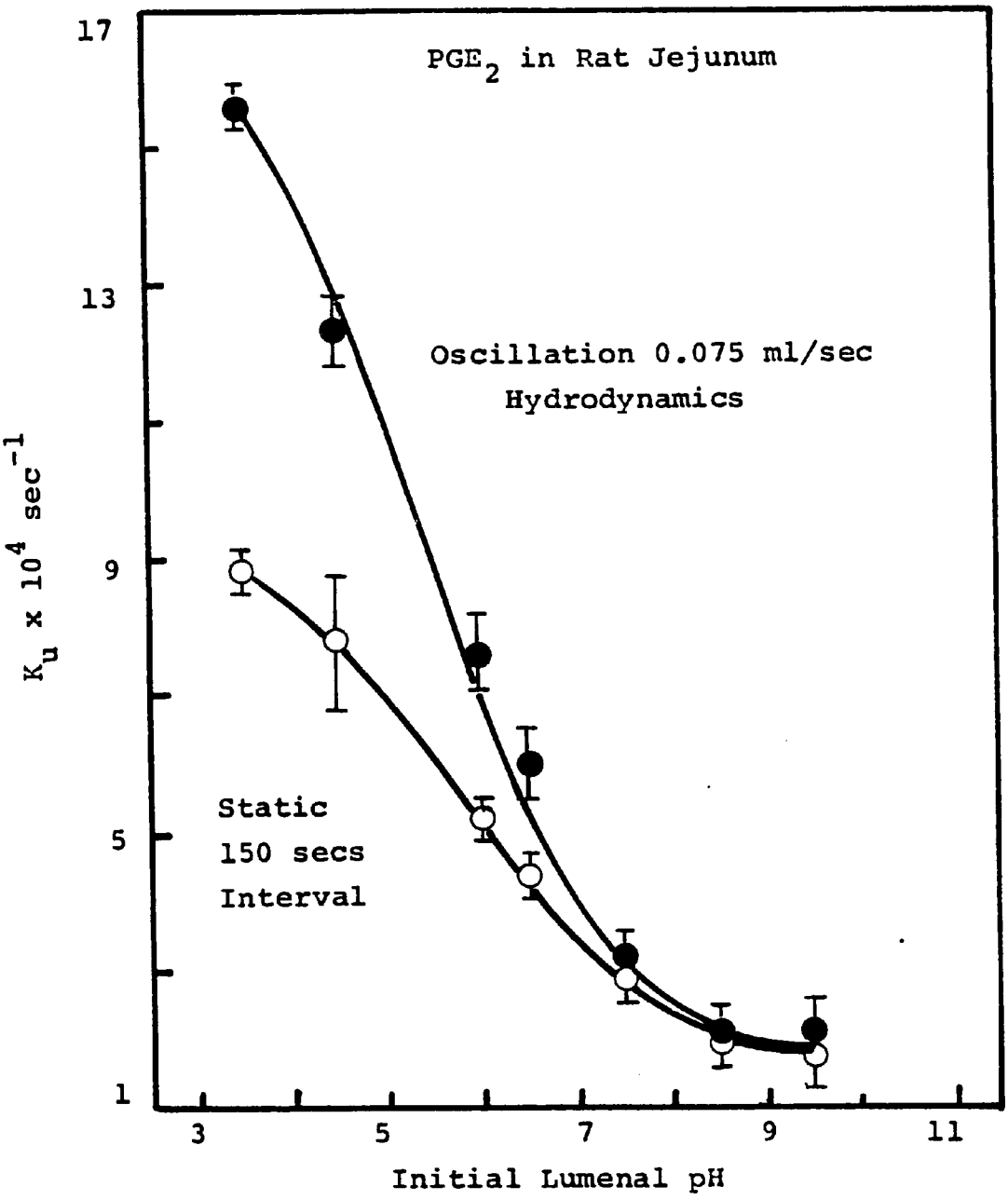


Figure 32. Apparent absorption rate constants versus high buffer capacity pH under two hydrodynamic conditions.

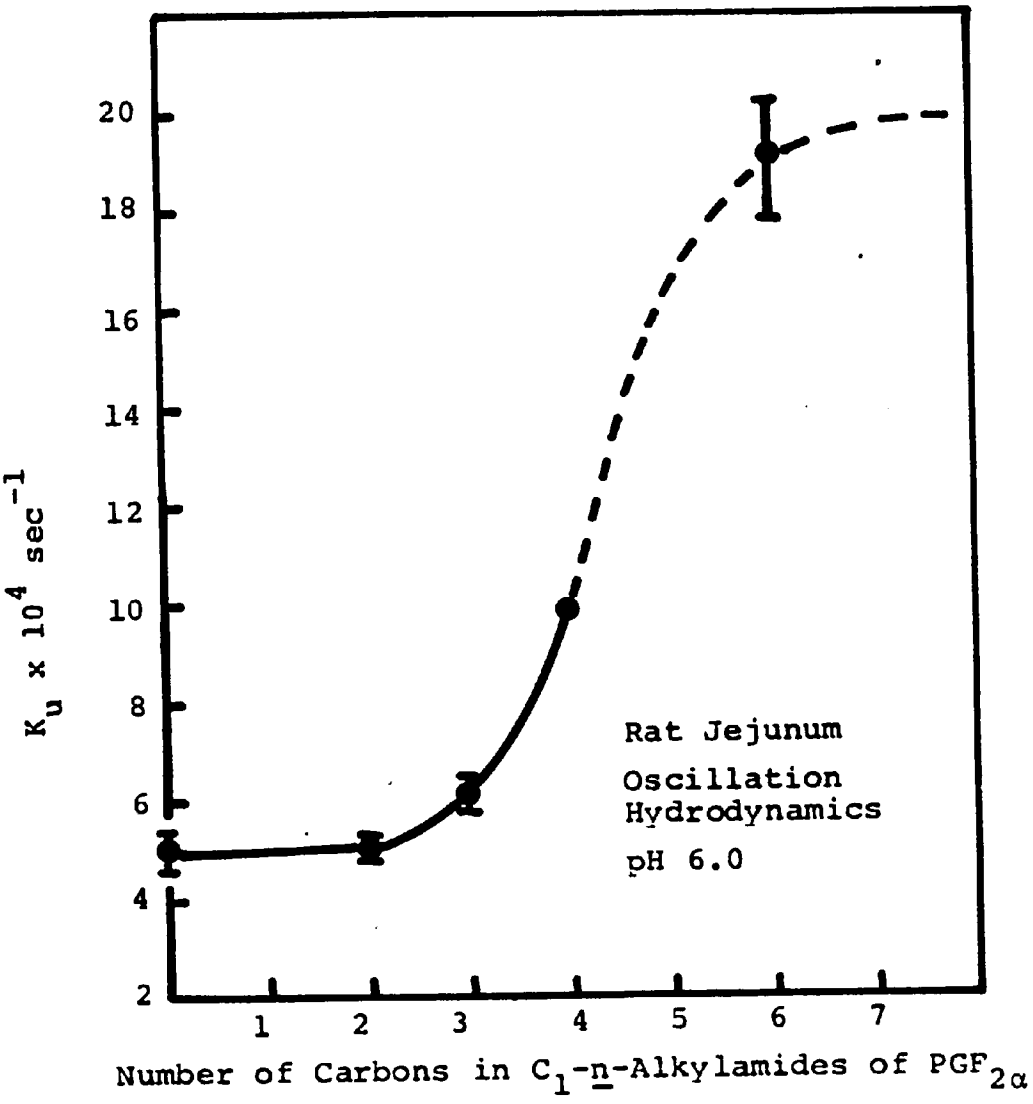


Figure 33. In situ absorption rate constants of the $PGF_{2\alpha}$ C_1-n-alkylamides, including $PGF_{2\alpha}$ amide. The sigmoidal shape of the profile (extrapolated by the dashed lines) is predicted by the theory.

Table XXIV. Permeability Coefficients of Various Prostaglandins Obtained from *In Situ* Rat Jejunal Studies at 37°C.

Prostaglandin		Permeability Coefficients x 10^4 cm/sec			
		P_{app}	P_{aq}	P_p	$P_{e,m}$
PGE_2	pH 3.5	1.38	1.8	0.2	5.6
	4.5	1.07	1.8	0.2	2.40
	6.0	0.68	1.8	0.2	0.9
$PGF_{2\alpha}$	pH 3.5	1.01	1.7	0.15	2.4
	4.5	0.83	1.7	0.15	1.2
	6.0	0.41	1.7	0.15	0.38
$PGF_{2\alpha}C_1$-carbamoylmethylamide		0.23	1.64	∿0	0.26
$PGF_{2\alpha}$ C_1-amide		0.45	1.7	0.15	0.47
$PGF_{2\alpha}$ C_1-ethylamide		0.47	1.67	∿0	0.65
$PGF_{2\alpha}$ C_1-*n*-propylamide		0.57	1.66	∿0	0.9
$PGF_{2\alpha}$ C_1-*n*-butylamide		0.89	1.64	∿0	1.94
$PGF_{2\alpha}$ C_1-*n*-hexylamide		1.54	1.62	∿0	32.0

P_{aq}, P_p and $P_{e,m}$ are the permeability coefficients of the aqueous diffusion layer, aqueous pores of the membrane and the membrane diffusional-bioconversion pathway, respectively. P_{app} is the apparent permeability coefficient.

lung prostaglandin dehydrogenase, $PGF_{2\alpha}$ C_1-carbamoylmethylamide is not. The maximum enzymatic rates, v_{max}, and Michaelis constants, K_M, are found in Table XXV. In the ensuing π^* analysis two basic assumptions are made with regards to the application of the *in vitro* metabolism data

Table XXV. Michaelis Constant and ν_{max} of Various Prostaglindins using Monkey Lung Prostaglandin Dehydrogenase.[82]

Prostaglandin	$K_M \times 10^6$ M	Relative ν_{max} with $PGF_{2\alpha}$ as 100%
PGE_2	11	112
$PGF_{2\alpha}$	59	100
$PGF_{2\alpha}$ C_1-carbamoyl methylamide	not a substrate	
$PGF_{2\alpha}$ C_1-amide	158	41
$PGF_{2\alpha}$ C_1-methylamide	439	39
$PGF_{2\alpha}$ C_1-ethylamide	333	24
$PGF_{2\alpha}$ C_1-n-propylamide	438	23
$PGF_{2\alpha}$ C_1-n-butylamide	196	17
$PGF_{2\alpha}$ C_1-n-hexylamide	149	16*

*Considered as rough estimate due to turbidity occurring during measurements.

$\nu_{max,PGF_{2\alpha}}$ = 740 nM/min/mg protein.

to the membrane situation: firstly, the metabolism of the prostaglandin to the 15-keto form is the rate-determining step; secondly, although the absolute values of the *in vitro* ν_{max} and K_M of each prostaglandin are generally not expected to be identical to those in the membrane, the ratio of the apparent first order rate constants between two prostaglandins (for example, PGE_2 and $PGF_{2\alpha}$ or $PGF_{2\alpha}$

C_1-amide and C_1-methylamide) can be more reasonably assumed to be the same in the membrane. As it turns out, these assumptions appear to be reasonable.

3. π^* Analysis Between PGE_2 and $PGF_{2\alpha}$: Prostaglandins $F_{2\alpha}$ and E_2 differ from each other by a hydroxyl and keto group at the C_9 position, respectively. By choosing $PGF_{2\alpha}$ as the reference and taking the logarithm of the ratio of the permeability coefficients at the same pH, the pH effects cancels out and the π^* is found to be reasonable invariant of pH as would be expected (Table XXVI). The average π^* is equal to + 0.35. The π_k is estimated from the *in vitro* ν_{max} and K_M in Table XXV; thus

$$\pi_k = 0.5 \log \frac{(\nu_{max}/K_M)_{PGE_2}}{(\nu_{max}/K_M)_{PGF_{2\alpha}}} = 0.38$$

Table XXVI. Analysis of Values Between PGE_2 and $PGF_{2\alpha}$

pH	$P_{e,m} \times 10^4$ cm/sec		n*	π^*	Estimated π_k and π_{PC}
	PGE_2	$PGF_{2\alpha}$			
3.5	5.6	2.4	2.33	0.37	$\pi_k = 0.38$
4.5	2.4	1.20	2.0	0.30	$\pi_{PC} = -0.04 \simeq 0$
6.0	0.9	0.38	2.37	0.37	
Average			2.23	0.35	

Physically, this means that the metabolism of PGE_2 is faster than that of $PGF_{2\alpha}$.

Accordingly, in evaluating the relative lipophilicity of the 9-hydroxyl and 9-keto moiety to passive diffusion across the biomembrane,

$$\pi_{PC} = \pi^* - \pi_k = 0.35 - 0.38 = -0.03$$

For practical purposes π_{PC} is zero. In a n-octanol/0.01N HCl log PC is 2.82 for PGE_2 and 2.73 for $PGF_{2\alpha}$[60] or π_{PC} (n-octanol/0.01N HCl) is 0.09. The estimated π_{PC} (isobutanol/0.1N HCl) is 0.06. Although PGE_2 is slightly more lipophilic than $PGF_{2\alpha}$, the π_{PC} in the above analysis (Table XXVI) for the rat jejunum was not able to detect the small differences in the lipophilicity within experimental error.

4. π^* Analysis Between $PGF_{2\alpha}$ and $PGF_{2\alpha}$ C_1-Amide: Here, $PGF_{2\alpha}$ is used as the reference prostaglandin. The more hydrophilic $PGF_{2\alpha}$ C_1-amide has a smaller $P_{e,m}$ than that for $PGF_{2\alpha}$ and the overall incremental constant n^* is less than unity and π^* is a negative quantity (Table XXVII). As can be seen, the metabolism of $PGF_{2\alpha}$ by dehydrogenase is more efficient and, in physical quantitative terms,

$$\pi_k = 0.5 \log \frac{(\nu_{max}/K_M)_{PGF_{2\alpha}\ C_1\text{-amide}}}{(\nu_{max}/K_M)_{PGF_{2\alpha}}} = -0.41$$

Table XXVII. Analysis of π Values Between $PGF_{2\alpha}$ and $PGF_{2\alpha}$ C_1-Amide

Prostaglandin	$P_{e,m} \times 10^4$ cm/sec	n*	π*	Estimated π_k	Estimated π_{PC}
$PGF_{2\alpha}$ C_1-amide	0.47	0.17	-0.77	-0.41	-0.36
$PGF_{2\alpha}$ (free acid)	2.75				

Subsequently,

$$\pi_{PC} = \pi^* - \pi_k = -0.77 - (-0.41)$$
$$= -0.36$$

This analysis shows that the $P_{e,m}$ of $PGF_{2\alpha}$ C_1-amide is smaller than that of $PGF_{2\alpha}$ because the C_1-amide derivative is not only more hydrophilic but also not metabolized as rapidly.

It is noteworthy in Table XXVIII that the π_{PC} values for the n-octanol/0.01N HCl and isobutanol/0.01N HCl systems give a close approximation to that estimated for lipoidal biophase of the rat jejunal membrane.

5. π* Analysis Between $PGF_{2\alpha}$ C_1-Amide and $PGF_{2\alpha}$ C_1-Carbamoylmethylamide: Between the carbamoylmethylamide and the more lipophilic amide derivatives in Table XXIX, the π* from the intestinal absorption experiments is -0.26. Because the carbamoylmethylamide derivative is not a substrate to dehydrogenase while $PGF_{2\alpha}$ C_1-amide is a sub-

Table XXVIII. *In Vitro* Partition Coefficients of $PGF_{2\alpha}$ and $PGF_{2\alpha}$ C_1-Amide*

System	log PC		π
	$PGF_{2\alpha}$	$PGF_{2\alpha}$ C_1-amide	
n-Octanol/0.01N HCl	2.73	2.28	-0.45
n-Butanol/0.01N HCl	2.28	1.97	-0.31

*Log PC of $PGF_{2\alpha}$ in n-octanol/0.01N HCl was experimentally determined. All other values were then obtained by estimation of the π additive approach.

Table XXIX. Analysis of π Values Between $PGF_{2\alpha}$ C_1-Amide* and $PGF_{2\alpha}$ C_1-Carbamoylmethylamide

Prostaglandin	$P_{e,m} \times 10^4$ cm/sec	n*	π*	Estimated π_{PC}
$PGF_{2\alpha}$ C_1-carbamoyl methylamide	0.36	0.55	-0.26	-0.26
$PGF_{2\alpha}$ C_1-amide	0.47			

*$PGF_{2\alpha}$ C_1-amide is used as the reference prostaglandin.

strate, the π_k as expressed by Eq. 52 is not relevant here since it will be mathematically absurd. Instead, one should use Eq. 58:

$$\pi^* = \pi_{PC} + \log \frac{\tanh(L\sqrt{k/D})}{L\sqrt{k/D}} \qquad \text{(Eq. 58)}$$

where

k,D = apparent first order rate constant and membrane diffusion coefficient for $PGF_{2\alpha}$ C_1-amide, respectively.

In assuming the logarithm term to be negligible as compared to π_{PC} in the first approximation, then

$$\pi^* \simeq \pi_{PC} = -0.26$$

6. π^* Analysis of $PGF_{2\alpha}$ C_1-n-alkylamide Homologs:

Table XXX shows the summary of the π analyses of the C_1-n-alkylamides of $PGF_{2\alpha}$. Each homolog was compared against the subsequent decrement in the series. It is seen with the amide-ethylamide and ethylamidepropylamide sets that the π^* quantities are identical; however, the π_k's are

Table XXX. Analysis of π Values Among $PGF_{2\alpha}$ C_1-n-alkylamides Including $PGF_{2\alpha}$ C_1-amide

$PGF_{2\alpha}$ C_1-n-alkylamide Homologs	$P_{e,m} \times 10^4$ cm/sec	n*	π^*	Estimated π_k	Estimated π_{PC}
$PGF_{2\alpha}$ C_1-amide	0.47	1.38	0.14	-0.28	0.42
$PGF_{2\alpha}$ C_1-ethylamide	0.65	1.38	0.14	-0.07	0.21
$PGF_{2\alpha}$ C_1-n-propylamide	0.9	2.16	0.34	0.11	0.23
$PGF_{2\alpha}$ C_1-n-butylamide	1.94				

different. After factoring π_k from π^*, one gets π_{PC} for membrane partitioning which is 0.21 per carbon in the n-alkyl chain. This π_{PC} of 0.21 is in remarkable agreement with the π_{PC} = 0.2-0.25 per CH_2 group found with the n-alkanols and n-alkanoic acids for the rat jejunal membrane.[7]

The rationale for the identical π^* (= 0.14) between the amide-ethylamide and ethylamide-propylamide combinations becomes evident from the above analysis. Initially, one's reaction would usually be that the π^* between the former pair would be greater than the π^* of the latter pair because of the greater degree of lipophilicity provided by the ethyl group increment as compared to a methylene increment. However, one should remember that π^* consists of π_{PC} and π_k. It is seen that π_{PC} per carbon in the n-alkyl chain is about the same (π_{PC} = 0.21-0.25) and π_k becomes the pivotal parameter. The metabolism rate of the ethylamide is effectively less than the amide derivative. This is also the situation for the propylamide with respect to the ethylamide. In examining the π^* of the propylamide-butylamide pair, it is greater than 0.21 which would be expected for the membrane partitioning of a CH_2 group. This is due to the positive π_k.

SUMMARY

The physical model for passive absorption in the intestinal tract of the rat involving an aqueous boundary layer in series with the membrane consisting of parallel lipoidal and aqueous pore pathways was consistent with the results of *in situ* absorption studies using *n*-alkanoic acids and selected steroids and *n*-alkanols. The permeability coefficients of these solutes for the various transport barriers were quantitatively factored out. The π_{CH_2} constant of 0.25 as determined by the *n*-alkanoic acids was in excellent agreement with that reported in the literature for the CH_2 group.

In using the Doluisio method in *in situ* intestinal absorption studies in which the hydrodynamics of the lumenal solution are intermittently altered as often as the sampling intervals chosen, the sampling intervals should be kept constant throughout the time period of the experiment to maintain a level of consistency in the degree of stirring. This is particularly important when the transport rate is largely controlled by the aqueous boundary layer and least important when the transport rate is effectively membrane-controlled.

In the situation in which the solution is continuously oscillated in the lumen at a constant rate, the sampling interval taken does not affect the experimental results because of the uniformity and relative constancy of the

hydrodynamics.

Baseline *in situ* rat intestinal absorption studies and the physical model for passive diffusion coupled with membrane metabolism were established with prostaglandin $F_{2\alpha}$ used as the model drug. The studies also included $PGF_{2\alpha}$ C_1-amide, $PGF_{2\alpha}$ C_1-*n*-alkylamides and $PGF_{2\alpha}$ C_1-carbamoylmethylamide. The *in situ* permeability coefficients of these prostaglandins for the membrane passive diffusional-bioconversion pathway were interfaced with *in vitro* enzyme kinetic parameters of the above-mentioned compounds with purified monkey lung 15-OH prostaglandin dehydrogenase and analyzed by the π^* concept. This concept was developed and expressed mathematically to give specific quantitative assignment of substituent groups to membrane partitioning and bioconversion for such a complex absorption process as the simultaneous membrane transport and metabolism of drugs. The apparent success in this physical model π^* concept approach is evidenced by the identical π_{CH_2} for membrane partitioning among the $PGF_{2\alpha}$ C_1-*n*-alkylamides with respect to that for the *n*-alkanol and *n*-alkanoic acid homologs.

REFERENCES

1. D. H. Smyth, "Biomembrane," Intestinal Absorption, Volume 4A, Plenum Press, New York (1974).

2. A. G. E. Pearce and E. O. Riecken, "Intestinal Absorption," Brit. Med. Bull., 23, 217 (1967).

3. E. D. Jackson and L. L. Shanbour, "Gastrointestinal Physiology," Volume 4, University Park Press, Baltimore, Md., 1974.

4. J. S. Trier, "Handbook of Physiology," Morphology of the Small Intestine, Volume III, Amer. Physiol. Soc. (1968).

5. F. A. Wilson and J. M. Dietschy, Biochim. Biophys. Acta, 363, 112 (1974).

6. Y. L. Sallee, F. A. Wilson, and J. M. Dietschy, J. Lipid Res., 13, 184 (1972).

7. K. J. Desai, Thesis, The University of Michigan, Ann Arbor, 1976.

8. A. M. Ugolev, "Physiology and Pathology of Membrane Digestion," Plenum Press, New York (1968).

9. A. M. Ugolev, "Biomembrane," Membrane Digestion, Volume 4A, Plenum Press, New York (1974).

10. J. Grayson, "Gastrointestinal Physiology," The Gastrointestinal Circulation, Volume 4, University Park Press, Baltimore, Md. (1974).

11. W. Crouthamel, J. T. Doluisio, R. E. Johnson and L. Diamond, J. Pharm. Sci., 59, 878 (1970).

12. L. Ther and D. Winne, "Annual Review of Pharmacology," Drug Absorption, Volume 2, Annual Review, Palo Alto, California (1972).

13. L. Z. Benet, A. Greither and W. Meister, "The Effect of Disease States on Drug Pharmacokinetics," Gastrointestinal Absorption of Drugs in Patients with Cardiac Failure, A. Ph. A. Academy of Pharmaceutical Sciences, Washington, D.C. (1976).

14. A. A. Noyes and W. R. Whitney, Z. Phys. Chem., 23, 689 (1897).

15. W. Nernst, Z. Phys. Chem., 47, 52 (1904).

16. V. G. Levich, Physico-Chemical Hydrodynamics, Prentice-Hall Inc., Englewood Cliffs, N.J. (1962).

17. J. Dainty, Adv. Botan. Res., 1, 279 (1963).

18. J. Dainty and C. R. House, J. Physiol., 182, 66 (1966).

19. J. M. Diamond, J. Physiol., 183, 83 (1966).

20. A. W. Guthbert and Y. Dunant, Br. J. Pharmac., 40, 508 (1970).

21. F. A. Wilson, V. L. Sallee and J. M. Dietschy, Science, 174, 1031 (1971).

22. J. M. Dietschy, V. L. Sallee and F. A. Wilson, Gastroenterology, 61, 932 (1971).

23. V. L. Sallee and J. M. Dietschy, J. Lipid Res., 14, 475 (1973).

24. J. M. Dietschy, Helv. Med. Acta, 37, 89 (1973).

25. D. Winne, Biochim. Biophys. Acta, 298, 27 (1973).

26. L. D. Lewis and J. S. Fordtran, Gastroenterology, 68, 1509 (1975).

27. J. E. Pike, Sci. Amer., 226, 84 (1971).

28. S. Bergstrom, L. A. Carlson and J. R. Weeks, Pharmacol. Rev., 20, 1 (1968).

29. V. R. Pickles, Nature, 224, 221 (1969).

30. J. W. Hinman, Annu. Rev. Biochem., 41, 161 (1972).

31. J. R. Weeks, Annu. Rev. Pharmacol., 12, 317 (1972).

32. O. T. Oesterling, W. Morozowich and J. J. Roseman, J. Pharm. Sci., 61, 1861 (1972).

33. S. W. Waller, Gut, 14, 402 (1973).

34. V. V. Men'shikov, V. A. Orlov and N. V. Belyakov, Sov. Med., 11, 68 (1974).

35. P. Crabbe, Chem. Br., 11, 132 (1975).

36. E. W. Horton and I. H. M. Main, Br. J. Pharmacol., 21, 182 (1963).

37. E. W. Horton and I. H. M. Main, Br. J. Pharmacol., 24, 470 (1965).

38. A. Bennett and J. Posner, Br. J. Pharmacol., 42, 584 (1971).

39. A. Robert, J. E. Nezamis and J. P. Phillips, Amer. J. Dig. Dis., 12, 1073 (1967).

40. L. Way and R. P. Durbin, Nature, 221, 874 (1969).

41. D. E. Wilson and R. A. Levine, Gastroenterology, 56, 1268 (1969).

42. E. D. Jacobson, Proc. Soc. Exp. Biol. Med., 133, 516 (1970).

43. S. M. M. Karim and G. M. Filshie, Lancet, 1, 157 (1970).

44. J. J. Misiewicz, S. L. Waller, N. Kiley et al., Lancet, 1, 648 (1969).

45. N. F. Pierce, C. C. J. Carpenter, Jr., H. L. Elliot and W. B. Greenough, Gastroenterology, 60, 22 (1971).

46. T. M. Parkinson, J. C. Schneider, Jr., J. J. Krake and W. L. Miller, Life Science, 7, 883 (1968).

47. T. M. Parkinson and J. C. Schneider, Jr., Biochim. Biophys. Acta, 176, 78 (1969).

48. W. E. Magee, S. B. Armour and O. V. Miller, Biochim. Biophys. Acta, 306, 270 (1973).

49. A. Robert, W. E. Magee, O. V. Miller and J. E. Nezamis, Biochim. Biophys. Acta, 348, 269 (1974).

50. J. D. Rogers, Thesis, The University of Michigan, Ann Arbor, 1976.

51. K. Green, Biochim. Biophys. Acta, 231, 419 (1971).

52. E. Granström, Biochim. Biophys. Acta, 239, 120 (1971).

53. E. Granström and B. Samuelsson, J. Biol. Chem., 246, 5254 (1971).

54. E. Änggard, Ann. N.Y. Acad. Sci., 180, 200 (1971).

55. B. Samuelsson, E. Gramström K. Green and M. Hamberg, Ann. N.Y. Acad. Sci., 180, 138 (1971).

56. M. Hamberg and B. Samuelsson, J. Biol. Chem., 246, 6713 (1971).

57. M. Hamberg, Eur. J. Biochem., 6, 135 (1968).

58. C. Pace-Asciak, K. Morawska and L. S. Wolfe, Biochim. Biophys. Acta, 218, 288 (1970).

59. J. Nekono and A. V. Prancan, J. Pharm. Pharmacol., 23, 231 (1971).

60. Private Talking with Dr. Morozowich, The Upjohn Company, Kalamazoo, Michigan 49001.

61. F. F. Sun, Biochim. Biophys. Acta, 348, 249 (1974).

62. F. F. Sun and J. E. Stafford, Prostaglandin Symposium Acad. Pharm. Sci., Chicago, Ill., 2, 15 (1972).

63. K. Svanborg and M. Bygdeman, Eur. J. Biochem., 28, 127 (1972).

64. E. Granström and B. Samuelsson, Eur. J. Biochem., 10, 411 (1969).

65. E. Granström, Eur. J. Biochem., 20, 451 (1971).

66. E. Granström, Eur. J. Biochem., 25, 581 (1972).

67. E. Granström and B. Samuelsson, J. Biol. Chem., 246, 7470 (1971).

68. J. R. Paulsrud and O. N. Miller, Fed. Proc., 33, 590 (1974).

69. L. Z. Bito, Fed. Proc., 33, 590 (1974).

70. J. Fried, M. M. Mehra and B. J. Gaede, Supplementum to Advances in Biosciences 9, Pergamon Press, Vieweg (1972).

71. T. J. Roseman and S. H. Yalkowsky, J. Pharm. Sci., 62, 2933 (1973).

72. T. J. Roseman, B. Sims and R. G. Stehle, Amer. J. Hosp. Pharm., 30, 236 (1973).

73. S. M. M. Karim, J. Devin and K. Miller, J. Pharmacol., 4, 416 (1968).

74. J. T. Doluisio, G. H. Tan, N. F. Billups and L. Diamond, J. Pharm. Sci., 58, 1200 (1969).

75. K. Green and B. Samuelsson, J. Lipid Res., 5, 117 (1964).

76. N. F. H. Ho, W. I. Higuchi and J. Tuni, J. Pharm. Sci., 61, 192 (1972).

77. W. L. Hayton and G. Levy, J. Pharm. Sci., 61, 362 (1972).

78. J. T. Doluisio, W. G. Crouthamel, G. H. Tan, J. V. Swintosky and L. W. Dittert, J. Pharm. Sci., 59, 72 (1970).

79. J. Nakano, A. V. Prancan and N. H. Morsy, Jap. J. Pharmcol., 23, 355 (1973).

80. T. Nishibori, Y. Matsuoka and T. Matsumoto, Pharmacometrics (Japan), 8, 797 (1974).

81. L. Z. Bito, Prostaglandins, 9, 851 (1975).

82. F. F. Sun, S. B. Armour, V. R. Bockstanz and McGuire, Adv. in Prostaglandin and Thromboxane Research, Volume 1, Raven Press (1976).

APPENDIX

The permeability coefficient of the aqueous diffusion layer is defined by

$$P_{aq} = \frac{D}{h} \qquad \text{(Eq. 1')}$$

where D = aqueous diffusion coefficient, cm^2/sec

h = effective thickness of the aqueous diffusion layer, cm.

From convective-diffusion theory[16]

$$h \propto D^{1/3} Q^{-1/2} \qquad \text{(Eq. 2')}$$

and, accordingly,

$$P_{aq} \propto D^{2/3} Q^{1/2} \qquad \text{(Eq. 3')}$$

In Eq. 3' one has an explicit relationship of P_{aq} to the aqueous diffusivity of the molecule and the bulk fluid flow rate, Q. Furthermore, the Stokes-Einstein equation gives a relationship of D to the molecular weight (MW) and density (ρ) of the molecule.

$$D \propto \left(\frac{\rho}{MW}\right)^{1/3} \qquad \text{(Eq. 4')}$$

To account for differences between the permeability coefficients of two diffusants (for example, n-butyric and n-hexanoic acids) under the same hydrodynamic conditions, we have

$$\frac{P_{aq,butyric}}{P_{aq,hexanoic}} = \left(\frac{D_{aq,butyric}}{D_{aq,hexanoic}}\right)^{2/3}$$

$$= \left(\frac{MW_{hexanoic}}{MW_{butyric}}\right)^{2/9} \qquad \text{(Eq. 5')}$$

here, the relative densities are small.